Meereswissenschaftliche Berichte

Marine Science Reports

LEIBNIZ-INSTITUT FÜR
OSTSEEFORSCHUNG
WARNEMÜNDE

IOW

Hydrographic-hydrochemical assessment of the Baltic Sea 2021

Michael Naumann, Ulf Gräwe, Volker Mohrholz, Joachim Kuss, Marion Kanwischer, Helena Osterholz, Susanne Feistel, Ines Hand, Joanna J. Waniek, Detlef E. Schulz-Bull

Adressen der Autoren:
[1] Leibniz Institute for Baltic Sea Research (IOW), Seestraße 15, D-18119 Rostock-Warnemünde, Germany

Corresponding author: michael.naumann@io-warnemuende.de

Table of content

Kurz- /Zusammenfassung

Die Arbeit beschreibt die hydrographisch-hydrochemischen Bedingungen in der westlichen und zentralen Ostsee im Jahr 2021. Basierend auf den meteorologischen Verhältnissen werden die horizontalen und vertikalen Verteilungsmuster von Temperatur, Salzgehalt, Sauerstoff/ Schwefelwasserstoff und Nährstoffen mit saisonaler Auflösung dargestellt.

Nach dem warmen Rekordwinter 2019/20 (Kältesumme 0 Kd) belegt der Winter 2020/21 mit einer Kältesumme von 32,7 Kd, gemessen in Warnemünde, den 17. Platz der wärmsten Winter der Datenreihe seit dem Jahr 1948. Die Wärmesumme des Sommers 2021 ist mit 284,7 Kd deutlich über dem Mittelwert von 159,7 +/- 75,1 Kd und über dem Vorjahr 2020 mit 234,3 Kd.

Im gesamten Jahresverlauf 2021 blieben intensive Einstromereignisse aus. Kleinere Ereignisse sorgten für die Belüftung des Tiefenwassers im Gebiet des Arkona Beckens bis Bornholm Beckens.

In den tiefen Becken schreitet die Sauerstoffabnahme seit dem letzten "Major Baltic Inflow" (2014-2016) grundsätzlich weiter voran. Es treten in einzelnen Jahren auch immer mal wieder kurzzeitige Verbesserungen auf, die aber weder die schlechte Situation noch den Trend entscheidend verändern. So war der Zustand des Fårötiefs in 2020 und die westliche Gotlandsee (Landsort- und Karlsötief) in 2021 bezüglich des vorhandenen Schwefelwasserstoffs etwas besser. Allerdings gab es auch einen Schub von sauerstoffhaltigem Wasser bis in die südliche Gotlandsee im Bereich der Haloklinen, der sich danach weiter nördlich ausbreitete.

Die Winter-Nährstoffkonzentrationen von Phosphat und Nitrat im Oberflächenwasser waren deutlich höher als in den Jahren davor und entfernten sich von den HELCOM Zielwerten, die zumindest für Nitrat erreichbar schienen. In der Gotlandsee entsprachen die Werte für das Oberflächenwasser im Januar/Februar 2021 den Ergebnissen der vorigen Jahre. Nur für das Karlsötief war ein deutlich höherer Winternitratwert des Oberflächenwassers für 2021 dokumentiert.

Im Tiefenwasser verschlechterte sich die Situation der Hauptnährstoffe Phosphat und Ammonium entsprechend zur Entwicklung von negativem Sauerstoff (Schwefelwasserstoff) weiter. Höchste Konzentrationen wurden in 2021 für Phosphat im Tiefenwasser des Gotlandtiefs (5,4 µmol/l), des Fårötiefs (4,4 µmol/l) und des Karlsötiefs (4,0 µmol/l) seit 2017 gemessen. Nitrat war bei den euxinischen Bedingungen verbraucht und Ammonium akkumulierte zu Maxima in 2021 im Bornholmtief (4,0 µmol/l), Gotlandtief (22,8 µmol/l), Fårötief (12,2 µmol/l) und im Landsorttief (10,3 µmol/l) mindestens seit 2017.

Die Konzentrationen des partikulär gebundenen organischen Kohlenstoffs (POC) und Stickstoffs (PON) waren im Jahr 2021 im Oberflächenwasser besonders in März und Juli, induziert durch photosynthetische Primärproduktion, erhöht. Besonders an den sehr flachen Stationen vor Warnemünde, auf der Darßer Schwelle und im Fehmarn Belt war das Signal von März bis Juli bis in die unteren, durchmischten Wasserschichten sichtbar. Die partikulären C/N Verhältnisse lagen im Tiefen- und Oberflächenwasser signifikant unter den Langzeitmitteln, während nur die POC Konzentration an der Oberfläche unter dem Langzeitmittel blieb.

In diesem Bericht sind die während des Ostsee-Umweltmonitorings im Januar/Februar 2021 ermittelten Oberflächenwasserkonzentrationen für die chlorierten Kohlenwasserstoffe (CKW) Dichlordiphenyltrichlorethan (*o,p'*DDT, *p,p'*DDT) und die Metabolite *p,p'*DDE und *p,p'*DDD, polychlorierte Biphenyle (PCB$_{ICES}$) und Hexachlorbenzol (HCB) sowie polyzyklische aromatische Kohlenwasserstoffe (U.S. EPA PAH) zusammengefasst. Für die Summe von DDT und Metabolite (ΣDDT$_{sum}$) wurden Konzentrationen von 4,0 - 14,7 pg/L (Median: 5.8 pg/L) ermittelt; die höchste Konzentration von 14,7 pg/L für die Pommersche Bucht. Wie auch in den vergangenen Jahren waren die Konzentrationen des langlebigen Abbauproduktes *p,p'*-DDE höher im Vergleich zum *p,p'*DDT. Dies deutet darauf hin, dass aktuell keine wesentlichen neuen DDT-Einträge erfolgten. Für PCB$_{ICES}$ und HCB wurden Konzentrationen von 2,4 - 7,5 pg/L (Median: 2,8 pg/L) für ΣPCB$_{ICES,SUM}$ bzw. 5,1 - 8,1 pg/L (Median: 5,6 pg/L) für HCB$_{SUM}$ ermittelt. Auch hier wurden die jeweils höchsten Konzentrationen für die Pommersche Bucht nachgewiesen, d.h. 7,5 µg/L ΣPCB$_{ICES,SUM}$ und 8,1 µg/L HCB$_{SUM}$. Für die Belastung des Oberflächenwassers mit PAH (ΣPAH$_{SUM}$) wurden Konzentrationen von 3665 pg/L - 6939 pg/L (Median: 5414 pg/L) detektiert. Im Gegensatz zu den CKW wurden für die PAH die höchsten Konzentrationen in den Untersuchungsgebieten Central Baltic Sea (6639 pg/L) und Eastern Gotland Sea (*South*: 6939 pg/L, *North*: 6000 pg/L) (Abb. 6) verzeichnet. Die für die Pommersche Bucht ermittelten Daten verweisen auf die Oder als Quelle für den Eintrag der hier untersuchten Schadstoffe, im Besonderen partikulär gebundener Schadstoffe (ΣDDT$_{part}$: 7,17 pg/L, ΣPCB$_{ICES,part}$: 4,36 pg/L, HCB$_{part}$: 1,27 pg/L, ΣPAH$_{part}$: 1873 pg/L).

Die Zeitreihenanalysen der Oberflächenwasserdaten, zum Teil zurückliegend bis zum Jahr 2001, zeigen anhaltende abnehmende Trends der Konzentrationen für PCB$_{ICES}$ sowie DDT und dessen Metabolite.

Die Auswertung der ermittelten Daten anhand der Umweltqualitätsnormen (UQN) der Wasserrahmenrichtlinie zeigt, dass vor allem die Konzentrationen des hochmolekularen PAK Benzo(*b*)fluoranthen für Meeresorganismen besorgniserregend sein könnten, hauptsächlich in den Gebieten von der Pommerschen Bucht bis zur Gotlandsee. Hier wurden die Jahresdurchschnitts-UQN überschritten.

Abstract /Summary

The article summarizes the hydrographic-hydrochemical conditions in the western and central Baltic Sea in 2021. Based on the meteorological conditions, the horizontal and vertical distribution of temperature, salinity, oxygen/hydrogen sulphide and nutrients are described on a seasonal scale.

After the record warm winter 2019/20 (cold sum 0 Kd) are a "cold sum" of 32.7 Kd recorded for wintertime 2020/21 at station Warnemünde. It is classified as a mild winter on 17th position of warm winters over the past 73 years (1948-2021). The summer "heat sum" of 284.7 Kd is far above the long-term average of 159.7 +/- 75.1 Kd and above the previous year 2020 of 234,3 Kd.

In the course of the year 2021 no larger inflow events occurred, but the deepwater of the Arkona Basin and Bornholm Basin was ventilated by weak inflow events.

The oxygen decline since the last Major Baltic Inflow (2014-2016) generally continued in the central Baltic Sea deep basins. However slight improvements in certain years occured, but didn't change the general bad situation and the trend. So the situation in the deep water of the Fårö Deep was a little better in 2020 with regard to present hydrogen sulphide and the western Gotland Sea (Landsort and Karlsö Deep) somehow better in 2021. However, in 2021 a pulse of oxygenated water brought some oxygen to the southern Gotland Sea in the halocline range that was distributed further North.

The winter nutrient concentrations of phosphate and nitrate in surface water were clearly higher in 2021 as in a couple of previous years and moved further away from HELCOM target values that appeared within reach for nitrate in recent years. For the Gotland Sea the winter nutrient concentrations of surface water in January/February 2021 were within the range of recent years. Only for the Karlsö Deep a clearly higher nitrate concentration in surface water is documented for winter 2021 in surface water.

In the deep water, a worsening of the situation of the major nutrients phosphate and ammonium occured in the year 2021 in agreement with the development of negative oxygen (hydrogen sulphide). Highest values for 2021 were determined for phosphate in the deep water of the Gotland Deep (5.4 µmol/l), Fårö Deep (4.4 µmol/l), and Karlsö Deep (4.0 µmol/l) since 2017. Nitrate was depleted in euxinic condition and ammonium accumulated to maxima in 2021 in the Bornholm Deep (4.0 µmol/l), Gotland Deep (22.8 µmol/l), Fårö Deep (12.2 µmol/l) and Landsort Deep (10.3 µmol/l) at least since 2017.

The concentrations of particulate organic carbon (POC) and nitrogen (PON) were in surface waters notably increased in March and July induced by photosynthetic primary production. Especially at coastal and shallow stations like at Warnemünde, at the Darss Sill and Fehmarn Belt this signal was measured down to the mixed deep-water from March to July. The ratio of particular C/N were significant below the long-term means at the deep-water and surface layer, whereas POC concentrations were lowered only in surface waters.

This report summarizes surface water concentrations determined during the Baltic Sea environmental monitoring in January/February 2021 for the chlorinated hydrocarbons (CHC) dichlorodiphenyltrichloroethane (DDT) and its metabolites, polychlorinated biphenyls (PCB$_{ICES}$) and hexachlorobenzene (HCB), as well as polycyclic aromatic hydrocarbons (U.S. EPA PAH).

Seawater samples were collected in study areas from Kiel Bight to the Gotland Sea by transect sampling during the expedition EMB256.

Concentrations ranging from 4.0 to 14.7 pg/L (median: 5.8 pg/L) were determined for DDT and its metabolite (ΣDDT_{sum}); the highest concentration of 14.7 pg/L for the Pomeranian Bight. As in previous years, too, concentrations of the long-lived degradation product p,p'-DDE were higher as compared to p,p'-DDT. This implies that there are currently no significant new DDT inputs.

Concentrations ranging from 2.4 to 7.5 pg/L (median: 2.8 pg/L) and from 5.1 to 8.1 pg/L (median: 5.6 pg/L) were detected for PCBs ($\Sigma PCB_{ICES,sum}$) and HCB (HCB_{sum}). Highest concentrations were detected for the Pomeranian Bight.

Surface water PAH concentrations (ΣPAH_{sum}) ranged from 3665 pg/L to 6939 pg/L (median: 5414 pg/L). In contrast to the CHC, highest PAH concentrations were determined in the areas of the Central Baltic Sea to the Eastern Gotland Sea.

The data obtained for the Pomeranian Bight point to the river Odra as a source of the studied pollutants, in particular for the particle bound ones (ΣDDT_{part}: 7.2 pg/L, $\Sigma PCB_{ICES,part}$: 4.4 pg/L, HCB_{part}: 1.3 pg/L, ΣPAK_{part}: 1872 pg/L).

Analysis of time series data show continuing decreasing trends for concentrations of PCB_{ICES} as well as DDT and its metabolites.

The evaluation of the determined data on the basis of the environmental quality standards (EQS) of the Water Framework Directive shows that especially the concentrations of the high molecular PAH benzo(b)fluoranthene are of concern for the marine organisms, mainly in the areas from the Pomeranian Bight to the Gotland Sea. Here the annual average EQS values are exceeded.

1 Introduction

This assessment of hydrographic and hydrochemical conditions in the Baltic Sea in 2021 has partially been produced on the basis of the Baltic Sea Monitoring Programme that the Leibniz Institute for Baltic Sea Research Warnemünde (IOW) undertakes on behalf of the Federal Maritime and Hydrographic Agency, Hamburg and Rostock (BSH). Within the scope of an administrative agreement, the German contribution to the Helsinki Commission's (HELCOM) monitoring programme (COMBINE) for the protection of the marine environment of the Baltic Sea has been devolved to IOW. It basically covers Germany's Exclusive Economic Zone. Beyond these borders, the IOW is running an observation programme on its own account in order to obtain and maintain long-term data series and to enable analyses of the conditions in the Baltic Sea's central basins, which play a decisive role in the overall health of the sea.

The combination of both programmes leads to a yearly description of the water exchange between the North Sea and the Baltic Sea, the hydrographic and hydrochemical conditions in the study area, their temporal and spatial variations, as well as the investigation and identification of long-term trends.

Five routine monitoring cruises are undertaken each year covering all four seasons. The data obtained during these cruises, as well as results from other research activities by IOW, form the basis of this assessment. Selected data from other research institutions, especially the Swedish Meteorological and Hydrological Institute (SMHI) and the Maritime Office of the Polish Institute of Meteorology and Water Management (IMGW), are also included in the assessment.

HELCOM guidelines for monitoring in the Baltic Sea form the basis of the routine hydrographical and hydrochemical monitoring programme within its COMBINE Programme (HELCOM 2000). The five monitoring cruises in January/February, March, May, July/August and November were performed by RV Elisabeth Mann Borgese. Details about water sampling, investigated parameters, sampling techniques and their accuracy are given in NEHRING et al. (1993, 1995).

Ship-based investigations were supplemented by measurements at three autonomous stations within the German MARNET environmental monitoring network, the ARKONA BASIN (AB), the DARSS SILL (DS) station and the ODER BANK (OB) station. At the Darss Sill the autonoumous measuring pile was removed for a usual 10-years general overhaul in mid March and brought to Rostock harbour. A mooring was deployed as replacement. The Oder Bank bouy was in operation from mid-March to beginning-December 2021 and taken out of service over the winter of 2021/2022. A second system of a new buoy construction more resistant against damages caused by ice was operated in parallel at the Oder Bank position.

Besides meteorological parameters at these stations, water temperature and salinity as well as oxygen concentrations were measured at different depths:

AB: 8 horizons T + S   +   2 horizons O_2

DS: 6 horizons T + S   +   2 horizons O_2

OB: 2 horizons T + S   +   2 horizons O_2

All data measured at the MARNET stations are transmitted via METEOSAT to the BSH database as hourly means of six measurements (KRÜGER et al. 1998, KRÜGER 2000). An acoustic doppler

current profiler (ADCP) records current speeds and directions at AB and DS. The ADCP arrays are located on the seabed in some two hundred metres distance from the main stations and protected by a trawl-resistant bottom mount mooring. They are operated in real time: via an hourly acoustic data link, they send their readings to the main station for storage and satellite transmission. For quality assurance and service purposes, data stored by the devices itself are read retrospectively during maintenance measures at the station once or twice a year.

As a general overview of the state of the Baltic Sea Fig. 1 shows the recent hypoxic to euxinic conditions. Oxygen deficiency is one of the major factors influencing the Baltic Sea ecosystem. An overlay of the conditions in winter and summer are shown in this map, visualising the development during the year 2021. A large extend of bottom water in the deep basins is influenced by hypoxia (black dotted areas) and the situation is more or less stagnant. Compared to the winter situation measurements at the northern stations 283, 282, 285 showed no occurrence of hydrogen sulphide in summer but the situation worsened at the Bornholm basin with a spreading of hydrogen sulphide.
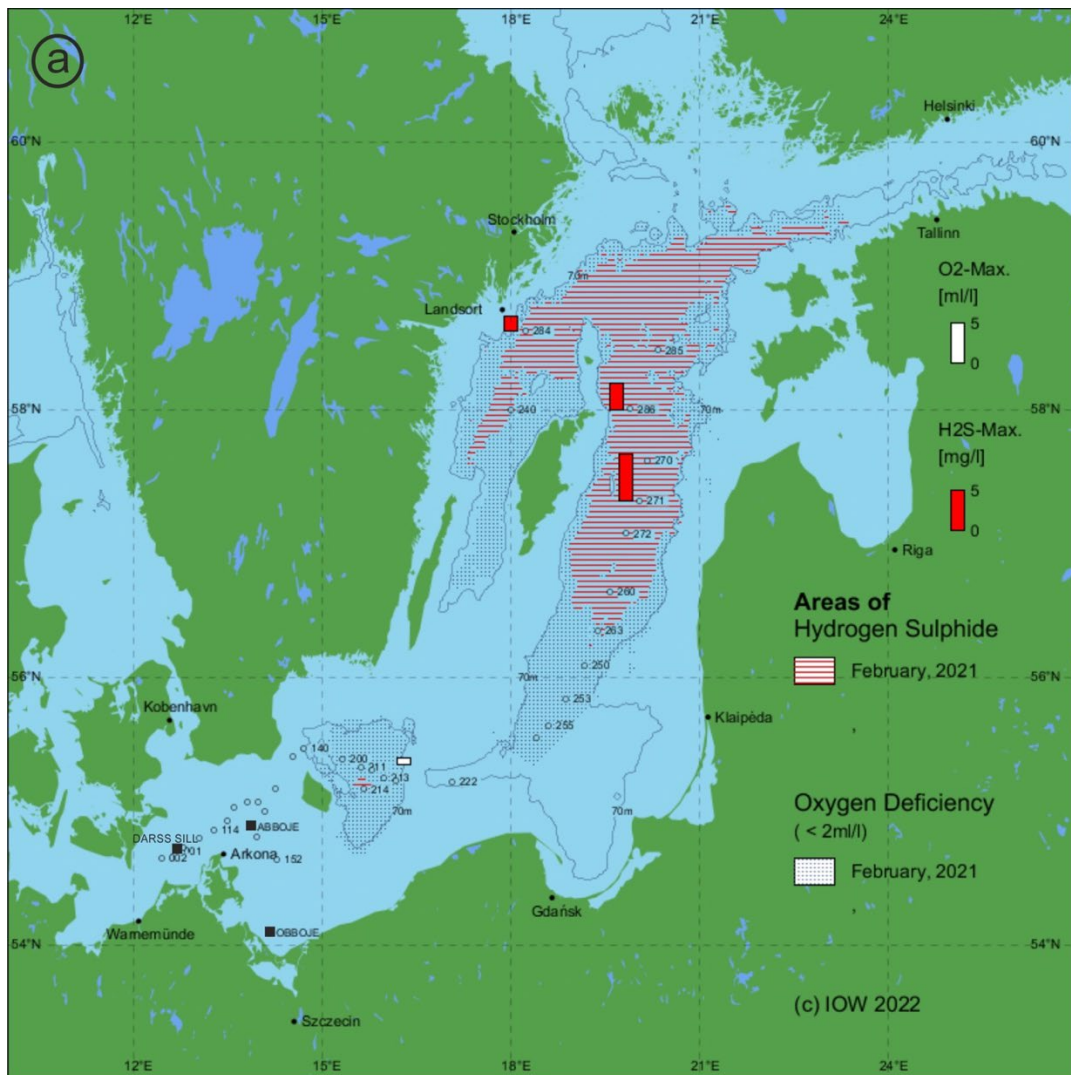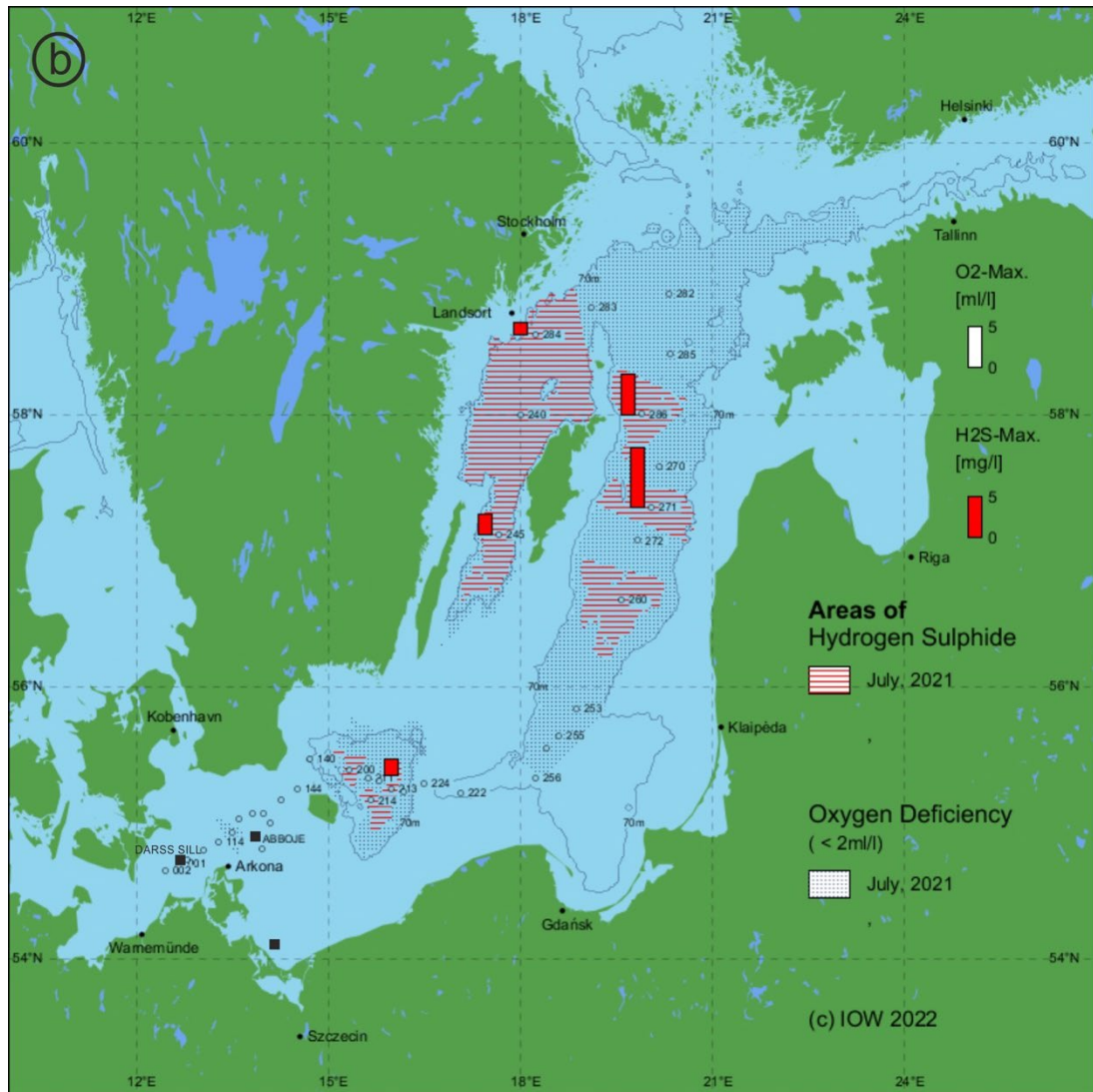
Fig. 1: Location of stations (■ MARNET- stations) and areas of oxygen deficiency and hydrogen sulphide in the near bottom layer of the Baltic Sea. Bars show the maximum oxygen and hydrogen sulphide concentrations of this layer in 2021; the figure additionally contains the 70 m -depth line. a) The situation in February 2021. b) The situation in July 2021.

2   General meteorological conditions

The following description of weather conditions in the southern Baltic Sea area is based on an evaluation of data from the Germany's National Meteorological Service (DWD), the Federal Maritime and Hydrographic Agency (BSH), the Swedish Meteorological and Hydrological Institute (SMHI), the Institute of Meteorology and Water Management (IMGW), Freie Universität Berlin (FU) as well as IOW itself. Table 1 gives a general outline of the year's weather with monthly mean temperature, sunshine duration, precipitation as well as the number of days of frost and ice at Arkona weather station. Solar radiation at Gdynia weather station is given in addition. The warm and cold sums at Warnemünde weather station, and in comparison with Arkona, are listed in Table 2 and Table 3.

According to the analysis of DWD (DWD 2022), 2021 like previous years was too warm, in the mid range of precipitation and of a longer sunshine duration than usual. With 9.1 °C, Germany's annual mean temperature was 0.9 K warmer than those of the reference period 1961-1990 and - 0.2 K colder compared to the reference period 1991-2020. It was the eleventh year in a row of a too warm mean temperature. The beginning of the year was characterized by temperature differences between polar airmasses and springlike phases. In February locally new negative temperature records were set in the mid of Germany, for example at Mühlhausen with -26.7 °C at February 10th. April was the coldest one since 40 years in Germany. In contrast, June was the third warmest in history after the years 2019 and 2003. In general, no new temprature records in the summertime occured. The annual maximum was measured at station Baruth (south of Berlin) with 36.6 °C at June 19th. Focussing at the Baltic Sea, the meteorological data reflect the same situation (cf.Table 1). Most monthly mean temperature values were above average, but April, May, August and December below average. At the southern Baltic Sea coast a warm sum of 284.7 Kd was reached (station Warnemünde, cf. Table 2), which is far above the longterm mean of 159.7 +/- 75.1 Kd and on 6th place of warmest summers (1948-2020). The warm sum of June (87.6 Kd) is more than twice as high as the longterm monthly mean of 42.4 Kd and is second placed in this time series.

The mean amount of precipitation in Germany in 2021 was 805 l/m², 75 l/m² more than in 2020, and above the long-term mean value (791 l/m² - reference period 1991-2020 and former reference period 1961-1990 of 789 l/m²). After a decade of too dry conditions, when only in 2017 precipitation was above average, forests could recover a bit in 2021. In contrast, it was a year high water levels in rivers and flooding desasters in western and central Europe caused by heavy rainfall events of historic magnitude. After the year 2001, 2021 is second placed in the number of heavy rainfall during the sommer months May-September. The highest daily rainfall of 198,7 l/m² was registered in Ludwigsburg /Uckermark in the south of the Oder lagoon (northeastern Germany). The lowest precipitation with values below 500 l/m² per year was observed in east of the Harz mountains (central Germany). In the coastal states along Germany's Baltic Sea coast precipitation ranged from 750 l/m² (avg. 788 l/m²) in Schleswig-Holstein to 630 l/m² (avg. 595 l/m²) in Mecklenburg-Vorpommern.

In Germany, the average annual sum of 1,650 hours was lower than in 2020 (1,901 hours) but on average (reference period 1991-2020). The record-breaking value of 2,020 hours of sunshine was observed in the year 2018. At the coast the sunshine duration was as well on average. Schleswig-

Holstein registered 1,570 hours in 2021 (long-term mean: 1,567 hours) and Mecklenburg-Vorpommern recorded 1,650 hours (long-term mean: 1,648 hours), far below its value from 2018, when it reached the nation-wide highest value of 2,085 hours.

At Gdynia station (Gdansk Bight), an annual sum of 383,544 J/cm² of solar radiation was recorded. Within a data series covering 66 years back in time (first compiled by FEISTEL et al. 2008, continued to date), this value takes the 27th rank in the midrange of these longterm data series. It is much lower than the long-term maximum in 1959 with 457,751 J/cm², but slightly above the mean value of 375,320 J/cm². The sunniest month in 2021 by far was June (Table 1). With 73,990 J/m², it takes the third place in the long-term comparison of monthly mean values, but still falls well short of the peak value of 80,389 J/m² in July 1994, which represents the absolute maximum of the entire series since 1956. February set a new record with 15,358 J/cm² and August was ranked on 55th place (43,307 J/m²). All other months showed solar radiation monthly mean values compared to those of the last 66 years as follows: January rank 51, March rank 23, April rank 39, May rank 47, July rank 25, September rank 34; October rank 14; November rank 50, December rank 28.

Table 1: Monthly averaged weather data at Arkona station (Rügen Island, 42 m MSL) from DWD (2022). t: air temperature, Δt: air temperature anomaly, s: sunshine duration, r: precipitation, Frost: days with minimum temperature below 0 °C, Ice: days with maximum temperature below 0 °C. Solar: Solar Radiation in J/cm² at Gdynia station, 54°31' N, 18°33' O, 22 m MSL from IMGW (2022). Percentages are given with respect to the long-term mean. Maxima are shown in bold.

Month	t/°C	Δt/K	s/%	r/%	Frost	Ice	Solar
January	1.7	0.2	71	113	14	1	4957
February	1.6	0.0	137	179	**16**	**8**	15358
March	3.9	0.6	105	100	10	-	28637
April	5.4	-1.2	105	104	1	-	40447
May	10	-0.8	85	129	-	-	53566
June	17.2	**2.6**	**122**	28	-	-	**73990**
July	**18.8**	1.4	86	**212**	-	-	60965
August	16.6	-1.2	93	115	-	-	43307
September	15.3	0.6	85	111	-	-	32082
October	11.2	1.0	110	165	-	-	19794
November	7.2	1.3	49	117	-	-	6052
December	2.2	-0.6	89	124	14	1	4389

Table 2: Sums of daily mean air temperatures at the weather station Warnemünde (data: DWD 2022). The 'cold sum' (CS) is the time integral of air temperatures below the line t = 0 ºC, in Kd, the 'heat sum' (HS) is the corresponding integral above the line t = 16 ºC. For comparison, the corresponding mean values 1948–2020 are given.

Month	CS 2020/21	Mean	Month	HS 2021	Mean
November	0	2.3 ± 5.9	April	0	1.0 ± 2.4
December	0	20.0 ± 27.5	May	4.5	6.0 ± 7.5
January	3.9	37.5 ± 39.0	June	87.6	25.0 ± 17.1
February	28.8	29.7 ± 37.1	July	124.3	58.5 ± 36.3
March	0	8.2 ± 12.0	August	43.1	55.2 ± 34.0
April	0	0 ± 0.2	September	24.9	12.5 ± 13.2
			October	0.3	0.5 ± 1.5
Σ 2020/2021	**32.7**	97.8 ± 84.5	Σ 2021	**284.7**	159.7 ± 75.1

Table 3: Sums of daily mean air temperatures at the weather station Arkona (data: DWD 2022). The 'cold sum' (CS) is the time integral of air temperatures below the line t = 0 ºC, in Kd, the 'heat sum' (HS) is the corresponding integral above the line t = 16 ºC.

Month	CS 2020/21	Month	HS 2021
November	0	April	0
December	0	May	0
January	5.3	June	50.4
February	24.9	July	87.2
March	0	August	27.8
April	0	September	13.8
		October	0
Σ 2020/2021	**30.2**	Σ 2021	**179.2**

2.1   Ice winter 2020/21

For the southern Baltic Sea area, the Warnemünde station shows a **cold sum of 32.7 Kd** (Table 2) referring to the air temperature of the winter 2020/2021. After the record winter 2019/2020 (cold sum of 0 Kd) the recent winter season is ranked on 17th place of warm winters in comparative data from 1948 to date. It continues the series of warm winters during the latest years showing low cold sums: 2018/2019 (18.3 kd), 2017/18 (67.7 Kd) and 2016/17 (31.7 Kd). Since the year 2012 all values plot below the long-term average of 97.8 Kd. In comparison, the cold sum at Arkona station is in the same magnitude of 30.2 Kd (Table 3) and represents as well a warm winter. Recent winter seasons show at Arkona slightly lower values than in Warnemünde (station Arkona: 2019/20 with 0 Kd, 2018/2019 with 14.6 Kd, 2017/18 with 53.8 Kd and 2016/17 with 27.2 Kd). Given the exposed location of the Arkona station at a headland surrounded by water masses at the northernmost coast of Rügen Island, the local air temperature development is under an even stronger influence by the water temperature of the Baltic Sea than at Warnemünde. Thus, winter values at Arkona are frequently higher, while summer values are lower.

The winter season recorded **45 days of frost and 9 ice days** (daily mean below 0 ºC) in the time span December 2020 to April 2021 (Table 1). A longer cold spell occurred from February 1st to 16th

with 16 days of frost and 8 ice days. At station Arkona a cold sum of 24.9 Kd was registered and January reached 5.3 Kd (Table 3). All other winter months showed cold sums of 0 Kd.

Water temperatures lowered as well during this cold spell in the beginning of February. The **local ice conditions at the German Baltic Sea** coast were generally classified as weak (HOLFORT 2021). First icing occurred in small areas in sheltered lagoons for a short period in mid of January. In February all lagoons showed an ice cover and some drift ice along the eastern coast of Rügen island (Fig. 3). Another measure for the strength of an ice winter is the accumulated areal ice volume (KOSLOWSKI 1989, BSH 2009). The season 2020/21 showed **a low accumulated areal ice volume** of 0.37 m (HOLFORT 2021), like typical for the last two decades. Winter season 2009/2010 was the only exception with a high value of 4.22 m. In contrast, the highest values recorded in this data series are as follows: 26.83 m in 1942; 26.71 m in 1940; 25.26 m in 1947; and 23.07 m in 1963. In all other winters, values were well below 20 m (KOSLOWSKI 1989).

For the whole Baltic Sea area a **maximum ice coverage** of 120 373 km² was observed at February 12th (Fig. 3). This maximum extent of ice corresponds to some 29 % of the Baltic Sea's area (415 266 km²), and was largely centred in the Bothnian Bay, Gulf of Finland and Gulf of Riga. The observed maximum ice extent is classified as mild in the time series of 302 years (Fig. 2).
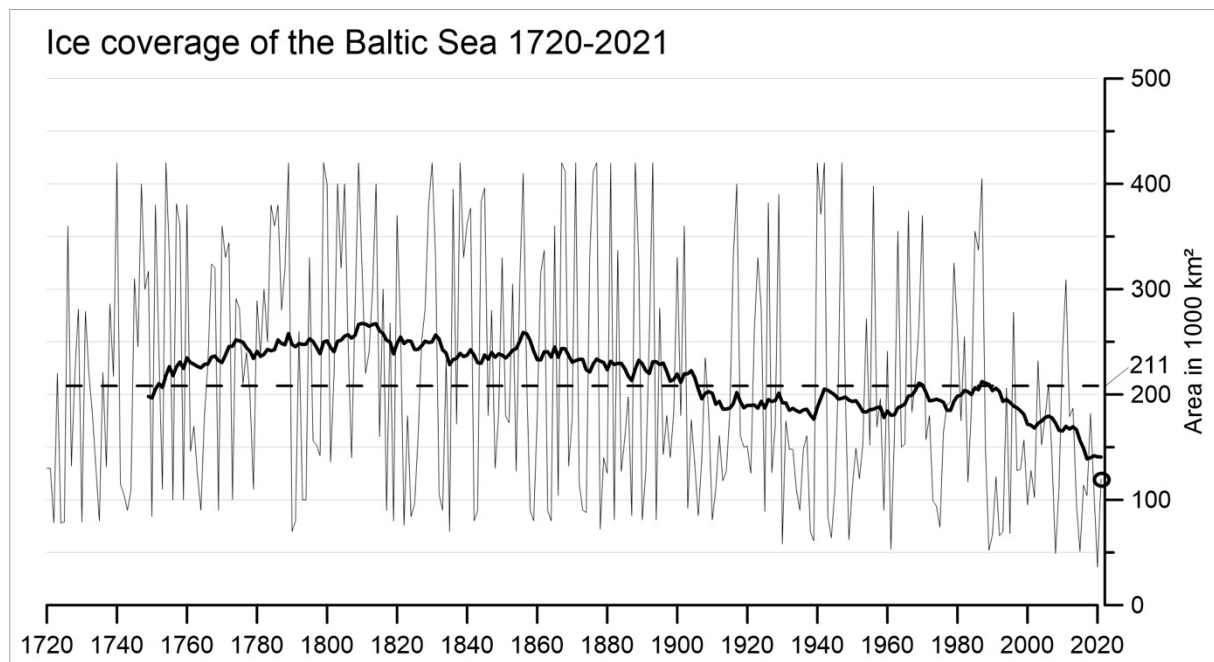
Fig. 2: Maximum ice covered area in 1 000 km² of the Baltic Sea in the years 1720 to 2021 (from data of SCHMELZER et al. 2008, HOLFORT 2021). The long-term average of 211 000 km² is shown as dashed line. The bold line is a running mean value over the past 30 years. The ice coverage in the winter 2020/2021 with 120 373 km² is encircled.
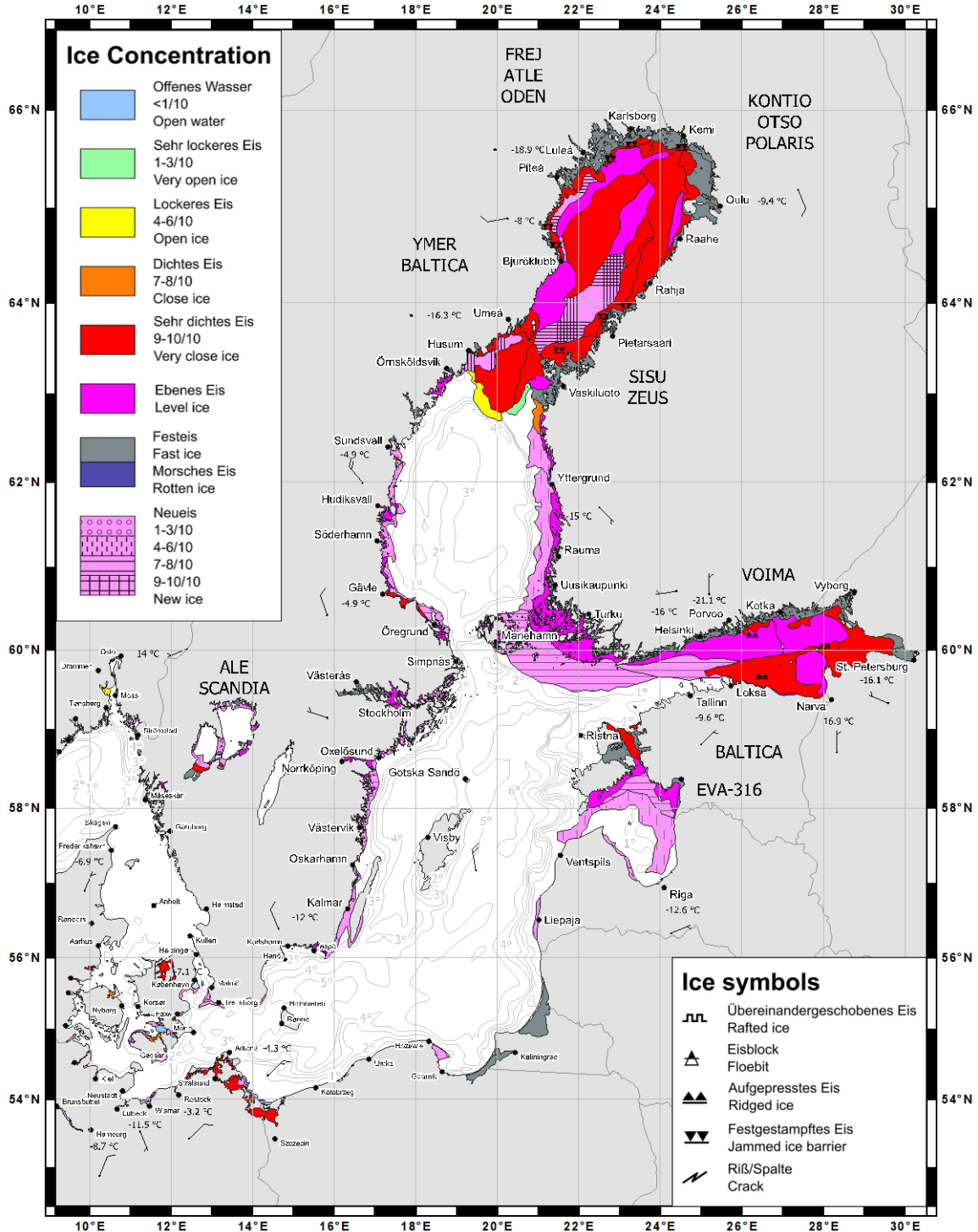
Fig. 3: Maximum ice coverage in the winter 2020/2021 on February 12ᵗʰ – ice concentration in colour code and ice type in symbols (HOLFORT 2021).

2.2 Wind conditions

The year 2021 was again a light windy one and westerly to south-westerly wind directions dominated the situation, comparable to the climatic mean for this region.

Fig. 4 to Fig. 5 illustrate the **wind conditions at Arkona** throughout 2021. The year 2021 of intensified westerly to southwesterly winds (Fig. 5) match with the **trend towards prevailing south-west winds** that began in 1981 (HAGEN & FEISTEL 2008) and continues today. Comparing the east component of the wind (for westerly winds, i.e. wind directed eastward) with an average of 2.46 m/s (Fig. 4b) with the climatic mean of 1.9 m/s (reference period 1991-2020), westerly winds were in 2021 much more dominant than the mean.

According to the wind-rose diagram (Fig. 5), north-western to south-western directed winds account for about 67 % of the annual sum, which is a bit higher compared to 2020 (61 %) and 2019 (62 %). These directions can potentially lead to inflow conditions of saltwater from the North Sea. Easterly to north-easterly winds account for another 18 % in 2021 (24 % in 2020, 22 % in 2019) and can induce outflow conditions. The **annual mean wind speed** of 6.77 m/s (Fig. 4a) is below the average and root mean square of 7.37 +/- 0.44 m/s of the 49 years long time-series at staion Arkona (1973-2020). The maximum wind speed in that period was reached with 8.41 m/s in 1990 and the minimum value occurred in 2018 – the warmest year on record – with 6.5 m/s (based on DWD data, 2022b). Only three high-wind days of over 15 m/s daily mean are registered at February 8th (20.2 m/s) of north-eastern direction, November 19th (16.4 m/s) of western direction and January 4th (15.7 m/s) of north-eastern direction. In addition to the daily means, a view at high values of hourly means and maximum gusts enables to detect short, but intensive wind events of violent character. Some storms are regionally restricted to some hours only with no significant impact on the daily mean value. However, they can lead to major damages. At February 8th the maximum daily mean (20.2 m/s), maximum hourly mean (23.5 m/s) and the **maximum gust of the year** (29.7 m/s, 11 Bft) occurred at the same day. All these 2021 maximum values are below previous peak values, for example an hourly mean of 30 m/s in 2000, 26.6 m/s in 2005; and 25.9 m/s in December 2013.

This windiest day of the year (February 8th) caused a **storm surge** of slight category at the coast of Schleswig Holstein (WEIDIG, 2021). The highest water levels were reached during the afternoon at Flensburg (+1.16 m MSL), Kiel-Holtenau (+1.06 m MSL), Neustadt (+1.13 m MSL), Tarvemünde (+1.14 m MSL) and Lübeck (+1.19 m MSL). At the adjacent coast of Mecklenburg-Vorpommern high water levels were registered (Wismar +0.98 m MSL, Rostock +0.81 m MSL, Greifswald +0.81 m MSL).
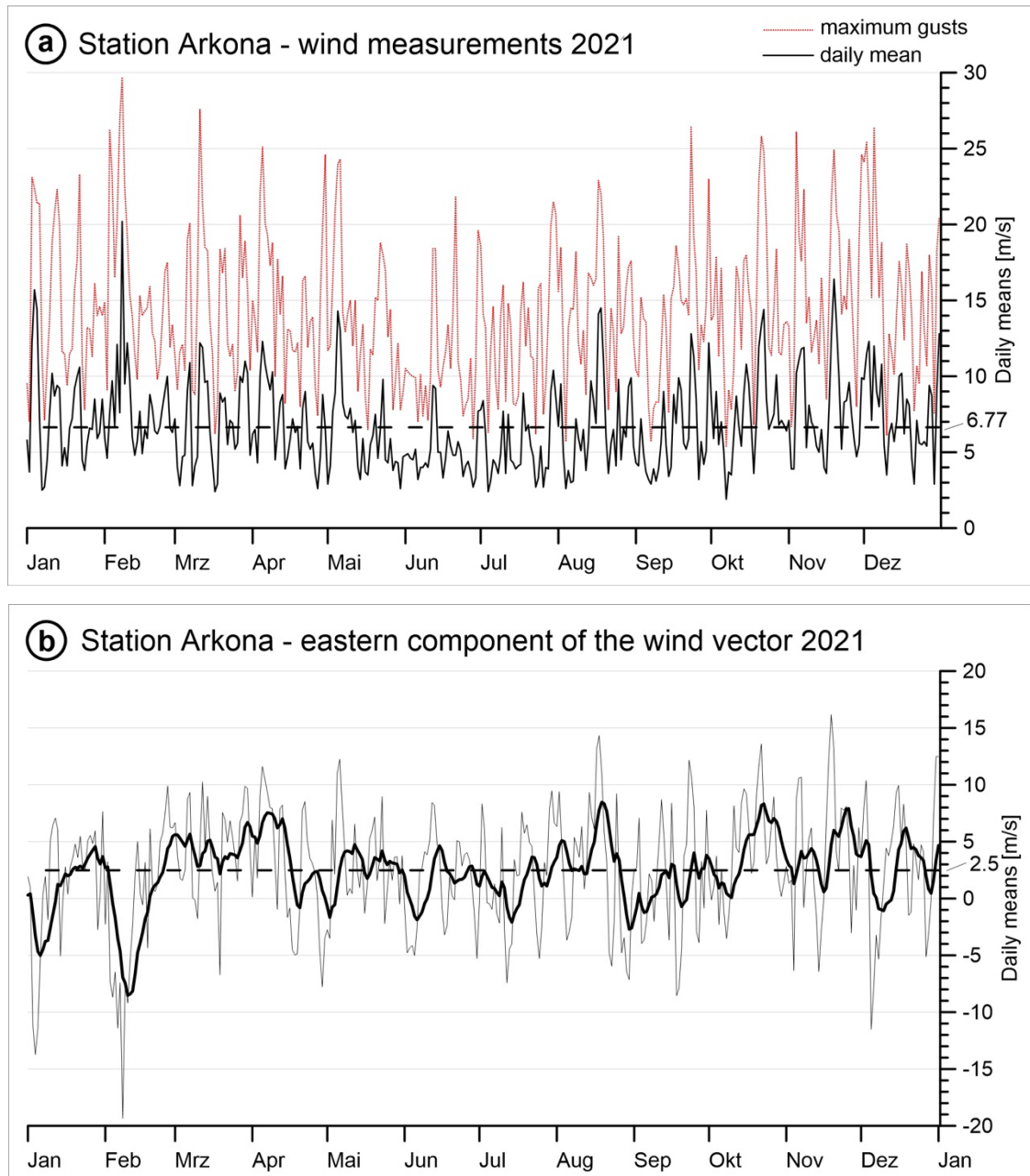
Fig. 4: Wind measurements at the weather station Arkona (from data of DWD, 2022a). a) Daily means and maximum gusts of wind speed, in m/s, the dashed black line depicts the annual average of 6.77 m/s. b) Daily means of the eastern component (westerly wind positive), the dashed line depicts the annual average of 2.46 m/s. The line in bold is filtered with a 10-days exponential memory.
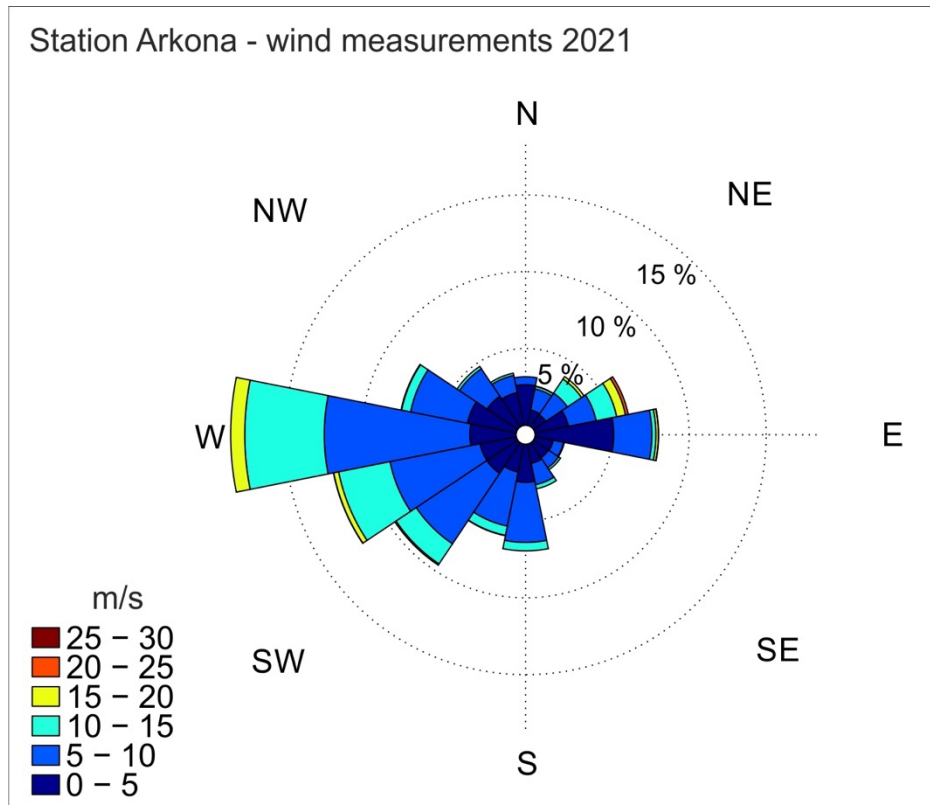
Fig. 5: Wind measurements at the weather station Arkona (from data of DWD 2022a) as windrose plot. Distribution of wind direction and strength based on hourly means of the year 2021.

3 Water exchange through the straits

3.1 Water level at Landsort

The Swedish tide gauge station at Landsort Norra, south of Stockholm, provides a good description of the mean water level in the Baltic Sea (Fig. 6a), as it is more or less unaffected by windshift and located in the centre of the large scale seiche of the Baltic Basin (LISITZIN 1974, JACOBSEN 1980, FEISTEL et al. 2008). In the course of 2021, the Baltic Sea experienced again no strong inflow activity. Several minor inflow pulses with total volumes up to 115 km² occurred all over the year which ventilated the Arcona Basin. These total volumes of inflow water are calculated after NAUSCH et al. 2002, FEISTEL et al. 2008. No "classic" situations of continuous and rapid sea level changes of more than 50 cm could be observed, which indicate major events. Rapid rises of the sea level are usually only caused by an inflow of North Sea water through the Sound and Belts. They are of special interest for the ecological conditions of the deep-water in the Baltic Sea. Such events are produced by storms from westerly to north-westerly directions, as the correlation between the sea level at Landsort Norra and the filtered wind curves illustrates (Fig. 6b). No signs of longer intensified phases (weeks) of a positive southeastern wind component (northwesterly wind) occurred during 2021, which can cause a rapid sea level rise.

Sea level fluctuations in the course of the year 2021 registered a low stand of -31.65 cm MSL at February 16th right after a period of stronger easterly winds (Fig. 6a, Fig. 6b). The highest water level was reached at November 7th with +42.15 m MSL. For example, the large Major Baltic Inflow of December 2014 showed a rapid continnous sea level rise from -47 cm MSL to +48 cm MSL within 22 days (MOHRHOLZ et al. 2015).
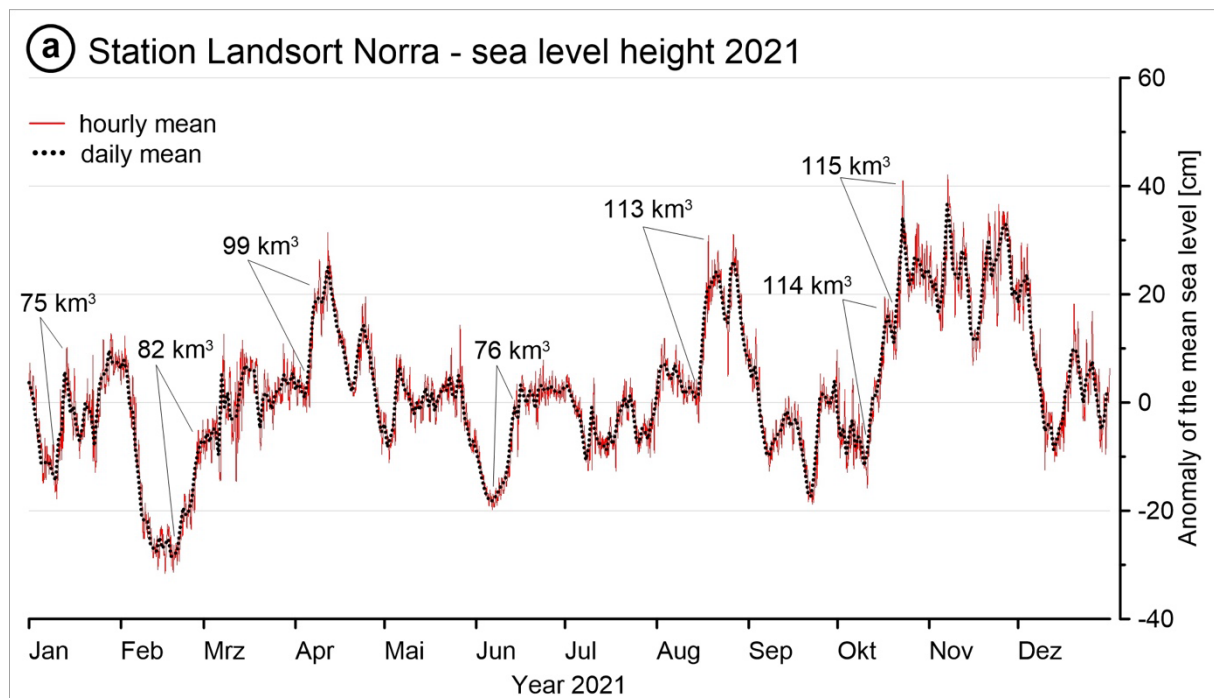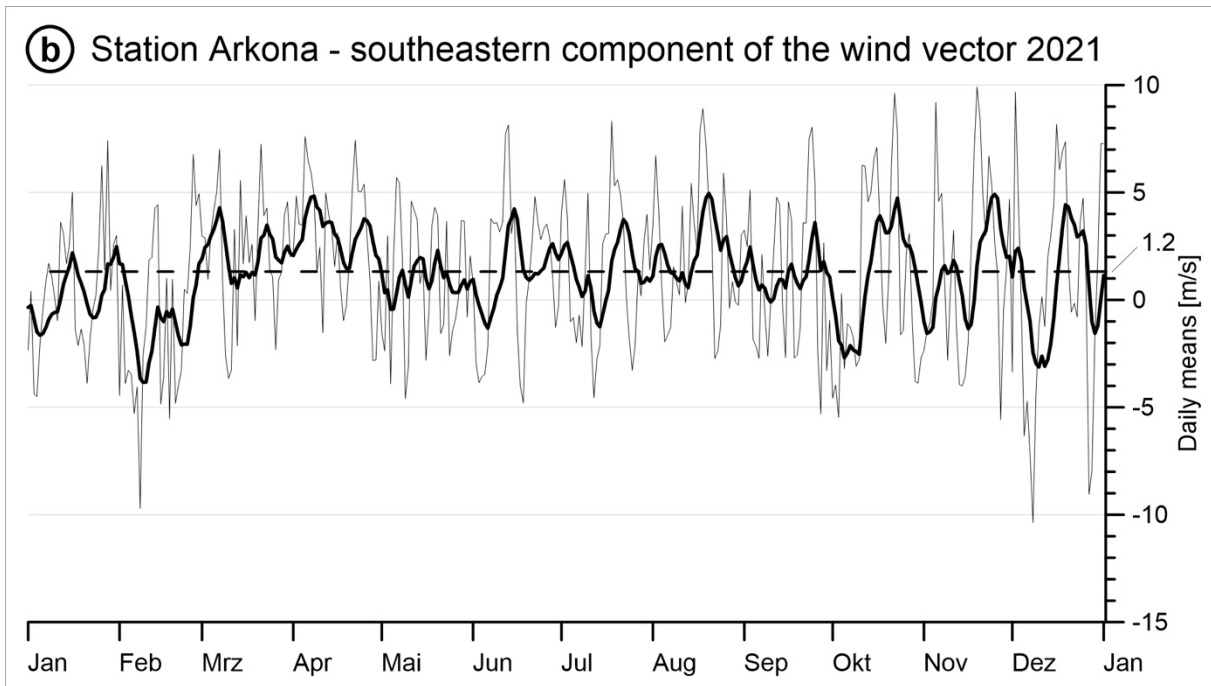
Fig. 6: above (a): Sea level at Landsort as a measure of the Baltic Sea fill factor (from data of SMHI 2022a). below (b): Strength of the southeastern component of the wind vector (northwesterly wind positive) at the weather station Arkona (from data of DWD 2022a). The bold curve appeared by filtering with an exponential 10-days memory and the dashed line depicts the annual average of 1.22 m/s.

An overview of the inflow situation at the **entrance of Baltic Sea** is shown in Fig. 7 and Fig. 8. The curve of the accumulated inflow volume through the Öresund runs mainly below the long-term mean 1977-2020 but within the standard deviation (SMHI 2022b). Single inflow pulses do not exceed 20-25 km³. In comparison, the previous year 2020, the year 2017 of very low inflow activity and the curve of 2014 is shown, the year in which in December the latest very strong Major Baltic Inflow occurred (MOHRHOLZ et al. 2015). Another measure which leads to the classification of inflow events is the salt mass import (Fig. 8), where the overflow volumes of saline water above 17 PSU are taken into account in more detail. MOHRHOLZ (2018) reviewed all sources of hydrographic long-term data for the historic events and set up a new calculation method in comparison to the criteria of MATTHÄUS & FRANCK (1992). The classic criterium for a Major Baltic Inflow is an import volume of at least 1 Gt. None of the smaller inflow pulses during 2021 reached this mark. In October, the second event of 115 km³ (Fig. 6a) showed a saline volume above 17 PSU of 34 km³ and salt mass import of 0.7 Gt as strongest event of the year.
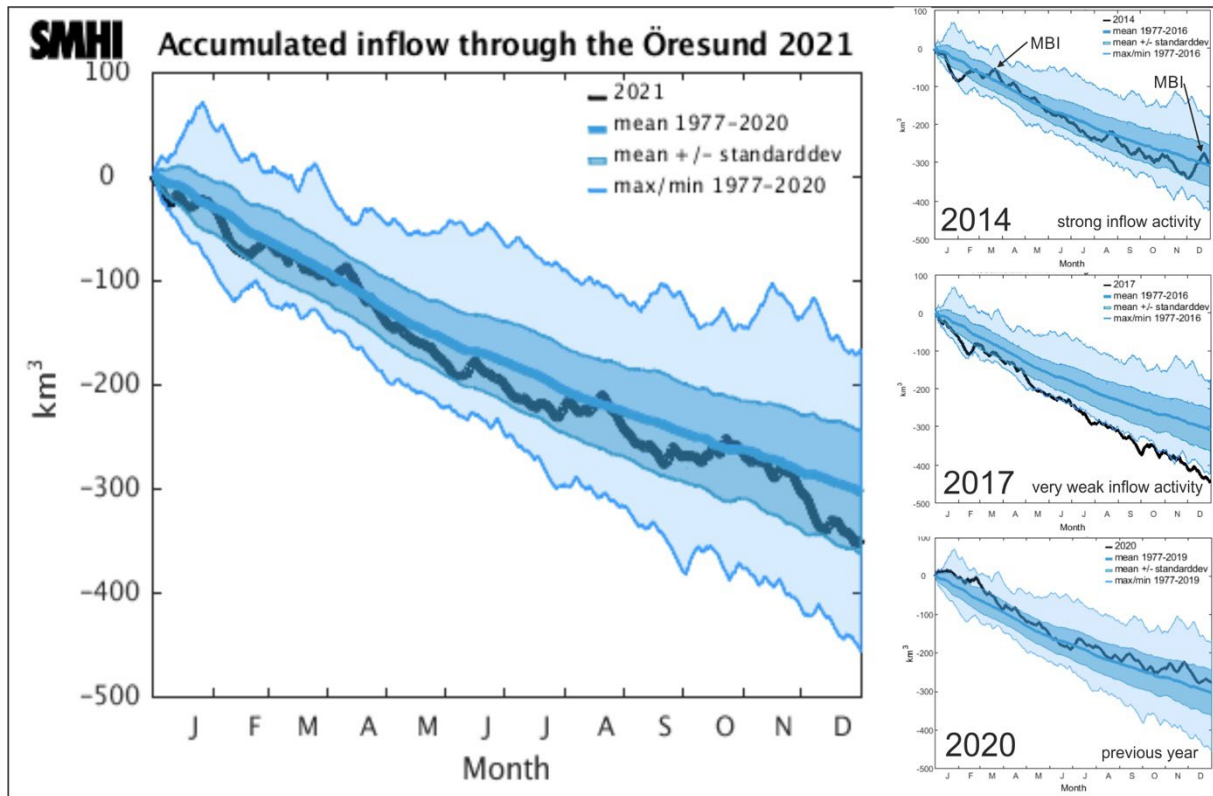
Fig. 7: Accumulated inflow (volume transport) through the Öresund during 2021 in comparison to the previous year and year 2017 of very weak inflow activity and 2014, characterized by the very strong Major Baltic Inflow in December (SMHI 2022b).
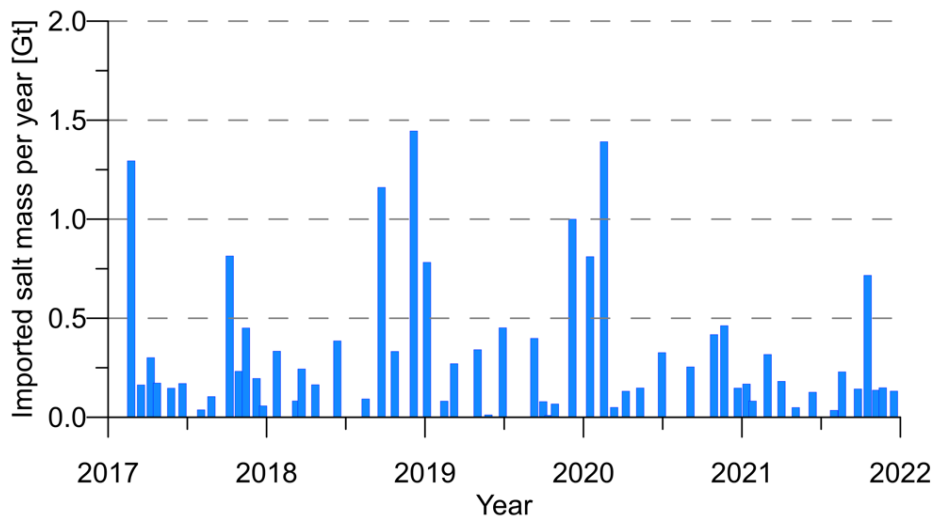
Fig. 8: Inflow activity into the Baltic Sea during 2017-2021 - salt mass import in Gt per event (calculated after MOHRHOLZ 2018).

3.2   Observations at the MARNET monitoring platform "Darss Sill"

The monitoring station at the Darss Sill supplied complete records during the year 2021. The ADCP provided data records for the first nine months of 2021. However, due to some synchronisation issues between the instantaneous online data and the analogue stored data, a data gap exists in the database for the remainder of the year. However, the raw data are recorded and will be soon fed into the database.

As usual, in addition to the automatic oxygen readings taken at the observation mast, comparative measurements of oxygen concentrations were taken at the depths of the station's sensors using the Winkler method (cf. GRASSHOFF et al. 1983) during the regular maintenance cruises. Oxygen readings were corrected accordingly.

3.2.1   Statistical Evaluation

We selected bulk parameters determining the water mass properties at Darss Sill from a statistical analysis based on the temperature and salinity time series at different depths.

To expand first on the larger picture, the year 2021 was globally among the seven warmest on record and experienced a summer of extremes, according to findings reported by the EU's Copernicus Climate Change Service. The report shows that the last seven years globally were the seven warmest on record by a clear margin. Within that time, 2021 ranks among the cooler years, alongside 2015 and 2018. Europe was just 0.1 K above the 1991-2020 average in 2021 but experienced its warmest summer.

Similar to the large-scale temperature trend, the **temperature** recordings of 2021 in the surface waters of Darss Sill were also well above the long-term mean. The yearly mean temperature (Table 4) for the year 2021 of 9.79 °Cwas lower than in 2020 (10.75 °C) and 2018 (10.54 °C). Annual mean surface-layer temperatures for 2021 are ranked in the top ten since 1992 (i.e. in the upper quartile). The standard deviation of the surface layer temperatures reveals average values. The lowest temperature recorded was 1.68 °C (Table 6), close to the mean minimum values.

This can also be seen in Figure 10. Here, we show the anomaly of the near-surface temperature. The climatology was based on the data set of REYNOLDS et al. 2007 and covered the period 1982 to 2011. This period is close to the national reference period (1981-2010). In winter and autumn, the water was up to 1.5 K warmer than the long-term mean. During Spring, the surface waters were close to normal, only interrupted by a cold anomaly in May (which was caused by lower than average air temperature). The summer temperatures were 2 K warmer, only lowered by sporadic upwelling events at Darss Sill during phases with easterly winds (beginning of June, end of July, and in the second week of August).

The mean **salinities** and their standard deviations at the station Darss Sill are given in Table 4. The values of the lowermost two sensors reflect the near-bottom variability in salinity. They are, therefore, a sensitive measure for the overall inflow activity. Unlike 2016 and 2014, both characterised by strong inflow activity, 2021 shows below-average mean salinity and average near-bottom salinity fluctuations. The variability at the 19 m sensors can be ranked below average. The low mean salinity, combined with the low variability, indicates a weak inflow activity in 2021.

Table 4: Annual mean values and standard deviations of temperature (T) and salinity (S) at the Darss Sill. Maxima in boldface.

	7 m Depth		17 m Depth		19 m Depth	
	T	S	T	S	T	S
Year	℃	g/kg	℃	g/kg	℃	g/kg
1992	9.41 ± 5.46	9.58 ± 1.52	9.01 ± 5.04	11.01 ± 2.27	8.90 ± 4.91	11.77 ± 2.63
1993	8.05 ± 4.66	9.58 ± **2.32**	7.70 ± 4.32	11.88 ± 3.14	7.71 ± 4.27	13.36 ± 3.08
1994	8.95 ± 5.76	9.55 ± 2.01	7.94 ± 4.79	13.05 ± 3.48	7.87 ± 4.64	14.16 ± 3.36
1995	9.01 ± 5.57	9.21 ± 1.15	8.50 ± 4.78	10.71 ± 2.27	–	–
1996	7.44 ± 5.44	8.93 ± 1.85	6.86 ± 5.06	13.00 ± 3.28	6.90 ± 5.01	14.50 ± 3.14
1997	9.39 ± 6.23	9.05 ± 1.78	–	12.90 ± 2.96	8.20 ± 4.73	13.87 ± 3.26
1998	8.61 ± 4.63	9.14 ± 1.93	7.99 ± 4.07	11.90 ± 3.01	8.10 ± 3.83	12.80 ± 3.22
1999	8.83 ± 5.28	8.50 ± 1.52	7.96 ± 4.39	12.08 ± **3.97**	7.72 ± 4.22	13.64 ± **4.39**
2000	9.21 ± 4.27	9.40 ± 1.33	8.49 ± 3.82	11.87 ± 2.56	8.44 ± 3.81	13.16 ± 2.58
2001	9.06 ± 5.16	8.62 ± 1.29	8.27 ± 4.06	12.14 ± 3.10	8.22 ± 3.86	13.46 ± 3.06
2002	9.72 ± 5.69	8.93 ± 1.44	9.06 ± 5.08	11.76 ± 3.12	8.89 ± 5.04	13.11 ± 3.05
2003	9.27 ± 5.84	9.21 ± 2.00	7.46 ± 4.96	**14.71** ± 3.80	8.72 ± 5.20	15.74 ± 3.27
2004	8.95 ± 5.05	9.17 ± 1.50	8.36 ± 4.52	12.13 ± 2.92	8.37 ± 4.44	12.90 ± 2.97
2005	9.13 ± 5.01	9.20 ± 1.59	8.60 ± 4.49	12.06 ± 3.06	8.65 ± 4.50	13.21± 3.31
2006	9.47 ± 6.34	8.99 ± 1.54	8.40 ± 5.06	14.26 ± 3.92	9.42 ± 4.71	**16.05** ± 3.75
2007	9.99 ± 4.39	9.30 ± 1.28	9.66 ± 4.10	10.94 ± 1.97	9.63 ± 4.08	11.39 ± 2.00
2008	9.85 ± 5.00	9.53 ± 1.74	9.30 ± 4.60	-	9.19 ± 4.48	-
2009	9.65 ±5.43	9.39 ±1.67	9.38 ±5.09	11.82 ±2.47	9.35 ±5.04	12.77 ±2.52
2010	8.16 ± 5.98	8.61 ± 1.58	7.14 ± 4.82	11.48 ± 3.21	6.92 ± 4.56	13.20 ± 3.31
2011	8.46 ± 5.62	-	7.76 ± 5.18	-	7.69 ± 5.17	-
2012	-	-	-	-	-	-
2013	-	-	-	-	-	-
2014	10.58 ± 5.58	**9.71** ± 2.27	10.01 ± 4.96	13.75 ± 3.53	9.99 ± 4.90	14.91 ± 3.40
2015	-	-	-	-	-	-
2016	10.23 ± 5.63	9.69 ± 1.98	9.27 ± 4.59	14.07 ± 3.53	9.11 ± 4.43	15.56 ± 3.45
2017	9.67 ± 5.05	9.40 ± 1.58	9.23 ± 4.54	11.65 ± 2.50	9.20 ± 4.45	12.39 ± 2.61
2018	10.54 ±**6.62**	8.76 ± 1.16	9.24 ± **5.41**	11.58 ±3.23	9.16 ± **5.27**	12.56 ± 3.56

Year						
2019	10.34 ±5.25	9.57 ± 1.89	9.83 ± 4.65	12.50 ±2.95	9.83 ± 4.50	13.41 ± 3.07
2020	**10.75** ±4.56	9.68 ± 1.59	**10.39** ± 4.25	11.75 ±2.95	**10.28** ± 4.11	12.44 ± 2.59
2021	9.79 ± 5.32	9.23 ± 1.36	9.23 ± 5.01	12.75 ± 2.67	8.97 ± 4.62	13.18 ± 3.02

Table 5: Amplitude (K) and phase (converted into months) of the yearly cycle of temperature measured at the Darss Sill in different depths. Phase corresponds to the time lag between temperature maximum in summer and the end of the year. Maxima in boldface.

	7 m Depth		17 m Depth		19 m Depth	
	Amplitude	Phase	Amplitude	Phase	Amplitude	Phase
Year	K	Month	K	Month	K	Month
1992	7.43	4.65	6.84	4.44	6.66	4.37
1993	6.48	4.79	5.88	**4.54**	5.84	**4.41**
1994	7.87	4.42	6.55	4.06	6.32	4.00
1995	7.46	4.36	6.36	4.12	–	–
1996	7.54	4.17	6.97	3.89	6.96	3.85
1997	8.60	**4.83**	–	–	6.42	3.95
1998	6.39	4.79	5.52	4.46	–	–
1999	7.19	4.52	5.93	4.00	5.70	3.83
2000	5.72	4.50	5.02	4.11	5.09	4.01
2001	6.96	4.46	5.35	4.01	5.11	3.94
2002	7.87	4.53	6.91	4.32	6.80	4.27
2003	8.09	4.56	7.06	4.30	**7.24**	4.19
2004	7.11	4.48	6.01	4.21	5.90	4.18
2005	6.94	4.40	6.23	4.03	6.21	3.93
2006	**8.92**	4.32	7.02	3.80	6.75	3.72
2007	6.01	4.69	5.53	4.40	5.51	4.36
2008	6.84	4.60	6.23	4.31	6.08	4.24
2009	7.55	4.57	7.09	4.37	7.03	4.32
2010	8.20	4.52	6.54	4.20	6.19	4.08
2011	7.70	4.64	6.98	4.21	7.04	4.14
2012	–	–	–	–	–	–
2013	–	–	–	–	–	–
2014	7.72	4.43	6.86	4.17	6.77	4.13

2015	–	–	–	–	–	–
2016	7.79	4.65	6.33	4.33	6.11	4.23
2017	7.00	4.56	6.20	4.31	6.15	4.28
2018	8.82	4.53	**7.31**	4.08	7.18	4.01
2019	7.29	4.47	6.42	4.21	6.22	4.18
2020	6.29	4.36	5.85	4.17	5.66	4.07
2021	7.22	4.37	6.60	4.01	6.38	3.81

We determined the amplitude and phase shift of the annual cycle from a Fourier analysis of the temperature time series at 7 m depth (surface layer) and the two lowermost sensors (17 m and 19 m depth). This method finds the optimal fit of a single Fourier mode (a sinusoidal function) to the data, from which amplitude and phase can easily be inferred as the characteristic parameters of the annual cycle. The results are compiled in Table 5.

Like the elevated mean temperatures and lower than average variability in 2021 discussed above, Table 5 shows that the annual cycle amplitudes at different depths vary around the long-term average. Thus, 2021 was characterised by a high mean temperature but a weak yearly cycle. Compared to the pronounced phase lag of approximately 0.5 months between the surface and near-bottom temperatures in 2021, the near-bottom water temperature closely follows the onset of surface warming. The near-bottom temperature at 19 m depth also shows an average annual cycle.

Table 6: Listing of the minimum and maximum temperature measured at 7 m water depth at Darss Sill (based on daily mean values). Time indicates the date of occurrence. The column Range provides the difference between the minimum and maximum temperature. Minima and maxima are highlighted in boldface. For the event of the annual maximum, we indicated in boldface the first-ever recording.

	Minimum		Maximum		
	Temperature	Time	Temperature	Time	Range
Year	°C		°C		°C
1995	0.98	30.12	20.54	05.08	19.56
1996	0.37	27.01	17.65	09.08	17.28
1997	0.16	21.01	22.50	19.08	22.34
1998	2.59	16.12	16.61	10.08	14.02
1999	1.55	18.02	19.84	31.07	18.29
2000	2.65	25.01	17.87	14.08	15.22
2001	2.33	28.03	20.65	29.07	18.32

2002	2.03	13.01	20.24	30.08	18.21
2003	0.09	11.01	21.92	13.08	21.83
2004	1.45	28.02	19.11	20.08	17.66
2005	1.50	13.03	19.79	13.07	18.29
2006	0.40	30.01	22.80	21.07	**22.40**
2007	3.36	25.02	18.70	14.08	15.34
2008	3.12	17.02	19.67	29.07	16.55
2009	1.65	25.02	19.62	10.08	17.97
2010	**-0.44**	05.02	20.33	21.07	20.77
2011	-0.12	05.01	17.94	12.07	18.06
2012	–	–	–	–	-
2013	–	–	–	–	
2014	1.54	09.02	21.61	09.08	20.07
2015	2.95	04.02	18.14	13.08	15.19
2016	1.81	23.01	20.42	28.07	18.61
2017	2.09	19.02	18.61	30.08	16.52
2018	1.11	18.03	**23.10**	04.08	21.99
2019	2.82	26.01	20.91	01.09	18.09
2020	4.74	07.01	19.51	22.08	14.77
2021	1.68	17.02	20.74	28.07	19.07

We evaluated the minimum and maximum temperatures recorded at 7 m water depth at Darss Sill to provide a final statistical measure. Table 6 indicates that we recorded 2021 as an average winter. The winter minimum temperature was 1.68 °C. As shown in Fig. 10, the winter was nearly 2 K too warm. The maximum value, recorded on 1st September, was 20.74 °C, ranked as the sixth-highest value. Additionally, the temperature range in 2021 was close to the long-term mean due to the warm winter and autumn.

3.2.2 Temporal development at Darss Sill

Fig. 9 shows the development of water temperature and salinity in 2021 in the surface layer (7 m depth) and the near-bottom region (19 m depth). As in previous years, the currents observed by the bottom-mounted ADCP in the surface and bottom layers were integrated in time to emphasise the low-frequency baroclinic (depth-variable) component, plotted in Fig. 11 as a 'progressive vector diagram' (pseudo-trajectory). This integrated view of the velocity data filters short-term fluctuations and identifies long-term phenomena such as inflow and outflow events. According

to this definition, the average current velocity corresponds to the slope of the curves shown in Fig. 11, using the convention that positive slopes reflect inflow events.

The year 2021 started with the aftermath of a marine heat wave, which started end of September 2020. Thus, water temperatures were higher than usual. Besides the high water temperatures, stratification in temperature and salinity was low, as indicated by the salinity stratification index G (MATTHÄUS & FRANK 1992), as shown in the lower panel of Fig. 9. Until June, salinity and stratification remained low, only interrupted by minor spill-over inflows. With the start of June, the wind speed dropped from 8 m/s in May to 5 m/s. The reduced wind mixing led to the development of thermal stratification, accompanied by an increase in salinity stratification. The rise in bottom salinity to 17 g/kg indicates some baroclinic inflow activity. The baroclinic inflow activity is also supported by the ADCP data, showing a pronounced two-layer flow structure. (Fig. 11). The two-layer flow leads to a decoupling of well-oxygenised surface waters from the stagnant bottom waters. End of July, the near-bottom oxygen saturation dropped to 55% (Fig. 12). During this time, thermal stratification reached a maximum temperature difference between the surface and bottom of 9 K and a salinity difference of 7 g/kg. At the beginning of August, winds of up to 15 m/s homogenised the water column at Darss Sill. They removed any stratification in temperature and salinity (Fig. 9). The stratification measure (Fig. 9 lower panel) was close to zero, indicating the lack of stratification.

In the second week of August, the wind turned to easterly directions and reached values of 12 m/s. During the following week, the surface temperature at Darss Sill dropped by 5 K. At the same time, the oxygen saturation fell below 35%. The change in water mass property was caused by an upwelling event, bringing colder, low-oxygen waters from the western Arkona Basin to Darss Sill.

Mid August, the wind turned again to westerly directions and calmed to 5 m/s. The decaying winds resulted in reduced vertical mixing and thus in a build-up of stratification in salinity due to the onset of weak baroclinic inflow activity. The warm inflow waters also resulted in a nearly homogenous vertical distribution in temperature during this period. Bottom salinity values reached again 17 g/kg. Intermittent baroclinic inflow activity characterized most of the month of September until gradually collapsing towards end of the month (Fig. 6). Then, the oxygen saturation reached an annual low of 30%. With the arrival of the first autumn storm (23.9. storm TIM) and peak wind speeds of 130 km/h at Dornbusch (Hiddensee), the stratification collapsed. The vertical mixing of the water column caused a recovery of oxygen saturation to nearly 90%.
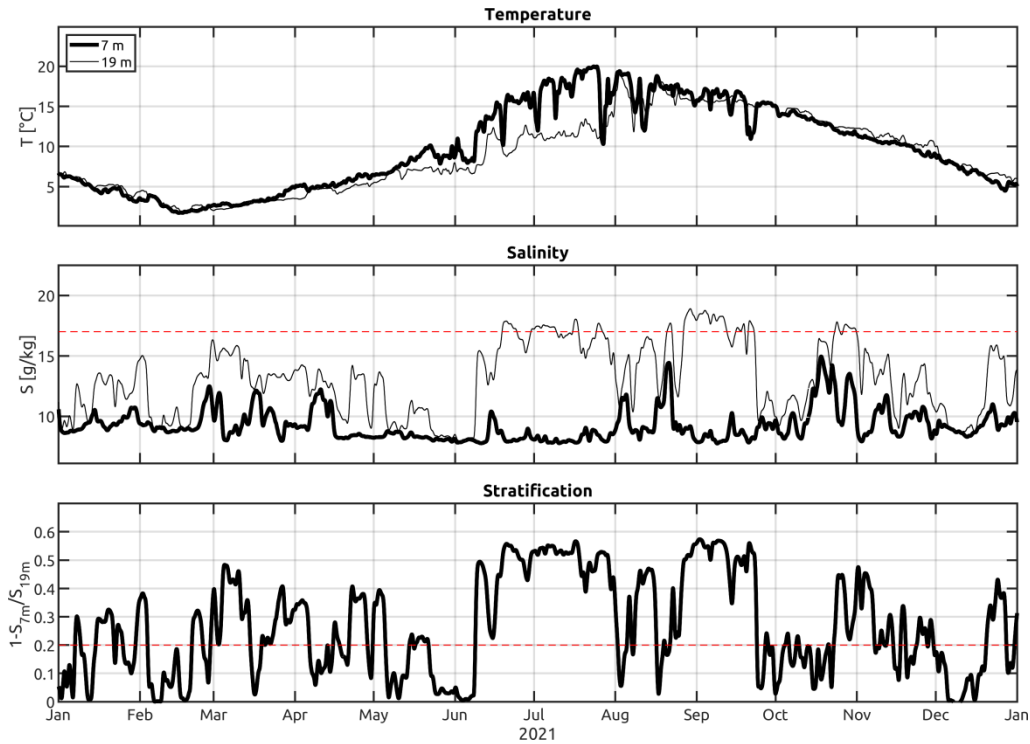
Fig. 9: Water temperature (upper panel) and salinity (middle panel) measured in the surface layer and the near-bottom layer at Darss Sill in 2021. The red dashed line indicates the salinity threshold of 17 g/kg. According to Matthäus & Frank (1992), we show a G stratification in the lower panel. Here the red dashed line marks the stratification threshold of 0.2.
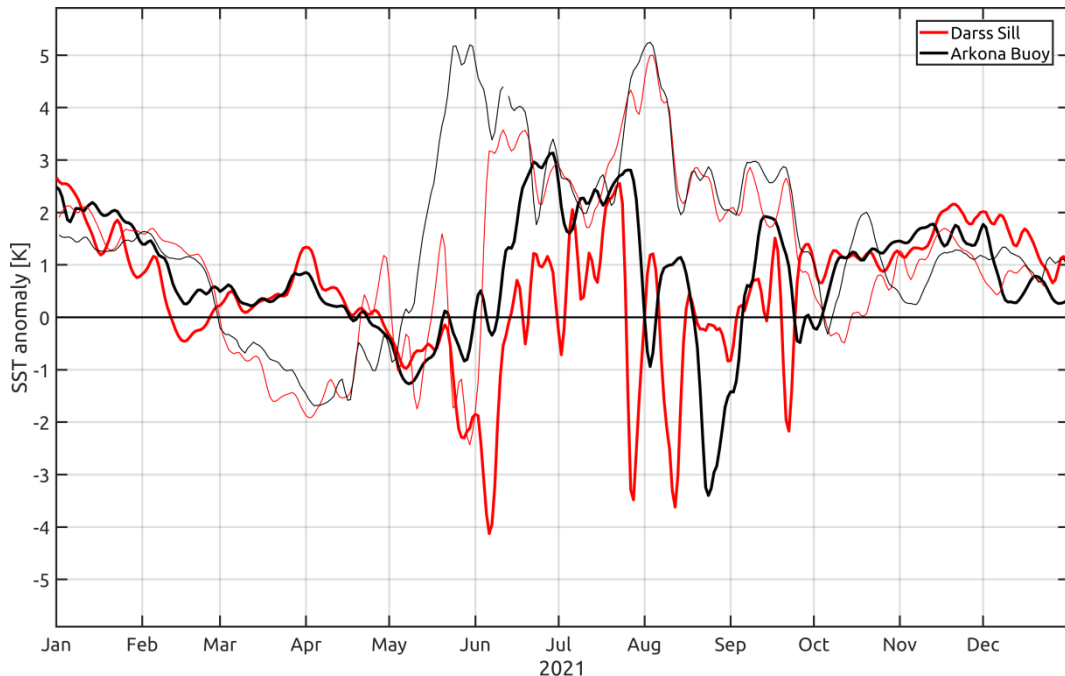

Fig. 10: Deviation of near-surface temperature from the climatology at Darss Sill and Arkona Buoy in 2021. The climatology was built for the national reference period 1982-2011 and is based on REYNOLDS et al., 2007. The thin lines show the anomaly from 2018.

The remaining part of the year was characterized by oxygen concentrations close to saturation throughout the water column (Fig. 12) due to both increased vertical mixing and two baroclinic inflow events in October and December (Fig. 6a). During the stronger event in October, a low-pressure system (storm HENDRIK), with wind speeds of 20 m/s, caused a barotropic inflow and thus elevated bottom salinity at Darss sill in combination with low stratification (G < 0.2, Fig. 9).
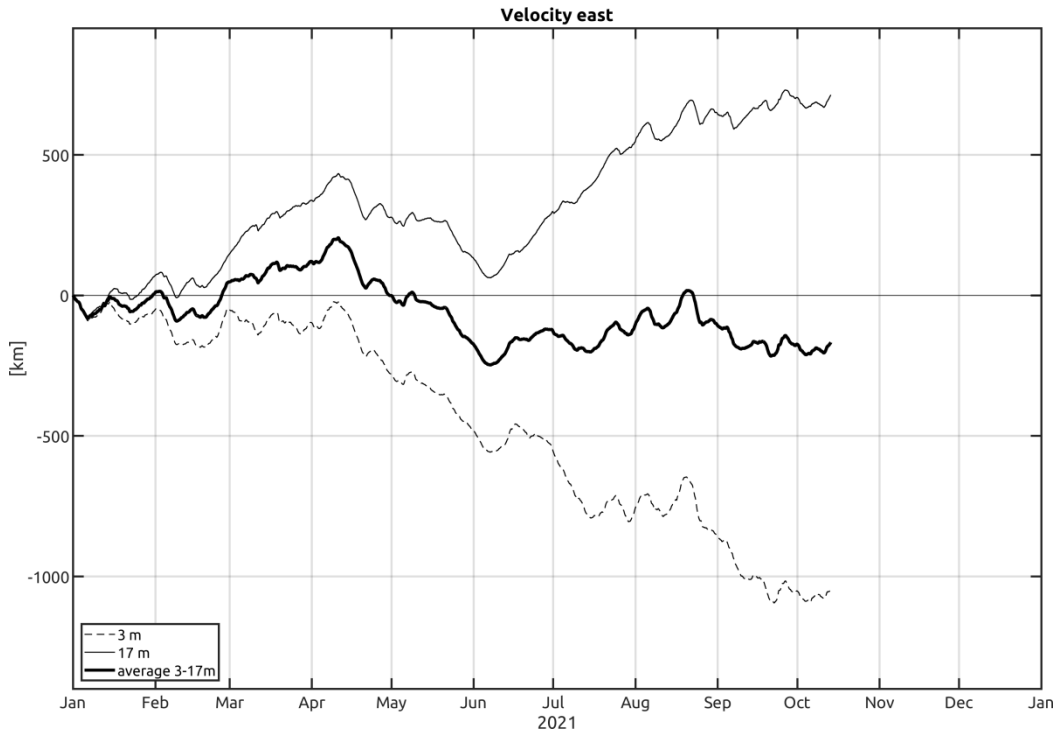

Fig. 11: East component of the progressive vector diagrams of the current in 3 m depth (dashed line), the vertical averaged current (thick line), and the currents in 17 m depth (solid line) at the Darss Sill in 2021.
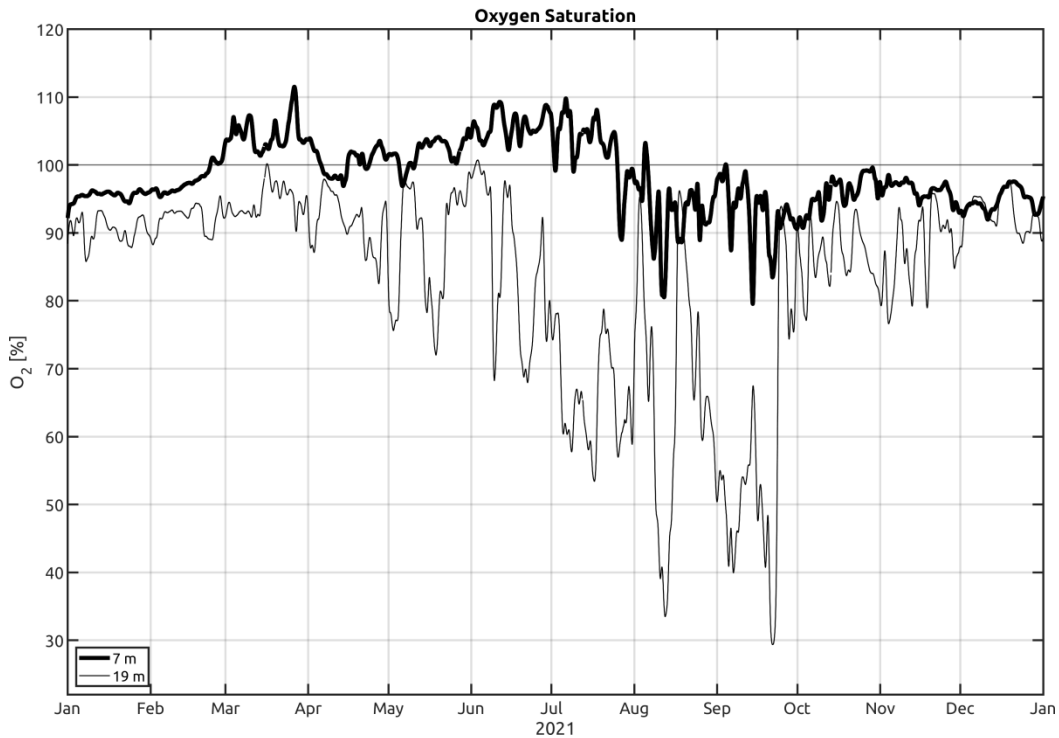
Fig. 12: Oxygen saturation measured in the surface and bottom layer at the Darss Sill in 2021.

3.3 Observations at the MARNET monitoring buoy "Arkona Basin"

3.3.1 Temporal development until summer

The Arkona Basin monitoring station (AB) described in this chapter is located almost 20 nm northeast of Arkona at 46 m water depth. The monitoring station in the Arkona Basin supplied complete records during the year 2021. As described in chapter 3.2, the optode-based oxygen measurements at the monitoring station were corrected with the help of the Winkler method, using water samples collected and analysed during the regular MARNET maintenance cruises. Due to some ongoing data synchronisation issues, oxygen and salinity data for November and December are still missing.

Fig. 13 shows the time series of water temperature and salinity at depths of 7 m and 40 m, representing the surface and bottom layer properties. As in the previous chapter, the corresponding oxygen concentrations plotted as saturation values are shown in Fig. 14.

Similar to the measurements at the Darss Sill and station AB, the first three months of the year were characterised by an abnormal warm surface layer (see also Fig. 10). The lowest daily mean temperatures of the year, approximately 2.45 °C, were reached on 24.02. (Fig. 13), about 0.3 K lower than the minimum temperatures measured 27 days earlier at the Darss Sill. While the local atmospheric fluxes largely determine the surface temperatures in the Arkona Basin, those at the Darss Sill are more strongly affected by lateral advection, which may explain the observed differences.
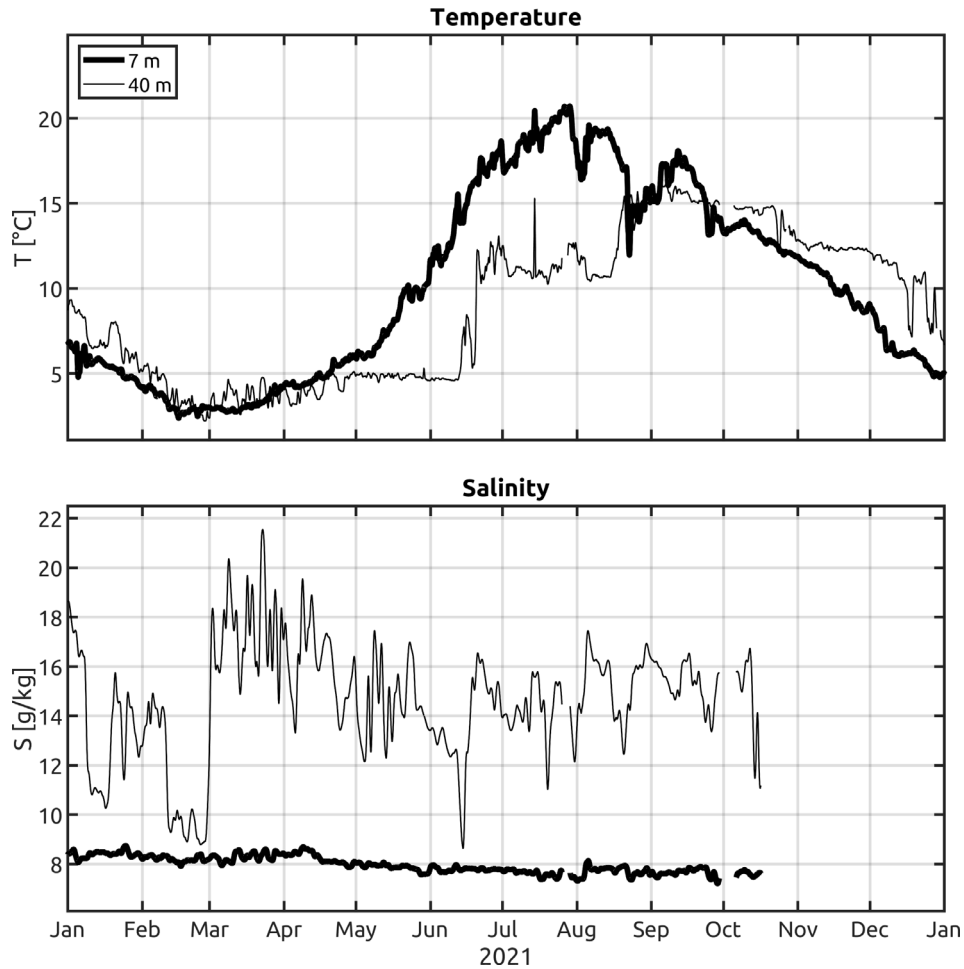
Fig. 13: Water temperature (above) and salinity (below) measured in the surface layer and near-bottom layer at the station AB in the Arkona Basin in 2021.

The water mass properties in the bottom layer during the first two weeks of 2021 were determined by the aftermath of small inflow events that occurred at the end of December 2020. Peak salinities in the bottom waters reached 18 g/kg. Since the maximum salinities at Darss Sill were reaching 17 g/kg, by the end of 2020, the water masses must originate from Drogden Sill. The declining bottom temperature indicates that the near-bottom region was not fully decoupled from direct atmospheric cooling. The slowly decaying salinities, interrupted by salinity spikes, indicate the draining of the bottom pool through the Bornholm Channel (Fig. 14) and some refilling through Drogden Sill. The oxygen demand due to respiration is usually small during this time of the year due to low water temperatures. Therefore, oxygen concentrations did not fall below approximately 80% of the saturation threshold (Fig. 14).

From March, the bottom salinity increased to values above 18 g/kg. Since the bottom salinity at Darss Sill did not exceed 16 g/kg (Fig. 9), those salty water masses must have originated from Drogden Sill. The high oxygen saturation levels of 90% (Fig. 14) support this. Thus well-oxygenised, salty water masses arrived in the Arkona Basin and moved slowly toward the Bornholm Basin. Until June, the renewal of the bottom pool slowly faded off. At the same time, the oxygen saturation also declined to 70%. The nearly constant bottom temperature of 5 °C indicates a virtually stagnant bottom pool.

With the establishment of the two-layer exchange flow at Darss Sill and the baroclinic inflow activity from mid-June, the bottom temperature increased by 6 K. In contrast, no clear signal in the salinity measurements was visible. Since the baroclinic inflows at Darss Sill were already decoupled from the surface, the oxygen saturation at Arkona Buoy further declined.

At the beginning of August, the surface temperature at the buoy transiently dropped by 5 K within a few days, quickly recovering afterwards. As the western Baltic Sea was forced by pulses of strong westerly winds during this period (Fig. 4), it is likely that the observed surface temperature drop was caused by the arrival of cold upwelled water from the Swedish coast. This is supported by oxygen saturations, which dropped from oversaturation (105%) to values of 98%. Starting around 12th August, the signals of a second, stronger and more lasting upwelling event hit the western Baltic Sea and were detectable at the Arkona Basin (Fig. 13). This event will be discussed in more detail and compared to model simulations in Section 3.3.2 below to clarify the mechanisms.

From mid of September on, the surface water cooled rapidly. Within two weeks, the near-surface temperature decreased by approx. 8 K. In the deeper layers, the most important was a strong and rapid increase of the near-bottom oxygen concentrations starting in the second week of October. Within three days, the near-bottom oxygen saturation recovered from 50% to nearly 90% (Fig. 14). As the water column remained stratified during this period (Fig. 12), we attribute this event to the intrusion of oxic inflow waters that were observed at the Darss Sill already end of September (Fig. 12).

Different from the gradual decrease of the surface temperatures in November and December (Fig. 13) that reflect the gradual loss of heat to the atmosphere, deep-water cooling was largely controlled by short events. It is likely that these events mirror the arrival of cooler inflow waters from the Darss Sill. Salinity measurements required to substantiate this hypothesis are unfortunately lacking for the lasts months of the year.
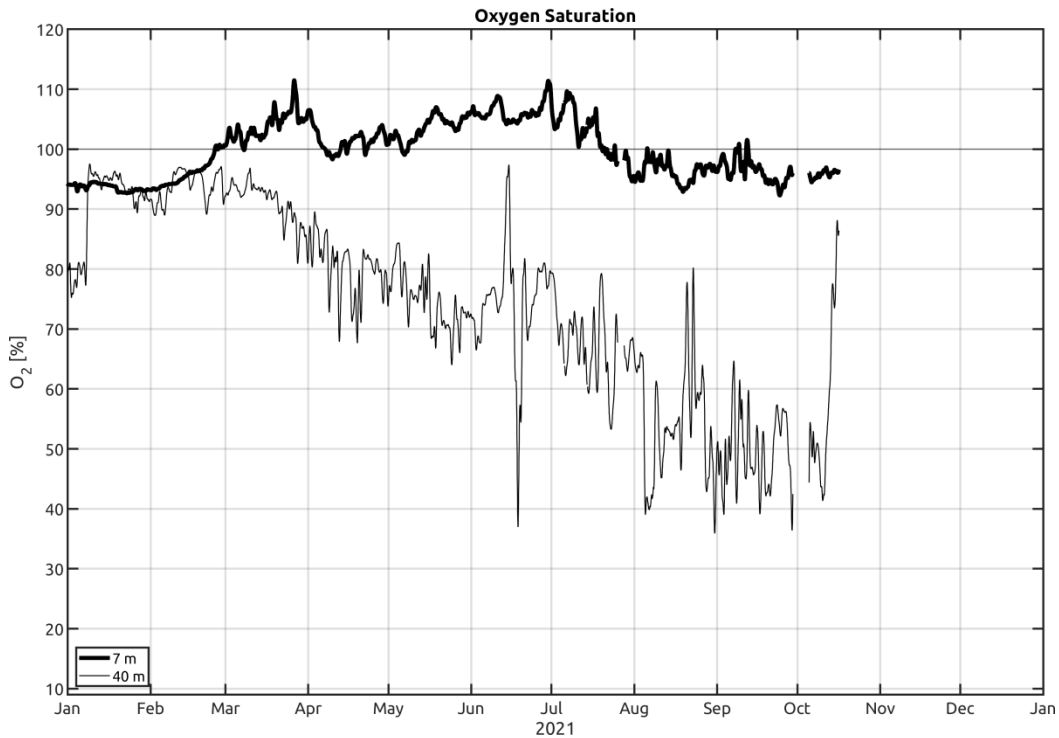
Fig. 14: Oxygen saturation measured in the surface and bottom layer at the station AB in the Arkona Basin in 2021.

3.3.2 An upwelling event

Fig. 13 shows a remarkable cooling event in the surface layer at the Arkona Buoy with temperatures decaying from values around 19°C mid of August to approximately 12°C within a week, accompanied by a steady increase in surface salinities. This cooling event is followed by gradual recovery with increasing temperatures and decreasing salinities until approximately the second week of September. The general tendency of westerly winds with a strong peak around mid of August, and the subsequent switching to easterly winds in the last week of August and beginning of September suggest that an upwelling cell developing on the Swedish coast might have affected the measurements at the Arkona Buoy.

To substantiate this hypothesis, we analysed the results of a realistic numerical model with 600 m spatial resolution (GRÄWE et al. 2015). A snapshot of the surface temperature is shown in Fig. 15. Here, we present the conditions on 18th August, a few days after the peak of the westerly wind event. Although the model underestimates the total extent of the upwelling cell, one can see that large parts of the southern Swedish coast from Falsterbo up to Öland were affected by this event. Upwelling filaments, generated along the coast of Ystad, were advected far south into the cetner of the Arkona Basin. Therefore, while none of the individual upwelling filaments reached the position of the Arkona Buoy in these simulations, it seems plausible that the upwelled waters from the Swedish coast affected the measurements at this MARNET station in reality. In the simulations, the upwelling lasted from the 12th August until the 24th August, consistent with the temporal evolution of the surface temperature in Fig. 13.
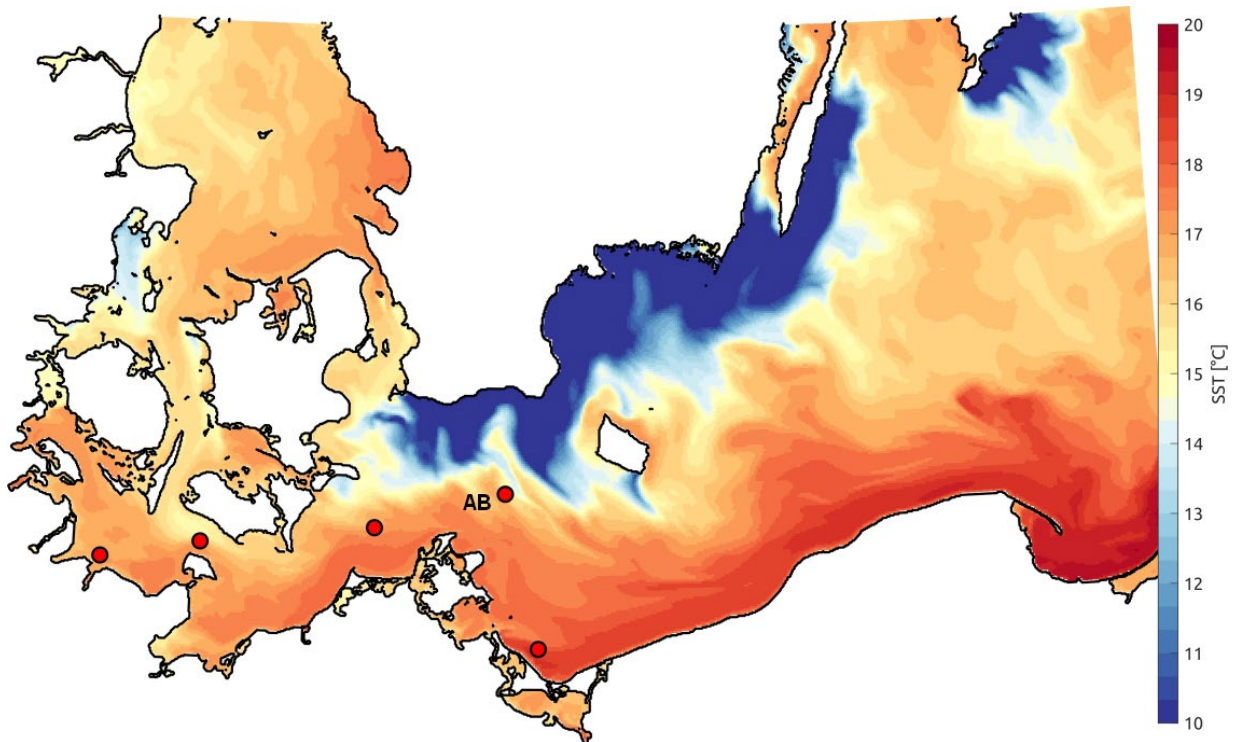
Fig. 15: Modelled sea surface temperature on 18th August in the western Baltic Sea. The red dots mark the location of the MARNET stations (AB = Arkona Buoy).

3.4 Observations at the MARNET monitoring buoy "Oder Bank"

The water mass distribution and circulation in the Pomeranian Bight have been investigated in the past as part of the TRUMP project (*TR*ansport und *UM*satzprozesse in der *P*ommerschen Bucht) (v. BODUNGEN et al. 1995; TRUMP 1998), and were described in detail by SIEGEL et al. (1996), MOHRHOLZ (1998) and LASS et al. (2001). For westerly winds, well-mixed water is observed in the Pomeranian Bight, with a small amount of surface water from the Arkona Basin mixed with it. For easterly winds, water from the Oder Lagoon flows via the rivers Świna and Peenestrom into the Pomeranian Bight, where it stratifies on top of the bay water off the coast of Usedom. As shown below, these processes influence primary production and vertical oxygen structure in the Pomeranian Bight.

The Oder Bank monitoring station (OB) is located approximately five nautical miles northeast of Koserow/Usedom at a water depth of 15 m, recording temperature, salinity, and oxygen at depths of 3 m and 12 m. The oxygen measurements were validated with the help of water samples taken during the regular maintenance cruises using the Winkler method. After the winter break, the monitoring station OB was returned to service early in the year, on 14th March 2021. From that date, the station provided continuous time series of all parameters until 4th December, when it was again demobilised to avoid damage from floating ice.

Temperatures and salinity at OB are plotted in Fig. 16; associated oxygen readings are presented in Fig. 17. Similar to the other MARNET stations, the maximum temperatures that were reached during the summer period were lower than in 2018 (the maximum temperature at OB was 24.8 °C) but comparable with the years 2010, 2013, and 2014, when temperatures of up to 23 °C were

observed at station OB. In 2021, the maximum hourly mean temperature reached on 16th July was 22.6 °C, similar to 2020 (22.6 °C). As in the previous years, surface temperatures at the monitoring station OB were significantly higher compared to those at the deeper and more energetic stations in the Arkona Basin and the Darss Sill (see Fig. 9 and Fig. 14), reflecting the shallower and more protected location of this station.

On average years, there is also a dynamic reason for the more substantial warming of the surface layer at station OB, related to the suppression of vertical mixing due to the transport of less saline (i.e., less dense) waters from the Oder Lagoon on top of the more salty bottom waters (e.g. LASS et al. 2001). However, in 2021 the precipitation over most of the Oder catchment was like in the previous years: lower than the long-term mean. The missing rain leads to lower water levels in the Oder until late autumn. Thus, the impact of the Oder plume in the Pomeranian Bight was of less dynamic importance than in average years.
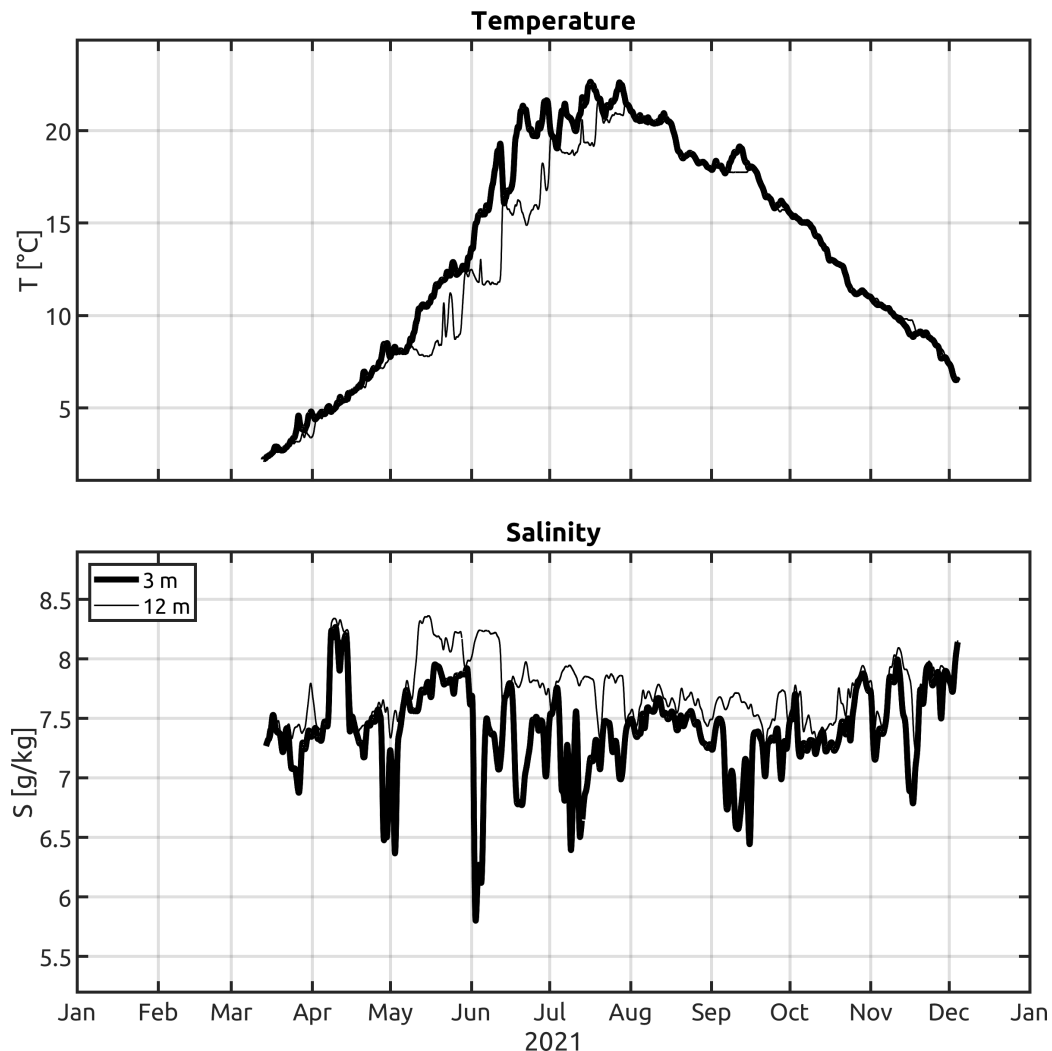

Fig. 16: Water temperature (above) and salinity (below) measured in the surface layer and near-bottom layer at the station OB in the Pomeranian Bight in 2021.

After the start of service in March, the water column was well mixed in salinity and temperature. At the beginning of May, a temperature and haline stratification developed. The temperature difference between the surface and bottom layers varied around 4 K and 0.5 g/kg in salinity. During June, peak values of 5 K were reached.

The upwelling along the Swedish Coast (see Sec. 3.2.3), caused by prolonged westerly winds during August, had only little consequence for the Pomeranian Bight. At first, thermal stratification was weak at Oder Bank. Secondly, the station is too far away from the Swedish coast to be affected by the upwelled waters. This is supported by the model results shown in Fig. 13.

From an ecological perspective, the most important consequence of the build-up of stratification and the suppression of turbulent mixing from May on was the decrease in near-bottom oxygen concentrations due to the decoupling of the bottom layer from direct atmospheric ventilation. Their impact on the oxygen budget of the Pomeranian Bight becomes evident in Fig. 17, showing oxygen concentrations at depths of 3 m and 12 m. For June and July, a distinct correlation between increasing oxygen saturation in the surface layer and a decrease in the near-bottom layer, reflecting the effects of primary production and the oxygen demand from remineralisation, respectively.

The lowest near-bottom oxygen concentrations (see Fig. 17) in 2021 were observed at the end of June, with hourly saturation values as low as 40%. With the onset of a slow atmospheric cooling and some stronger winds, the thermal stratification vanished, and near-bottom oxygen levels recovered to 95% saturation.
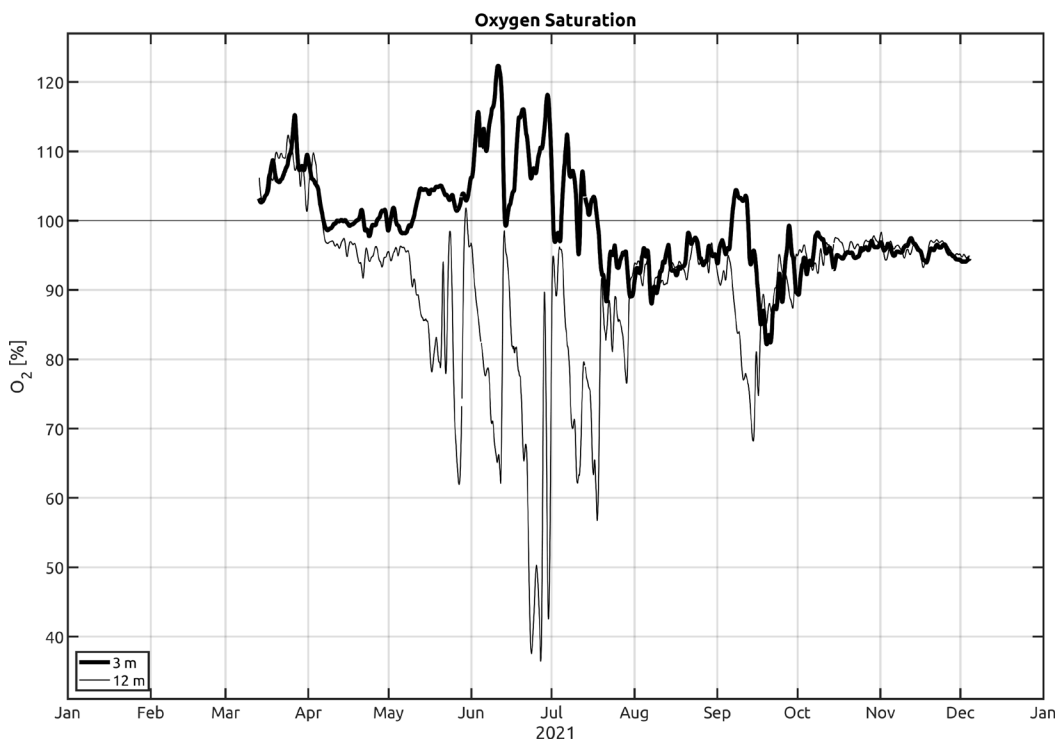
Fig. 17: Oxygen saturation measured in the surface and bottom layer at the station OB in the Pomeranian Bight in 2021.

Finally, it is worth noting that the increase in the primary production of biomass in the Oder Lagoon, induced by the lateral transport of lagoon water to station OB, is likely to have resulted in the super-saturated oxygen concentrations that were observed in the surface layer during all of the above events (Fig. 17). The highest near-surface oxygen concentrations, approximately 20% above the saturation level, were found in June. In addition, the lagoon water is known to export high nutrient concentrations toward the station. This may have resulted in locally increased production rates, which in turn may explain the increased oxygen concentrations in the surface layer. The correlation between the oxygen increase in the surface layer and the decrease in the near-bottom layer points to increased oxygen consumption rates induced by the decay of freshly deposited biomass ("fluff").

4 Results of the routine monitoring cruises: Hydrographic and hydrochemical conditions along the thalweg

The routine monitoring cruises carried out by IOW provide the basic data for the assessments of hydrographic conditions in the western and central Baltic Sea. In 2021, monitoring cruises were performed in February, March, May, July and November. Snapshots of the temperature distribution along the Baltic thalweg transect obtained during each cruise are depicted in Fig. 18 - Fig. 19. This data set is complemented by monthly observations at central stations in each of the Baltic basins carried out by Sweden's SMHI (SMHI 2022). Additionally, continuous time series data are collected in the eastern Gotland Basin. Here the IOW operates two long-term moorings that monitor the hydrographic conditions in the deep water layer. The results of these observations are given in Fig. 20 and Fig. 23.

4.1 Water temperature

The sea surface temperature (SST) of the Baltic Sea is mainly determined by local heat flux between the sea surface and the atmosphere. In contrast, the temperature signal below the halocline is detached from the surface and the intermediate winter water layer and reflects the lateral heat flows due to salt-water inflows from the North Sea and diapycnal mixing. The temperature of the intermediate winter water layer conserves the late winter surface conditions of the Baltic till the early autumn, when the surface cooling leads to deeper mixing of the upper layer.

In the central Baltic, the development of vertical temperature distribution above the halocline follows with some delay the annual cycle of atmospheric temperature. As in the previous years the winter of 2020/2021 was warmer than during the 30-years reference period 1961-1990. However, it was significantly cooler than the previous winter 2019/2020. The January, February and March 2021 depicted moderate positive temperature anomalies of about 1 K. Thus the surface cooling of the Baltic was reduced. The sea surface temperatures remained above the density maximum, except in the Gulf of Bothnia and the Gulf of Finland.

During April and May the mean air temperature was considerably cooler (-1 K) than the long term mean. The most extreme air temperature anomalies were observed in June 2021 with more than 3 K above the reference value. The air temperatures remained at a higher than normal level for the rest of the year. From July to December 2021, the monthly air temperature anomaly ranged between +0.5 and +2.0 K. Only the month of August was close the long term mean. The deep-water conditions in the central Baltic in 2021 were stagnant. The temperature in deep water was established by subsequent minor inflow events of 2016 to 2020 (MOHRHOLZ 2018).

The mean air temperature in January 2021 was about 1 °K above the long term mean. Thus, at the beginning of February also the sea surface temperature (SST) in the Baltic was relatively high with 3.5 °C to 5 °C. The lowest surface temperature was observed in the Belt Sea and at the Darss Sill with 3.5 °C to 4.0 °C. This exceeded the climatological mean of 1.8 °C by 2 K, but was 1 K below the extreme temperatures of February of 2020. At the central station of the Arkona Basin (TF0113) the SST of about 4.6 °C (climatological mean 1.9 °C) was considerably higher than in the Belt Sea. As in the previous years the surface temperatures were well above the density

maximum in the entire western and central Baltic. Therefore the temperature driven convection was still ongoing, and no shallow temperature stratification was observed in the beginning of February. The upper layer was homogenized and no remains of former winter water layer were found. Due to the high SST only a weak temperature gradient between the surface and halocline layer was observed. At station TF271 in the eastern Gotland Basin the thermocline was at about 54 m depth, slightly above the permanent halocline (61 m). The temperature increased in the upper layer from 5.02 °C at 2 m depth to 5.09 °C at 51 m depth. The surface temperatures in the central Baltic ranged between 4.95 °C and 5.4 °C. This range was similar to February 2020 and again about 3 K above the long term average. Together with the extreme warm temperatures in February 2016 and 2018 the series of warm winters is continued.

The temperature distribution below the halocline is governed by the inflow of saline water from the North Sea. In the second half of 2020 only very weak inflows occurred. Between October and December 2020 three of these inflows carried in total 55 km³ of warm saline water into the western Baltic. In February 2021 the bottom layer in the Arkona Basin was still partly covered by this warm water, forming a thin bottom layer in the eastern part of the Arkona Basin. Here the bottom temperature was about 6.8 °C. The major part of the warm autumn inflows covered the upper halocline of the Bornholm Basin and the Slupsk Furrow. The lower part of the halocline and the deeper layers were still covered by warmer water from the barocline summer inflows of 2020. The maximum temperature in the halocline of the Bornholm Basin was about 10.0 °C. Below 65 m depth the temperature decreased towards the bottom to about 9.1 °C. Parts of warm summer water were shifted eastward into the Slupsk channel and further into the eastern Gotland Basin. This water covered the bottom layer in the Slupsk Furrow (bottom water temperatures of 9 °C to 10°C). Between the eastern outlet of the Slupsk Furrow and the entrance of the eastern Gotland Basin another warm water plume was observed in the bottom layer. This plume spreads eastward and will be sandwiched into the permanent halocline in the Gotland Basin at depths of 110 to 120 m. The deep water in the Gotland Basin was slightly warmer than the halocline water above and the bottom water below. The warmer core of the deep-water layer was found at about 130 m to 140 m depth with a maximum temperature of 7.3 °C. The bottom temperature at station TF 0271 was 7.2 °C. The same value was observed also in February 2020. The bottom water temperature in the Farö Deep was increased by 0.05 K to 7.25 °C, due to the inflow of upper deep water from the eastern Gotland Basin.

In the end of March the higher than normal air temperatures during the winter month caused only a moderate surface cooling compared to temperatures observed in January. In the western Baltic the surface temperatures ranged between to 3.6 °C in the Fehmarn Belt and 3.0 °C in the Arkona basin, which was about 1 K above the climatological mean. Thus, the surface temperature of the western Baltic was still above the temperature of density maximum. At the central station of the Bornholm TF213 the SST was 3.5 °C. The SST decreased further to the east and reached 3.3 °C in the eastern Gotland basin, 3.0 °C in the Farö Deep, and 2.5 °C in the northern Gotland Basin.

In the western Baltic the eastward advection of saline water from minor inflows control the temperature distribution below the surface mixed layer. The thin warmer water layer at the bottom of the Arkona Basin nearly vanished. The deeper layers at the Darss Sill and the Arkona Basin are covered with cold water from winter inflows. The minimum temperature in the central Arkona Basin was 2.6 °C at 28 m depth. In the Bornholm Basin a rather patchy temperature

distribution was observed below the thermocline, which was found at about 50 m depth. Here the different inflow waters of autumn and winter cause strong horizontal temperature gradients. The bottom water temperature in the Bornholm basin was 9.05 °C, still at the level of February. A part of the cooler water from the upper halocline water crossed the Slupsk Sill and formed the new cooler bottom water layer in the Slupsk Furrow. Here the bottom water temperature decreased significantly to 6.2 °C to 7.4 °C. The warm inflow water patch that was observed in February at the entrance of the eastern Gotland Basin has moved further to the north and reached the eastern Gotland basin. The bottom temperature at station TF 0271 (Gotland Deep) and in the Farö Deep did not change significantly and were still at 7.2 °C and 7.25 °C respectively.

The cooler than normal air temperatures in April and May 2021 hampered the seasonal warming of the surface layer in spring. In the first half of May the surface temperatures varied between 8.4 °C in the Kiel Bight, 6.0 °C in the Arkona Basin, and 5.3 °C in the eastern Gotland Basin. This was 1 K to 2 K below the climatological mean values for May, but 2 K to 3 K lower than in the previous year. In the western Baltic a strong gradient was observed in SST from west to east, whereas the temperature distribution was more uniform in the Baltic Proper. In the Belt Sea the onset of the seasonal thermal stratification has started, in contrast to a still weak vertical temperature gradient in the western and central Baltic. In the Arkona Basin the thermocline depth was found at 33 m. Towards the eastern Gotland basin the thermocline depth decreased to about 40 m. Below the thermocline the winter water layer was well pronounced even in the western Baltic. In the Bornholm Basin the core temperature of winter was 4.1 °C. It decreased slightly to 3.7 °C in the eastern Gotland Basin. In the Slupsk Furrow winter water layer was somewhat warmer with 4.2 °C.

Below the intermediate layer the temperatures increase with depth. In the halocline of the Bornholm Basin the remains of the warm inflow waters from autumn 2020 were mixed up with the colder water from winter inflows. The bottom water temperature in the Bornholm Basin decreased between March and May by 0.5 K to 8.5 °C. In the Slupsk Furrow the deep-water conditions did not change significantly. Here the bottom water temperature was about 7.9 °C. At the eastern sill of the Slupsk Furrow an overflow of warm deep water towards the Gotland basin is visible. The warm water patch observed in the southern Gotland basin in March was mostly mixed up in the upper deep-water layer of the Gotland basin. Only a small patch of about 8 °C water was detected at the rim of the basin. There was no significant change observed in the deep water and bottom water layer of the eastern Gotland Basin. The maximum temperature of deep water (7.5 °C) was found at 105 m, due to the small warm intrusions. The bottom water temperature was found unchanged at 7.2 °C. This indicates that none of the inflowing warm plumes was dense enough to reach the bottom of the basin. The bottom water temperature in the Farö Deep was 7.24 °C.

The next cruise of the long-term observation program was conducted in the second half of July. After the cooler than normal spring the air temperature in June and July was well above the climatological mean. Especially the June was extremely warm. Thus, also the surface temperature in the Baltic has increased more than normal, and reached its annual maximum during the time of the cruise. A very strong summer thermal stratification was developed throughout the Baltic Sea. The seasonal thermocline, which separated the warm layer of surface water from the cooler intermediate water, was found at relatively shallow depths between 12 m and 18 m. The surface

temperatures in the Arkona Basin reached 20.0 °C in a surface layer of 12 m to 15 m thickness. Below this warm surface layer a cool layer of former winter water was still present, with a minimum temperature of 7.2 °C. The bottom layer in the Arkona basin was covered with warmer waters from barocline inflows, which led to an increase in bottom temperature to 11.4 °C. At station TF213 in the Bornholm Basin an SST of 20.9 °C was recorded, which was close to the SST of the extreme warm July 2018. The thermocline in the Bornholm Basin was located at 18 m depth. In the eastern Gotland Basin a SST 21.7 °C was observed in a very thin surface layer of 12 m thickness at station TF271. For this location the climatological mean value for July is 16.0 °C. Generally, in the central Baltic the SST was extremely high, but it did not reach the temperatures observed in July 2018, when a SST of 23.9 °C was recorded in the eastern Gotland Basin.

Despite of the high SSTs throughout the Baltic, below the thermocline a relatively strong winter water layer was present. Minimum temperatures in this intermediate water layer were about 4.0 °C in the eastern Gotland Basin, and 4.0 °C in the northern Gotland Basin, which caused a strong vertical temperature gradient between 15 m and 30 m. In the Bornholm Basin and the Slupsk Furrow the winter water layer was slightly warmer with core temperatures of about 4.8 °C. During calm summer conditions baroclinic inflow events are frequently observed, which transport warm saline water into the Arkona Basin. This water mass filled the bottom layer in the entire Arkona Basin, with warm water of 11.4 °C. This water body has partly passed the Bornholmgat, and is sandwiched in the halocline of the western Bornholm Basin. This plume depicted a core temperature of 10.2 °C at 58 m depth. The bottom water in the basin was still covered with water from the autumn/winter inflows of the previous year. In contrast the Slupsk Furrow was completely flushed with cool winter water from the central Baltic. As in May the deep water conditions in the central Baltic remain mainly unchanged. The bottom temperature in the eastern Gotland Basin was still at 7.2 °C. The weak diapycnal mixing in the Basin smoothed the vertical temperature gradients in the deep water layer near the former warm core of inflow water.

In November 2021 a number of planned stations in the central Baltic could not be performed due to bad weather conditions. The general temperature distribution during that cruise depicted the autumnal cooling and the erosion of the seasonal thermocline in the surface layer. Since the autumn months were also characterized by higher than normal air temperatures the SST depicted also a positive air temperature anomaly. The seasonal surface cooling has deepened the surface mixed layer to 30 m to 35 m in the western Baltic and to 40 m depth in the eastern Gotland Basin. Surface temperatures of about 11 °C were observed in the Arkona Basin, which was 2 K higher than the climatological mean. Also in the Bornholm Basin at station TF213 the SST of 10.2 °C was still high and about 1.5 K higher than normal. Towards east the SST became more patchy. In the Slupsk Furrow the SST was 10.1 °C. In the eastern Gotland Basin the SST ranged between 8.8 °C at station TF0271 and 10.4 °C at station TF0276. The deepening of the seasonal thermocline reduced the mixed upper part of the winter water layer with the surface water. This reduced vertical extent of the intermediate winter water layer in the central Baltic to a thin layer of 20 m to 30 m thickness, with minimum temperatures of 4.4 °C in the eastern Gotland basin. In the Bornholm Basin only smaller patches of intermediate winter water were found above the halocline. From the Belt Sea to the Arkona Basin the bottom water is significantly warmer than the surface water layer. This warm water originated from the barocline inflow events in the summer and autumn, which brought warm saline water into the western Baltic. This water

spreads from the Arkona basin into the halocline of the Bornholm Basin and further eastward. Parts of this warm water have reached the Slupsk Furrow and flushed the bottom layer there. The maximum temperature in this water body of 13.8 °C was observed in the western Arkona Basin. In the Bornholm Basin the core temperature of the warm water decreased from 13.0 °C in the west to 10.6 °C near the Slupsk Sill. The deep water temperature conditions in the Gotland basin remained still unchanged compared to July.
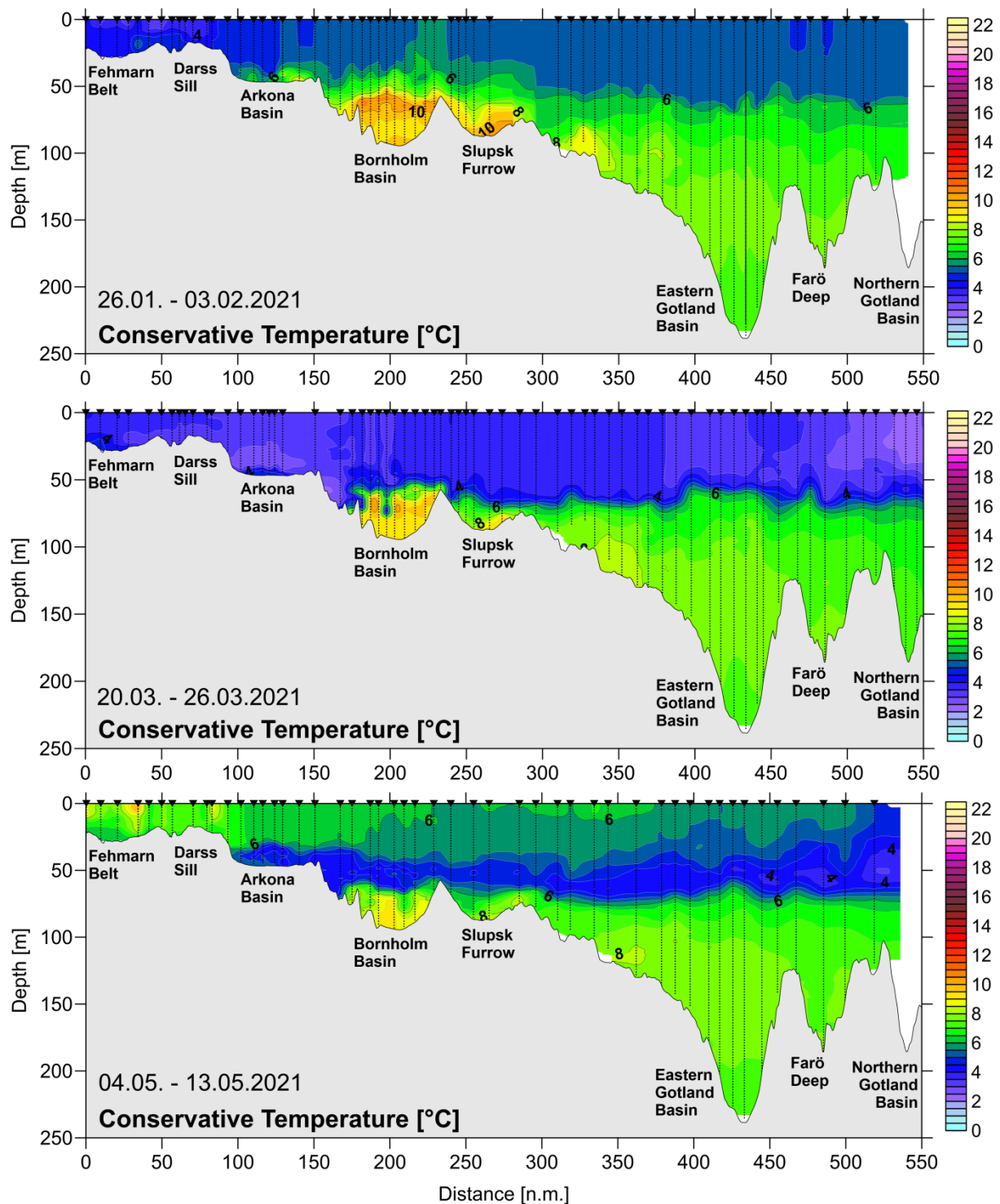

Fig. 18: Temperature distribution along the thalweg transect through the Baltic Sea between Darss Sill and northern Gotland Basin for February, March, and May 2021.
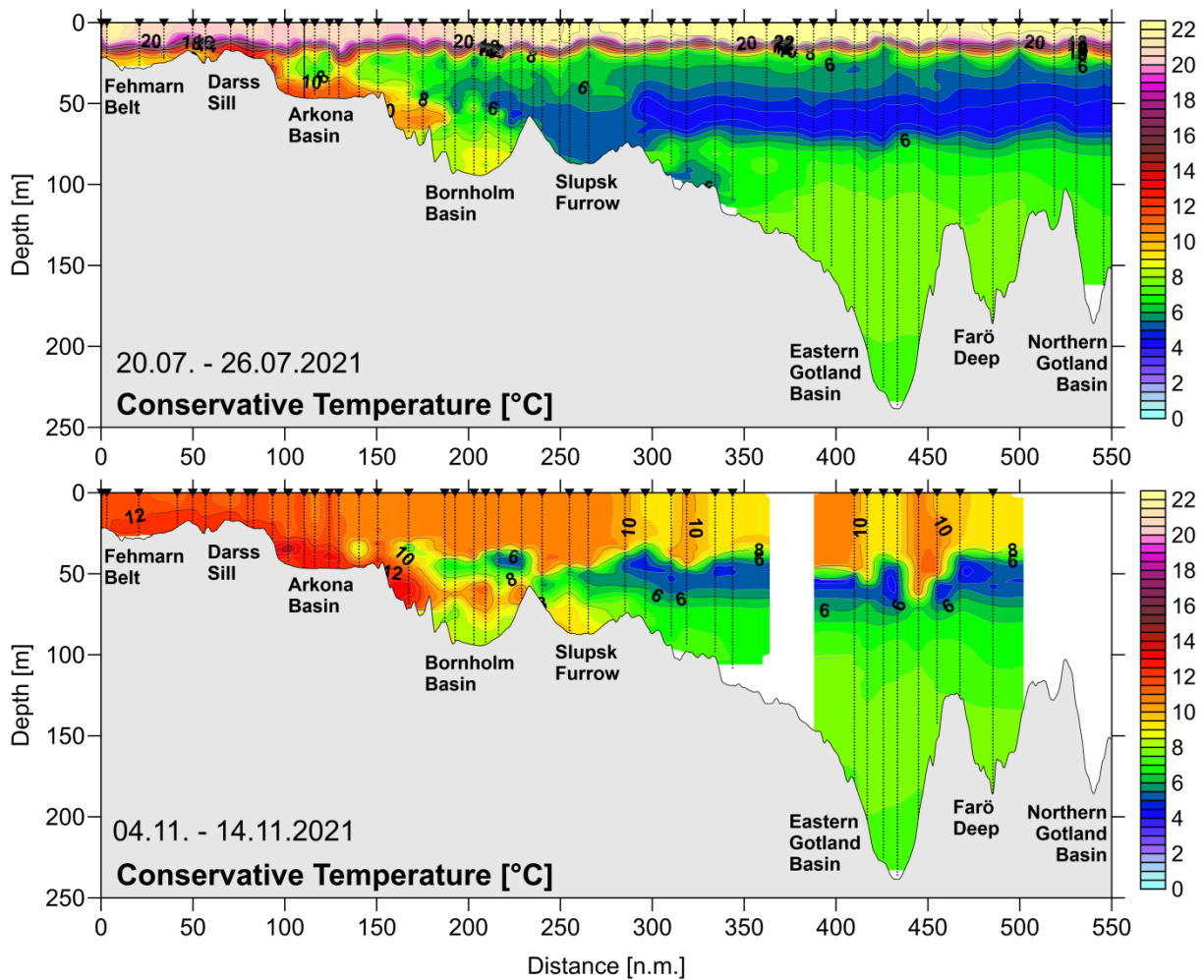
Fig. 19: Temperature distribution along the thalweg transect through the Baltic Sea between Darss Sill and northern Gotland Basin for July and November 2021.

As part of its long-term monitoring programme, IOW operates hydrographic moorings near station TF271 in the eastern Gotland Basin since October 2010. In contrast to the Gotland Northeast mooring, operational since 1998 and from where the well-known 'Hagen Curve' (FEISTEL et al. 2006, NAUMANN et al. 2017) is derived, the mooring at TF271 also collects salinity and oxygen data. The gathered time series data allow the description of the development of hydrographic conditions in the deep water of the Gotland Basin in high temporal resolution. This time series greatly enhances the IOW's ship-based monitoring programme. Figure 20 shows the temperature time series at five depths in the deep water of the eastern Gotland Basin between January 2020 and December 2021. During this period the temperature stratification in the deep water is characterized by a downward decreasing temperature, except the bottom layer before summer 2020. In 2020 the two uppermost levels at 140 m and 160 m depth depicted a pronounced temporal variability due to the interleaving of inflow water patches at this depth. Afterwards, the temperature fluctuations vanished in the entire deep-water range. The year 2021 was characterized by a stable temperature stratification. However, the temperature difference between 140 m depth and the bottom layer was very weak with about 0.1 K. In the entire year

2021 no signs of warm or cold water intrusion were detected in the deep water of the Gotland basin. The inflow events of the inflow period 2020/2021 were not dense enough to reach the deep layers. Thus the deep water temperature remained in 2021 constantly between 7.1 °C and 7.2 °C. The period of relatively warm deep water conditions is continued in 2021.
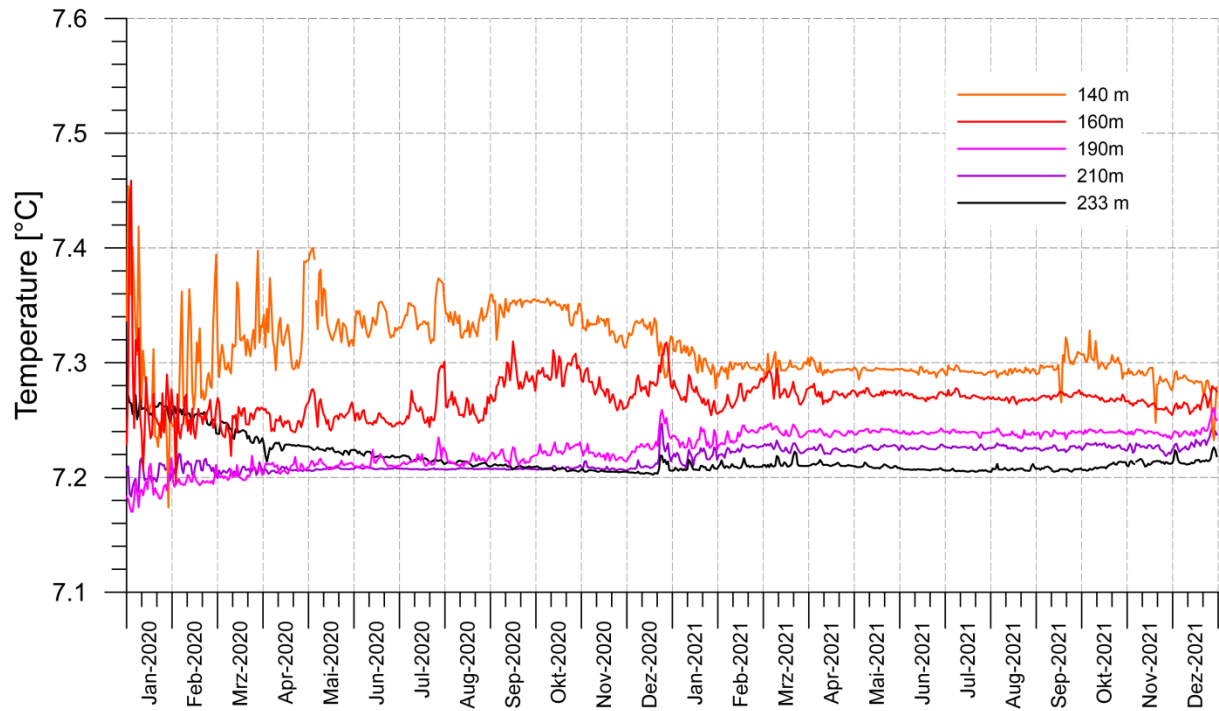

Fig. 20: Temporal development of deep water temperature in the Eastern Gotland Basin (station Tf271) from January 2020 to December 2021 (daily averages of original data with 10 min sampling interval).

Table 7.1 summarises the annual means and standard deviations of temperature in the deep water of the central Baltic based on CTD measurements over the past five years. As in the previous year the deep water temperatures in the entire Baltic increased in 2021, with the exception of the Bornholm Basin. This continued the generally increasing trend since the extreme Christmas MBI in 2014. However, the absolute increase in deep water temperatures was weak. In the eastern Gotland Basin increase at 200 m depth was only 0.02 K and can be attributed to vertical mixing processes with the warmer water above this layer. In the Farö Deep the temperature at 150 m depth was constant with an extreme low standard deviation. The weak increase in the Landsort deep and the Karlsö Deep might be caused by the ongoing slow spreading of warmer water from the halocline layer of the eastern Gotland basin which was fed by the warm saline summer and autumn inflows of the previous years.

In the Bornholm Basin the deep water temperature was nearly constant with a very weak reduction of the annual mean by 0.03 K. Compared to the high standard deviation of 0.39 K this change is not significant.

Table 7: Annual means and standard deviations of temperature, salinity and oxygen concentration in the central Baltic Sea: IOW- and SMHI data (n= 17-29).

Table 7.1: Deep water temperature (ºC; maximum in bold).

Station	Depth m	2017	2018	2019	2020	2021
213 (Bornholm Deep)	80	7.06 ±0.28	7.81 ±1.49	**8.65 ±0.12**	8.45 ±0.29	8.42 ±0.39
271 (Gotland Deep)	200	7.05 ±0.15	6.89 ±0.01	7.20 ±0.07	7.21 ±0.01	**7.23 ±0.00**
286 (Fårö Deep)	150	6.83 ±0.15	6.70 ±0.04	7.05 ±0.18	7.24 ±007	**7.24 ±001**
284 (Landsort Deep)	400	6.14 ±0.19	6.27 ±0.03	6.37 ±0.15	6.60 ±0.27	**6.67 ±0.02**
245 (Karlsö Deep)	100	5.53 ±0.06	5.67 ±0.12	5.64 ±0.12	5.83 ±0.11	**6.05 ±0.11**

Table 7.2: Deep water salinity (maximum in bold).

Station	Depth m	2017	2018	2019	2020	2021
213 (Bornholm Deep)	80	**17.40 ±0.46**	16.64 ±0.32	16.63 ±0.27	16.34 ±0.34	15.84 ±0.26
271 (Gotland Deep)	200	**13.30 ±0.04**	13.17 ±0.03	13.16 ±0.03	13.03 ±0.03	12.93 ±0.03
286 (Fårö Deep)	150	**12.58 ±0.07**	12.50 ±0.12	12.46 ±0.08	12.39 ±0.03	12.24 ±0.08
284 (Landsort Deep)	400	11.29 ±0.19	**11.41 ±0.05**	11.33 ±0.06	11.34 ±0.16	11.24 ±0.06
245 (Karlsö Deep)	100	10.28 ±0.11	**10.44 ±0.21**	10.35 ±0.24	10.40 ±0.18	10.36 ±0.18

4.2   Salinity

The vertical distribution of salinity in the western and central Baltic Sea during IOW's five monitoring cruises is shown in Fig. 21 and Fig. 22. The salinity distribution is markedly less variable than temperature distribution, and a west-to-east gradient in the surface and the bottom water is typical. Greater fluctuations in salinity are observed particularly in the western Baltic Sea where the influence of salt-water inflows from the North Sea is strongest. The duration and influence of minor inflow events is usually too small to be reflected in overall salinity distribution. Only combined they can lead to slow, long-term changes in salinity. The salinity

distributions shown in Fig. 21 and Fig. 22 are mere 'snapshots' that cannot provide a complete picture of inflow activity. In 2021 the evolution of salinity distribution was mainly controlled by the minor barotropic inflows in autumn and winter 2020/2021 and the baroclinic inflows in late summer and autumn 2021. However, none of the inflows could be completely covered by the IOW monitoring cruises. The salinity at the Darss Sill was well below 17 g/kg during all cruises, although there were significant volumes of high saline water observed in the Fehmarn Belt. It is not possible to produce meaningful statistics on inflow events, by using only the monitoring cruises. The analyses of the sea level changes and the salinity observations in the western Baltic revealed a very weak barotropic inflow activity in the winter season 2020/2021. Weak barotropic inflows were detected in November 2020 (0.42 and 0.46 Gt salt) and in February 2021 (0.32 Gt salt), which transported about 1.2 Gt salt into the western Baltic. Another minor inflow was observed in October 2021 (0.72 Gt salt). During summer and autumn 2021 barocline inflows dominated the water exchange with the North Sea.

The first monitoring cruise in 2021 was performed just before the weak inflow in February. The salinity in the Fehmarn Belt was rather low with a bottom value of 17.5 g/kg. The bottom salinity of 11.6 g/kg at the adjacent Darss Sill did indicate an eastward directed flow. In the Arkona Basin the remains of the small November inflows formed a thin saline bottom layer of about 5 m thickness, with a maximum salinity of 15.1 g/kg. Above the bottom water the basin was filled with the brackish Baltic surface water with a salinity of 8.5 g/kg to 9.0 g/kg. In the Bornholm Basin the halocline depth was at 54 m, close to the sill depth of the Slupsk Sill. In the deep water layer the salinity increased continuously to a bottom salinity of 16.7 g/kg. The Slupsk Furrow depicted relatively low saline waters in the deep layer. The bottom salinity was only 13.0 g/kg. However, the shallow halocline exceeds the sill depth at the eastern edge of the furrow and parts of the halocline water spreads into the southern Gotland Basin. Due to the lack of larger inflow events in the recent years the salinity in the deep water of the central Baltic Sea decreased continuously. The bottom salinity in the Gotland Deep was of 13.05 g/kg. Nevertheless, this is a high value compared with climatological data and still close to the overall maximum of 13.6 g/kg observed after the extreme inflow event in 1951. The 12 g/kg isohaline was at a depth of around 110 m, the same depth as observed one year ago. This points to balance between upward salt flux due to mixing and the lateral inflow saline water into the halocline layer. The 13 g/kg isohaline was found at 205 m depth, 23 m deeper than one year before. This indicates the slow upward directed salt flux in the deep-water layer during the absence of saline inflows at that depth. Further north in the Farö Deep the bottom salinity was 12.55 g/kg, nearly the same level as one year ago. The stagnation in the bottom waters of the central Baltic was still ongoing.

Until March 2021 the situation in the central Baltic did not change, whereas the salinity distribution in the western Baltic was affected by the minor barotropic inflow in the end of February. The bottom salinity in the Fehmarn Belt increased to 21.1 g/kg and the shape of the isohalines at the Darss Sill pointed to an active overflow. The total volume of the saline bottom pool in the Arkona Basin has strongly increased. Here a bottom salinity of 21.8 g/kg was found. The halocline depth rose by about 15 meters compared to February. Parts of the inflow waters has reached the halocline layer of the Bornholm Basin as seen in the temperature distribution, but caused only minor changes in the salinity. The bottom salinity in the Bornholm Basin was 16.4 g/kg, about 0.3 g/kg less than in February.

In May the distribution in the Fehmarn Belt and at the Darss Sill indicated an outflow situation. The maximum bottom salinity in the Fehmarn belt was still high with 21.2 g/kg, but the surface layer was covered by brackish Baltic surface water. At the Darss Sill the bottom salinity was only 8.7 g/kg. The saline bottom water pool in the Arkona Basin has lost most of its volume. The halocline was found at 35 m to 40 m depth in the centre of the basin. The bottom salinity amounted to 18.6 g/kg, which was 3 g/kg less than in March. In the Bornholm Basin the halocline depth was shallower than in March. With about 50 m it exceeded the sill depth of the Slupsk Sill, and sill forced an overflow of saline water into the Slupsk Furrow. The bottom salinity in the Bornholm Basin was further decreased to 16.1 g/kg at station TF0213. In the Slupsk Furrow the saline deep-water volume was slightly increased. Here the bottom salinity in was 13.5 g/kg. No significant changes of deep-water conditions were observed in the central Baltic. At station TF271 (Gotland Deep) the bottom salinity remained nearly unchanged at 13.03 g/kg. Due to the arriving inflow patches the salinity gradient in the upper halocline of the central Baltic decreased between February and May.

The calm summer conditions forced the onset of barocline inflows through the Belt Sea. In July 2021 the Fehmarn Belt and the Darss Sill depicted the two layer stratification, typical for the barocline inflow situation. In the Fehmarn Belt a strong halocline at about 15 m depth separated the brackish surface water from the saline inflow at the bottom, where a maximum bottom salinity of 27.9 g/kg was measured. At the time of the cruise the tip of the inflow had reached the Darss Sill were the bottom salinity increased to 15.6 g/kg. The pool of saline bottom water in the Arkona Basin was moderately filled with warm, but less saline water from a previous inflow. In the center of the basin the warm water with a salinity of 16.6 g/kg formed a 10 m thick layer. Parts of this water have passed the Bornholmgat. However, the saline stratification in the central Bornholm Basin was not changed significantly. The bottom salinity at station TF0213 remained at 16.1 g/kg. The halocline depth in the Basin was found at 55 m, the depth of the Slupsk Sill. Further east, in the central Baltic basins, again no significant changes were observed. The depth of the 13 g/kg isohaline in the Gotland deep was at 220 m, 15 m deeper than in February, pointing to the ongoing weak salt flux. The bottom salinity in the Gotland Deep and the Farö Deep was 13.01 g/kg and 12.42 g/kg, respectively. The surface salinity in the central Baltic decreased according to its usual seasonal cycle, and was at 7.22 g/kg in the eastern Gotland Basin.

The signature of the weak barotropic inflow from late October is visible in the salinity distribution gathered in November 2021. In the Fehmarn Belt the bottom salinity amounted to 23.0 g/kg. At the Darss Sill brackish Baltic surface water covered most of the water column. Only in a thin bottom layer saline water was found. However, in the Arkona Basin warm and saline water from the summer/autumn inflows covered the bottom layer. The maximum bottom salinity of 16.3 g/kg did not change significantly compared to July. The saline layer was relatively thin with a maximum vertical extent 12 m. The warm saline water from the inflows has filled the halocline layer of the Bornholm basin. Due to the low salinity the inflow water did not reach the bottom of the Basin. Thus, due to the vertical salt flux the bottom salinity in the basin decreased further to 15.77 g/kg. The salinity in the bottom water pool of the Slupsk Furrow was slightly increased by the input of halocline water from the Bornholm Basin. The bottom salinity at station TF0222 was 13.6 g/kg. The stagnation in the deep water of the central Baltic was still ongoing. The bottom salinity decreased very slowly in the Gotland Deep to 12.97 g/kg.
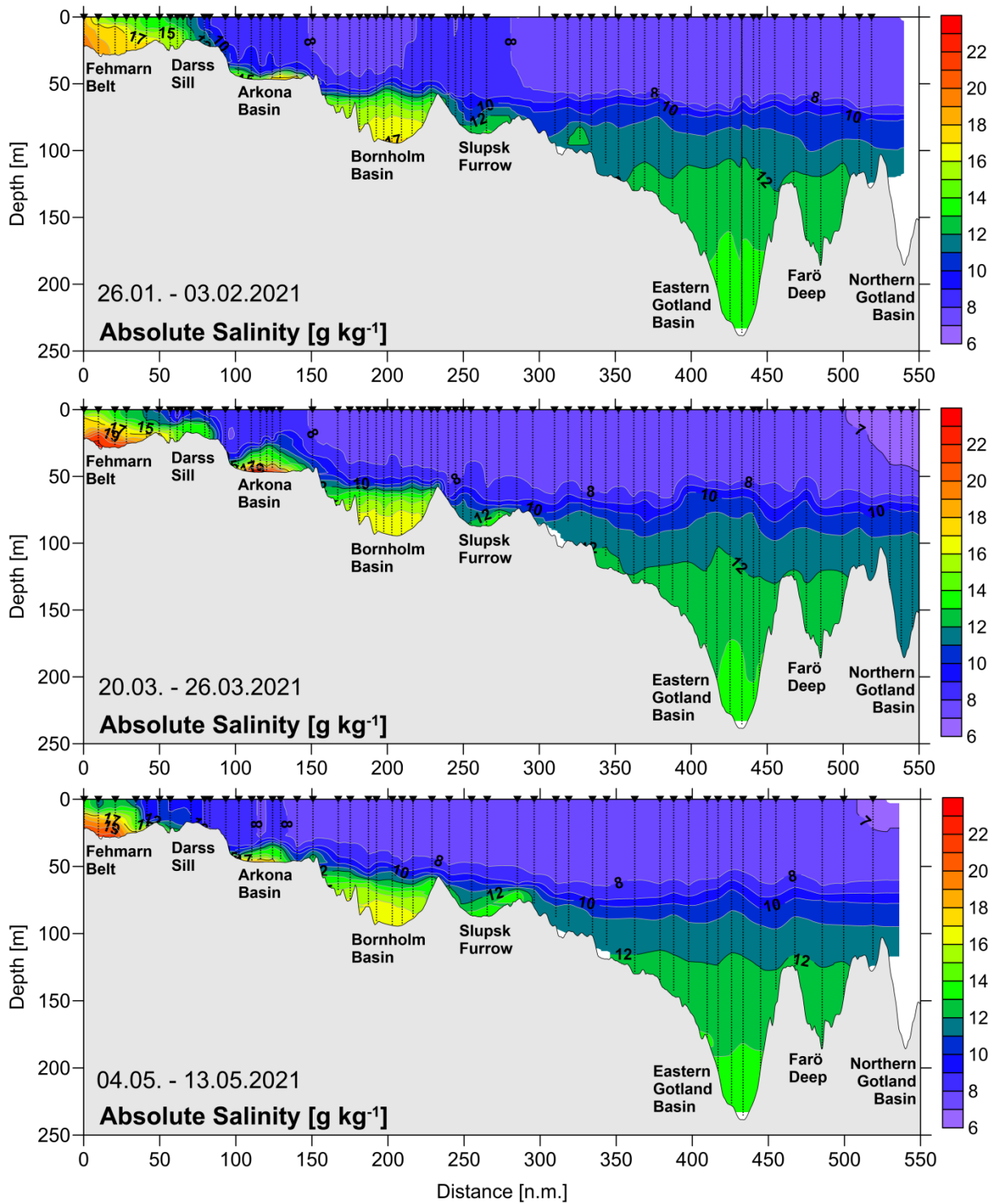
Fig. 21: Salinity distribution along the thalweg transect through the Baltic Sea between Darss Sill and northern Gotland Basin for February, March, and May 2021.
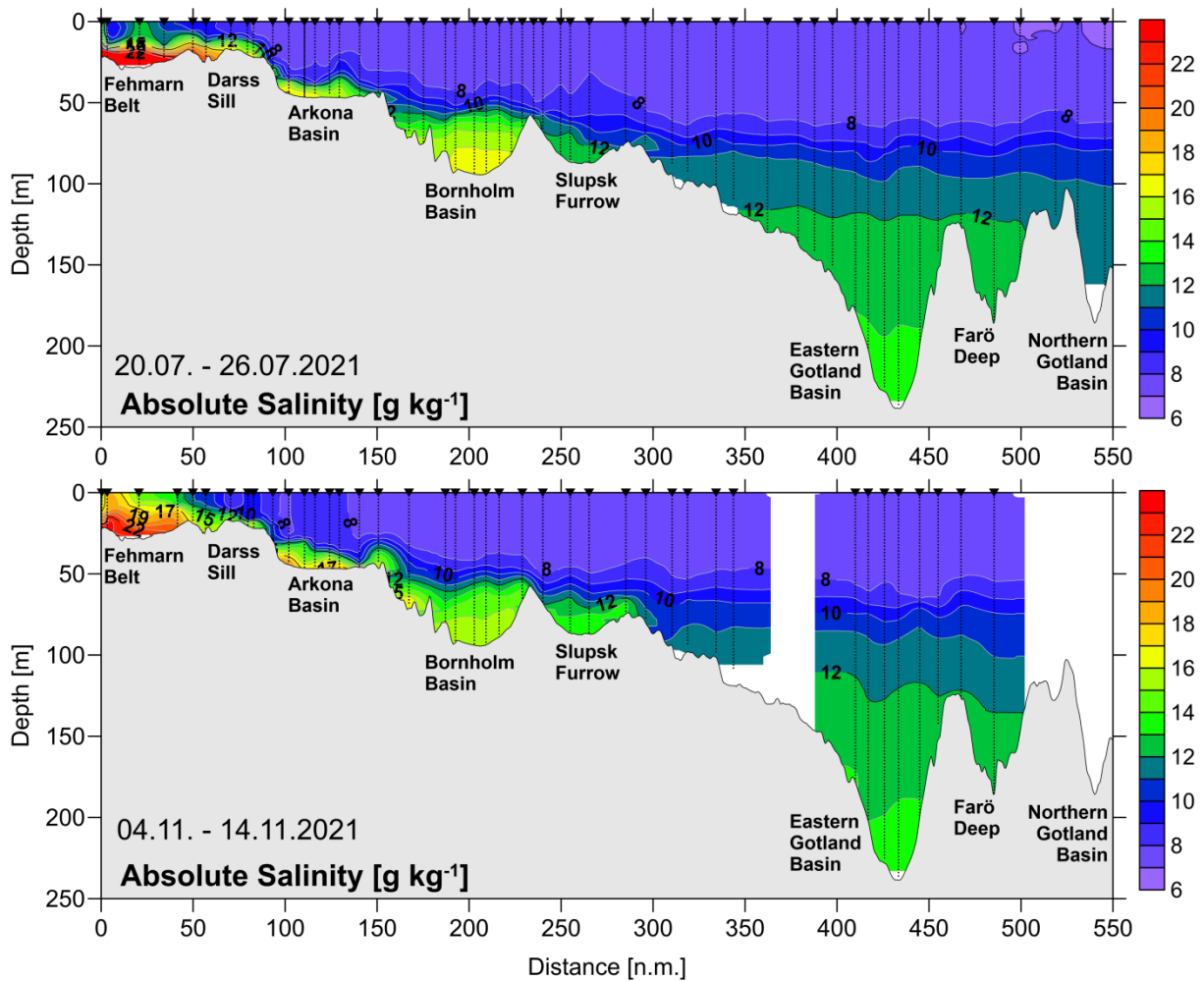
Fig. 22: Salinity distribution along the thalweg transect through the Baltic Sea between Darss Sill and northern Gotland Basin for July and November 2021.

Table 7.2 shows the overall trend of salinity in the deep water of the Baltic in the past five years. After the series of stronger inflow events in 2014 to 2016 the bottom salinity in the Gotland Deep and Farö Deep reached its maximum in 2016 and 2017. Since then only weak changes in salinity stratification were observed in the central Baltic. The deep-water salinity in the eastern Gotland Basin dropped slightly due to vertical mixing by 0.01 g/kg to 0.13 g/kg per year. In the Farö Deep the annual salinity decrease is only about 0.04 g/kg to 0.15 g/kg. Also in the Karlsö Deep and Landsort Deep the slow decrease of deep water salinity has started. In the Bornholm Basin the mean deep-water salinity decreased also in 2021. The high standard deviation of salinity in the Bornholm basin points to rapid fluctuations, caused by particular inflow events.

As previously no clear trend emerges over the past five years for salinity in the surface layer of the Baltic. Table 7.3 summarises the variations in surface layer salinity.

Table 7.3: Annual means of 2017 to 2021 and standard deviations of surface water salinity in the central Baltic Sea (minimum values in bold, n= 17-29). The long-term averages of the years 1952-2005 are taken from the BALTIC climate atlas (FEISTEL et al., 2008).

Station	1952-2005	2017	2018	2019	2020	2021
213 (Bornholm Deep)	7.60 ±0.29	**7.46 ±0.20**	7.53 ±0.08	7.63 ±0.11	7.80 ±0.18	7.54 ±0.26
271 (Gotland Deep)	7.26 ±0.32	7.33 ±0.22	**7.09 ±0.27**	7.19 ±0.25	7.33 ±0.16	7.36 ±0.13
286 (Fårö Deep)	6.92 ±0.34	7.13 ±0.43	6.92 ±0.34	**6.78 ±0.33**	7.07 ±0.29	7.12 ±0.23
284 (Landsort Deep)	6.75 ±0.35	6.54 ±0.34	6.59 ±0.32	6.52 ±0.26	6.58 ±0.50	**6.33 ±0.33**
245 (Karlsö Deep)	6.99 ±0.32	6.93 ±0.18	7.06 ±0.18	6.89 ±0.24	7.16 ±0.12	**6.86 ±0.25**

Fig. 23 shows the temporal development of salinity in the deep water of the eastern Gotland Basin between January 2020 and December 2021, based on data from the hydrographic moorings described above. The stratification in this period was controlled by stagnation and weak vertical mixing. This led to a slowly decreasing salinity in the entire deep-water body, and in a slight reduction of the vertical salinity gradient below 190 m depth. The higher temporal variability in the 140 m depth level was caused by pulse like inflows of saline water plumes into the halocline of the eastern Gotland Basin.
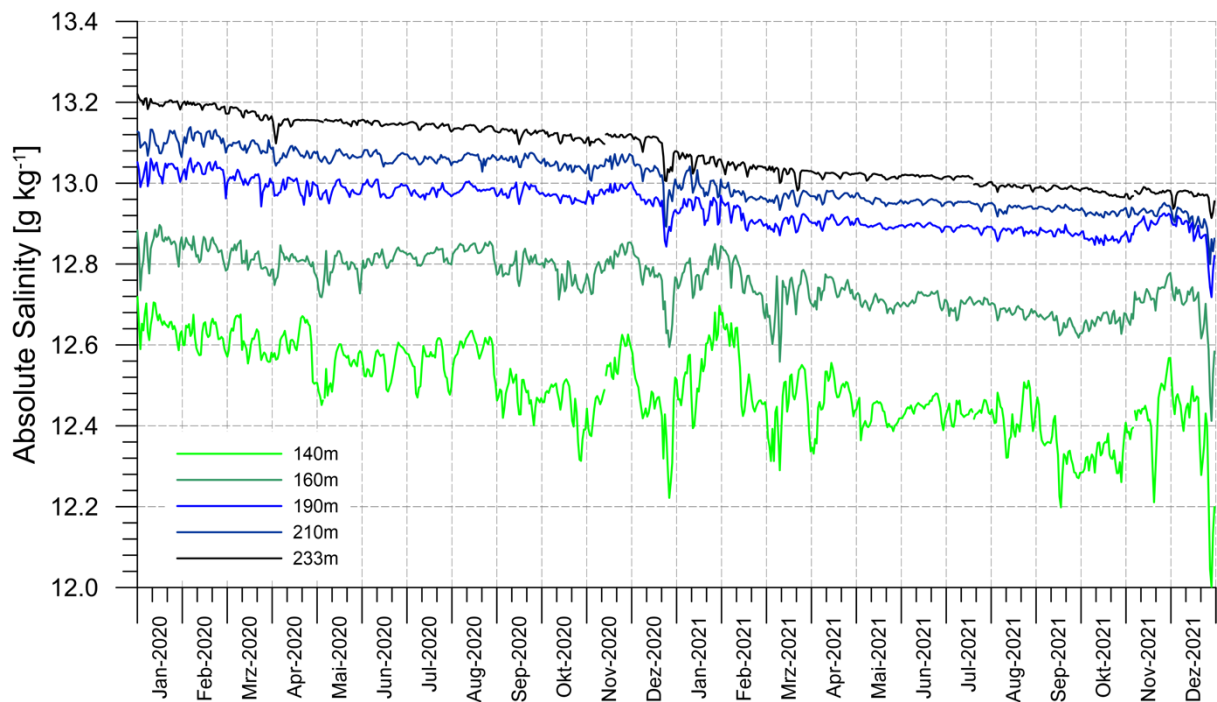

Fig. 23: Temporal development of deep-water salinity in the Eastern Gotland Basin (station TF271) from January 2020 to December 2021 (Daily averages of original data with 10 min sampling interval).

4.3 Oxygen distribution

Availability of sufficient oxygen reflects a precondition for the survival of higher marine life. Low oxygen concentration appears an issue especially in density gradients and at the sea floor. For the Baltic Sea, it is a natural phenomenon that oxygen supply to the deep basins is limited by a shallow and narrow transition area between the North Sea and the Baltic Sea, with an almost permanent slow and an episodic strong entrainment of oxygenated waters to the Baltic Sea's deeper basins. The effect is mainly determined by the supplied volume and the density of the water. However, after a "Major Baltic Inflow" a few years of stagnation follow and the water below the permanent halocline turns into anoxic and then to euxinic conditions again. This is caused by the elevated density hindering further supply of oxygenated water and a continuous consumption of oxygen during the mineralization of organic matter. After oxygen depletion, other oxidants are used. Sulphate, a major constituent of seawater is converted to poisonous hydrogen sulphide that turns Baltic Sea deep waters into dead zones for aerobic life. This process is fostered by eutrophication and excessive supply of organic matter to the seafloor (DIAZ & ROSENBERG 2008). The lack of oxygen below the halocline of the Baltic Sea areas is evaluated by using the HELCOM oxygen debt indicator for the deep basins to estimate the deviation from a "good environmental status" (HELCOM 2013). However, recently it became obvious that also shallow Baltic Sea areas are more often subjected to temporally low oxygen values. Shallow areas in this context are regions, which are too shallow to establish a permanent halocline, usually shallower than about 60 m. Here, deep winter mixing each year oxygenates the water column down to the bottom. However, during summer the microbial decomposition of large amounts of organic matter requires considerable amounts of the present oxygen.

Excess nutrient supply to the Baltic Sea and internal mobilization processes of especially phosphorus primarily cause increased phytoplankton blooms. Subsequently, the episodic remineralization activity of accumulated organic matter on the sea floor is intensified. To observe and finally to recommend measures, the bottom water oxygen concentration in shallow areas is for the first time assessed for test purposes during HOLAS III (HELCOM "Third Holistic Assessment of the Ecosystem Health Of the Baltic Sea") by an indicator based on the long-standing application of the "Iltsvind" (Oxygen loss) model for the western Baltic Sea proposed by the Danish party in HELCOM.

In surface waters as well as in shallow areas, the gas exchange with the atmosphere maintains an oxygen concentration of seawater controlled by temperature. This includes release of oxygen during primary production in spring as well as uptake of oxygen during elevated remineralisation activity in summer and autumn. The situation changes, when a stable thermocline develops separating oxygenated surface waters from the waters below. Then, assimilation and dissimilation processes that change the oxygen content in seawater are mainly separated, and in deeper waters without contact to the atmosphere, oxygen concentration clearly declines by respiration in summer. Strong temperature and/or salinity changes hinders mixing between the bottom and upper waters. Lasting oxygen consumption and finally denitrification and subsequent reduction of sulphate result in the building of toxic hydrogen sulphide (shown as negative oxygen), which is worsening the conditions.

We generally use ml/l as the standard unit for oxygen concentration. In the hydrographic analysis of oxygen displayed in Fig. 25/Fig. 26 we use the chemical oceanographic unit µmol/kg, in comparison to Fig. 18/Fig. 19 of temperature and Fig. 21/Fig. 22 of salinity. For the discussion of Fig. 25/Fig. 26 we give both units for clearity.

The decreasing trend of the oxygen concentration in deep waters of the five selected Baltic Sea deeps at respective reference depths was basically ongoing (Table 7.4 - Oxygen). The choice of reference depths in the middle of the respective deep waters secure annual averages basically unbiased from episodic smaller inflows that frequently occur in the depth range of the pycnocline and partly in the bottom layer but disappear soon. At Gotland Deep station, the decline of oxygen continued since 2017 (0.13 ml/l) and showed in 2021 an accumulation of hydrogen sulphide equivalent to -4.23 ml/l oxygen at 200 m depth. Similarly at the Fårö Deep station in 150 m depth, where oxygen decreased since 2017 (0.34 ml/l) to -2.12 ml/l oxygen in 2021. In the western Gotland Basin the worst situation of the last years was in 2020 and subsequently showed a reduced deficit in 2021. The annual average oxygen concentration in the Landsort Deep decreased from -0.41 ml/l in 2017 to -2.19 ml/l in 2020 and was 1.66 ml/l in 2021. Likewise at Karlsö Deep from -0.75 ml/l to -2.28 ml/l in 2020 and to -2.07 in 2021 (Table 7.4). Bornholm Deep more frequently receives oxygenated waters from the Arkona Basin. Even in summer and autumn at higher temperatures, the density is often high enough to reach the deep waters. So the annual and interannual changes are more pronounced. So Bornholm Deep station showed a change of the annual average oxygen concentration between 1 ml/l and almost 0.16 ml/l between 2017 and 2021 (Table 7.4).

Table 7.4: Annual means of 2017 to 2021 and standard deviations of deep water oxygen concentration (ml/l; hydrogen sulphide is expressed as negative oxygen equivalents; maximum in bold).

Station	Depth/ m	2017	2018	2019	2020	2021
213 (Bornholm Deep)	80	0.90 ±0.83	0.16 ±0.37	0.97 ±1.50	0.89 ±1.34	0.17 ±0.92
271 (Gotland Deep)	200	0.13 ±0.11	-0.85 ±0.50	-2.48 ±1.18	-4.13 ±1.30	-4.23 ±0.38
286 (Fårö Deep)	150	**0.34 ±0.33**	-0.73 ±0.42	-1.74 ±0.41	-1.42 ±0.64	-2.12 ±0.40
284 (Landsort Deep)	400	**-0.41 ±0.31**	-0.57 ±0.40	-1.49 ±0.25	-2.19 ±0.45	-1.66 ±0.09
245 (Karlsö Deep)	100	**-0.75 ±0.66**	-1.89 ±0.72	-1.95 ±1.25	-2.28 ±0.65	-2.07 ±0.86

As stated before, in surface waters the seasonal cycle of the water temperature basically controls the oxygen concentration by oxygen's solubility (Fig. 24a). However deep mixing or upwelling may cause intermediate deviations. The highest oxygen concentrations were consequently observed in January/February, March and May in 2021 between 8.0 ml/l and 9.5 ml/l oxygen. Thereby, the March values were the highest value as March usually shows the lowest water temperatures. Additionally, the spring bloom may also significantly contribute to the oxygen concentration in March and May. After the summer minimum in July between 6.0 ml/l and 6.5 ml/l oxygen in 2021, the concentration of oxygen was then higher in November likely caused by cooling and wind mixing at autumn weather conditions.

The bottom water of the shallow western Baltic Sea (Fig. 24b) showed a similar seasonal pattern as the surface water (Fig. 24a), however at a slightly lower concentration level. The maximum oxygen concentration in 2021 occurred in March with values between 7.7 ml/l and 8.8 ml/l oxygen in the Belt Sea, the Mecklenburg Bight and the Arkona Sea. The corresponding lowest average oxygen concentration in bottom waters was about 4.5 ml/l recorded in the Mecklenburg Bight and the Arkona Sea in July 2021. In the Belt Sea, the oxygen concentration further decreased from March (8.7 ml/l) to November, but was relatively high with almost 6 ml/l in November compared to the deeper basins of the Baltic Sea. The sampling schedule with five monitoring cruises annually, is relatively coarse and insufficient to cover the dramatic oxygen depletion events in August and September and thus gives a rough impression of the oxygen situation of shallow Baltic Sea waters only. Partly this is also true for the Bornholm Sea, which also appeared a considerable variability through the year in 2021, with oxygen concentrations in bottom water between weak oxic (0.33 ml/l oxygen) in March and euxinic conditions in January/February, May, July and November, with the worst average concentration of -1.22 ml/l in July. In the relatively shallow southern Gotland Sea an average weak oxic situation is established during the measurements in 2021 with 0.8 ml/l to 2.3 ml/l oxygen. The passage of oxygen bearing filaments is also visualized in the Fig. 25 and Fig. 26. The situation in the deep basin is different and bottom waters usually reflect more stable conditon. So during the year 2021 in the eastern Gotland Sea the oxygen equivalent concentration of hydrogen sulphide was between -5.8 ml/l and -7.1 ml/l, in the northern Gotland Sea between -1.6 ml/l and -2.0 ml/l, and in the western Gotland Sea between -1.7 ml/l and -2.2 ml/l oxygen equivalents, respectively.
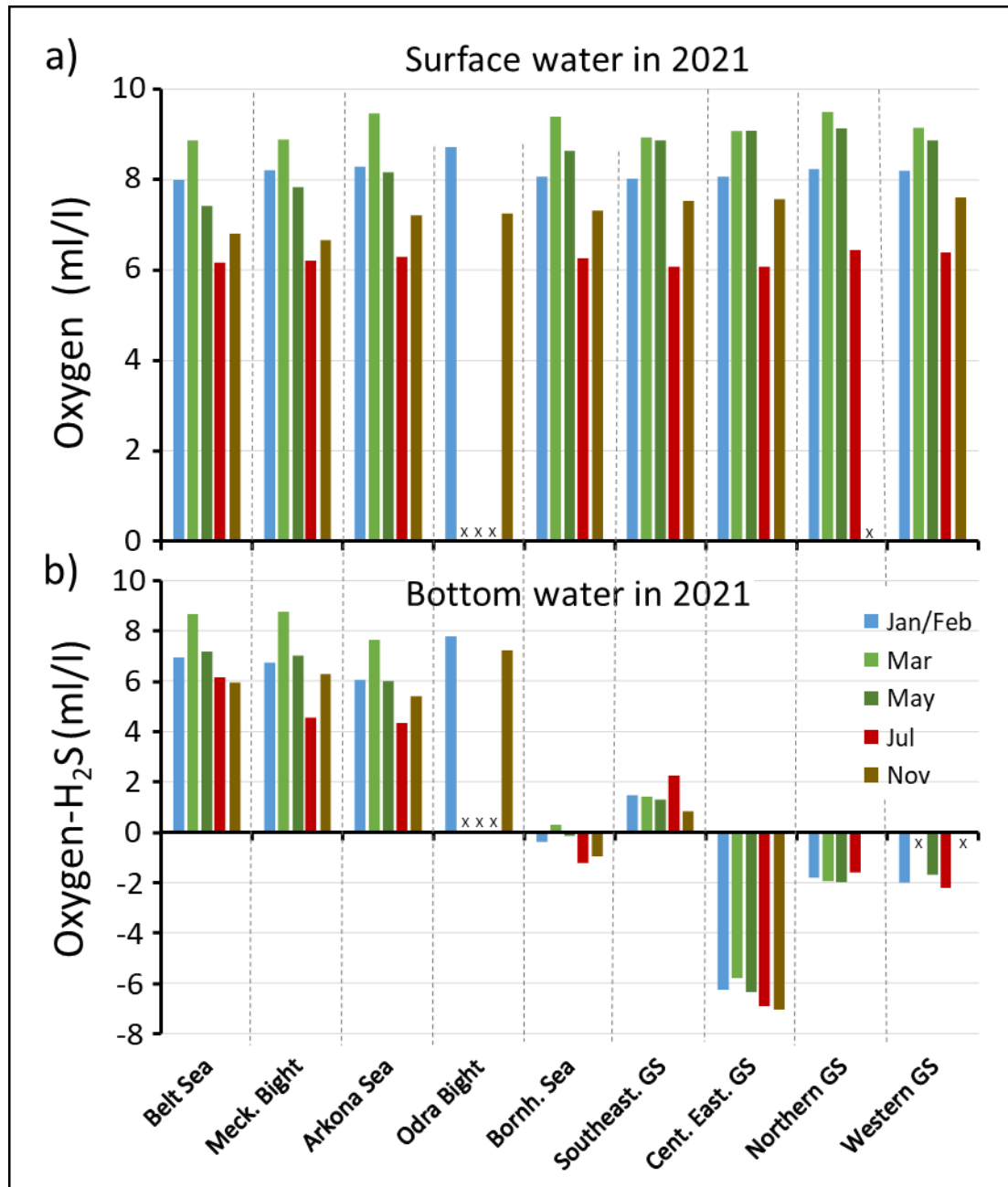
Fig. 24: Comparison of average oxygen concentrations in surface waters (a), including O₂-sensor data and average oxygen/hydrogen sulphide concentrations in bottom waters (b), without sensor data of the studied Baltic Sea areas of February to November 2020: Belt Sea, Mecklenburg Bight, Arkona Sea, Odra Bight, Bornholm Sea, southeastern Gotland Sea, central Eastern Gotland Sea, Northern Gotland Sea, and Western Gotland Sea.
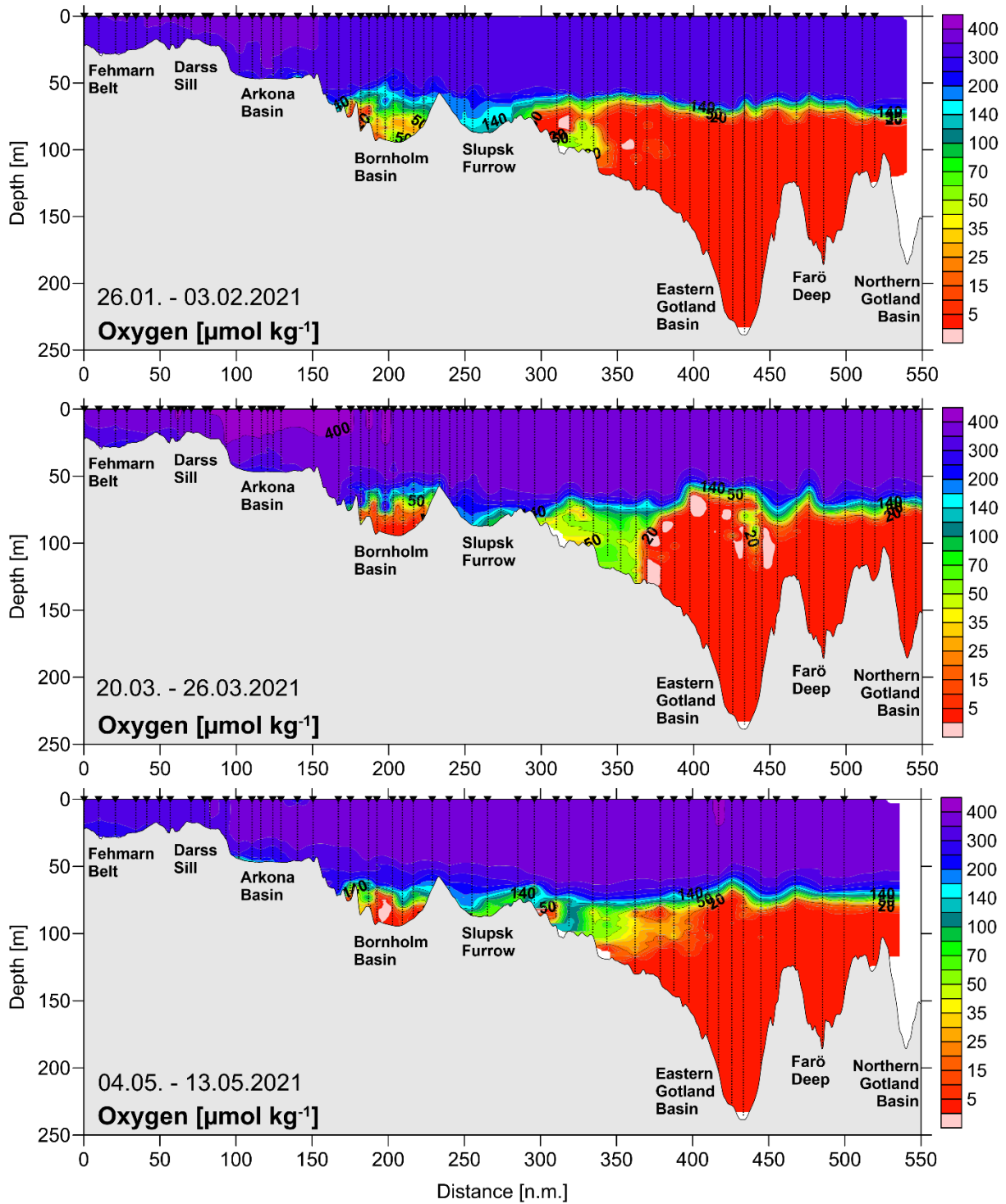
Fig. 25: Vertical distribution of oxygen (without H2S) during the January/February, March, and May cruises in 2021 between the Darss Sill and the northern Gotland Basin. Values below 5 µmol/kg can not be distinguished from 0 µmol/kg.
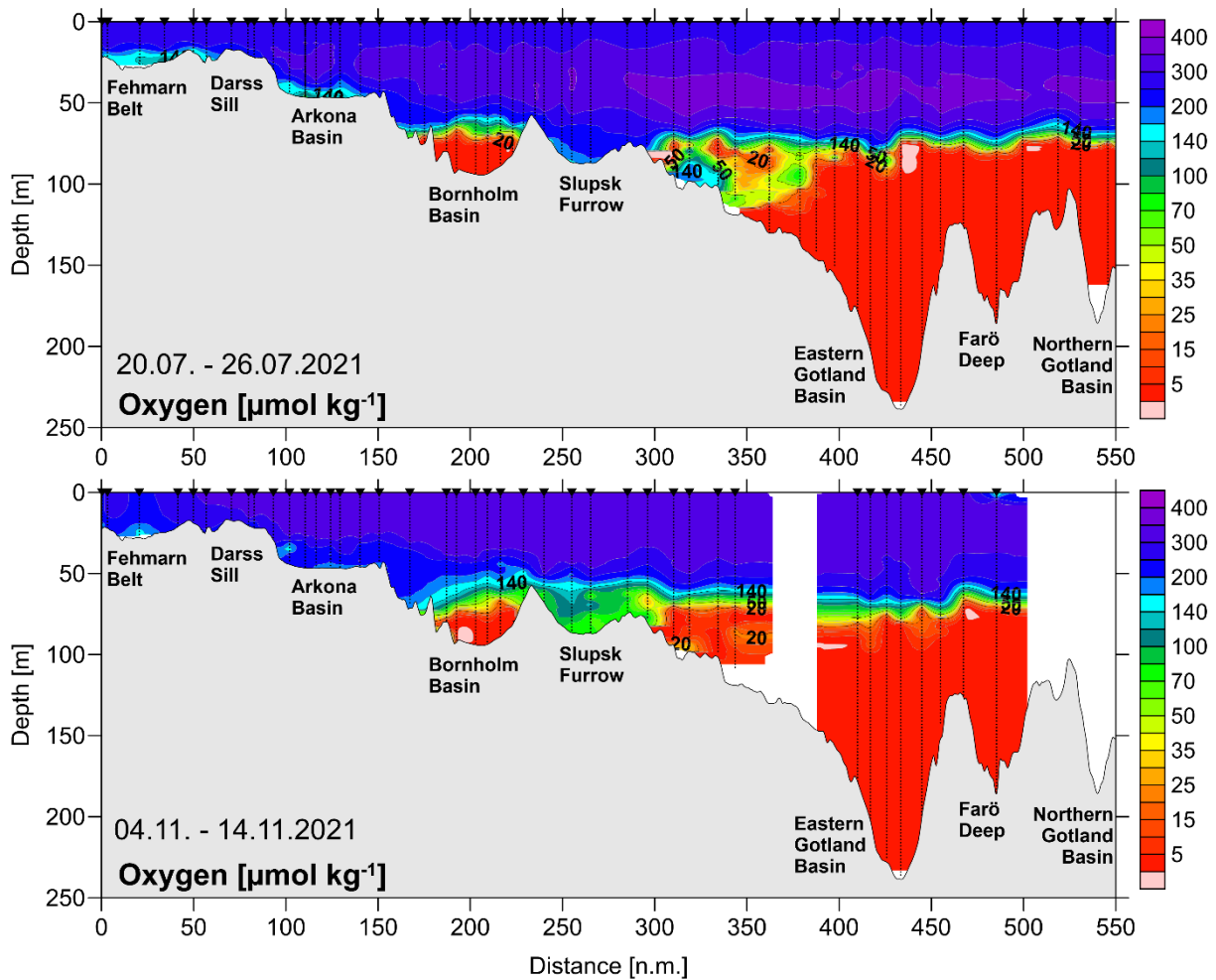
Fig. 26: Vertical distribution of oxygen (without H2S) during the July and November cruises in 2021 between the Darss Sill and the northern Gotland Basin. Values below 5 µmol/kg can not be distinguished from 0 µmol/kg.

The oxygen conditon of the deep water of the central Baltic Sea is primarily influenced by the occurrence or absence of moderate and strong barotropic and/or baroclinic inflows. Likely end of 2020 a major pulse of warm oxygenated haline water entered the Bornholm basin and moved further to the southern Gotland Sea. Thereby, the dense water that remained in the Bornholm basin was subsequently overflown between January and March in a depth of above 60 m by less haline colder water carrying 170 µmol/kg to 250 µmol/kg (~ 4 ml/l to 6 ml/l) oxygen, right from the Arkona Basin, across Slupsk sill, via the Slupsk furrow and further to the southern Gotland Basin. In January/February 2021 the eastern Gotland Basin showed values of 40 µmol/kg to 50 µmol/kg (0.9 ml/l to 1.2 ml/l) oxygen in the pycnocline between 70 m and 120 m. In May and July more oxygen reached the southern part of the eastern Gotland basin with concentrations of up to 200 µmol/kg (about 4.5 ml/l). Water bearing 40 µmol/kg to 80 µmol/kg (0.9 ml/l to 1.8 ml/l) spreaded further north to the central basin but appeared to be mostly consumed in November 2021 with some oxygen left in the halocline range to the northern end of the basin.

4.4   Nutrients: Inorganic nutrients

Many reduction measures that have been implemented in the last decades could not prevent the Baltic Sea from being eutrofied. In Germany, riverine inputs of total phosphorus declined between 2006 and 2014 by 14 %. In the same time-period, total nitrogen input decreased by 31 % (HELCOM 2018a). Despite this positive development, German territorial waters and bordering sea areas of the Baltic Sea remained hypertrophied by up to 50 % in the western and up to 100 % in the eastern part (HELCOM 2018b). To determine the effects of changes in nutrient inputs and to evaluate the results of reduction measures undertaken, the frequent monitoring of the nutrient situation is mandatory. Nutrients are core parameters since HELCOM established a standardized monitoring programme at the end of the 1970ies.

A drastic description of the consequences of eutrophication is given by DUARTE et al. (2009) "The effects of eutrophication include the development of noxious blooms of opportunistic algae and toxic algae, the development of hypoxia, loss of valuable seagrasses, and in general a deterioration of the ecosystem quality and the services they provide". According to the second "State of the Baltic Sea" report, 97 % of the Baltic Sea area is affected by eutrophication and 12 % is assessed as being in the worst status category (HELCOM 2018a).

4.4.1   Surface water processes

The long-standing observation that nitrate and phosphate concentrations in the surface waters of temperate latitudes exhibit a typical annual cycle with high concentrations in winter, depletion during spring and summer, and recovery in autumn (NAUSCH & NEHRING 1996, NEHRING & MATTHÄUS 1991) seems partly no longer valid. In recent years it appears more and more clear that nitrate is still completely taken up by the spring bloom and is replenished during late autumn and winter, whereas phosphate significantly declines in April/May, but persists at low concentration almost throughout the summer. Thus, blooms of diazotrophic cyanobacteria, which use dinitrogen gas in addition to phosphate for growth, are enabled also during summer starvation.

Fig. 27 illustrates the annual cycle of nitrate and phosphate concentrations in surface waters at the stations Gotland Deep and Bornholm Deep in comparison to the surface water temperature development in 2021. For this purpose, the data of five monitoring cruises of the IOW were combined with data of the Swedish Meteorological and Hydrological Institute (SMHI) to get a better resolution of the seasonal patterns. In the central Baltic Sea, a typical phase of elevated nutrient concentrations usually develops during winter, which lasted two to three months (NAUSCH et al. 2008). In 2021, the maximum nitrate concentration was measured in early February of 4.1 µmol/l in the central eastern Gotland basin and in mid-February of 4.1 µmol/l in the central Bornholm Sea, respectively. A maximum phosphate concentration was determined in mid-March of 0.75 µmol/l at Gotland Deep and in mid-February of 0.85 µmol/l at Bornholm Deep site. The decline of nitrate started at the Gotland Deep station in mid-March and reached the detection limit in mid-April at a surface water temperature of 4.0 °C. At Bornholm Deep station nitrate already declined at the end of February/first half of March and reached the detection limit end of March at 3.5 °C. The phosphate reserves lasted at both stations well during the summer of 2021. Only one week phosphate appeared to be below the detection limit, in mid-July at Bornholm Deep and end of July at Gotland Deep station. Thus, the spring bloom in 2021 likely ended in the

Bornholm Sea at the end of March, and in mid-April at the Gotland Deep station, similarly as in 2019, but earlier than in 2020. A significant increase of these basic major nutrients in the surface waters did not take place at both stations before early November. At that time, cooling to below 7 °C, clearly lower than the 12 °C in 2020, enabled wind induced mixing in autumn weather conditions and a supply of nutrients from deeper layers. Mineralization processes at depth released the nutrients that were subsequently mixed to surface waters and replenished the nutrients reservoir of surface waters until February of the next year.

The early exhaustion of nitrate at low temperatures likely enabled availability of phosphate almost throughout the year 2021. Algae growth is limited by nitrate availability, and phosphate remains unused at prevailing spring temperatures. This is seen in a low dissolved inorganic nitrogen/phosphorus ratio (DIN/DIP) present in the winter surface water of the Baltic Sea (Fig. 28). The favourable uptake ratio of about 16 was already shown by an early study of Redfield (REDFIELD et al. 1963) and was proven to be a valuable approximation many times thereafter. The DIN/DIP ratio (mol/mol) was determined from the sum of ammonium, nitrate, and nitrite concentrations versus the phosphate concentration. The surface water DIN/DIP ratio in the Baltic Sea in winter 2021 ranged between 5 mol/mol and 14.2 mol/mol in the investigated sea areas. Closest to the ideal ratio were the data of Odra Bight in the last 6 years with the mentioned N/P maximum 14.2 mol/mol. In 2021 the N/P-ratios were well in the range of previous years, with the exception of the western Gotland Sea, where the N/P ratio increased from an average of N/P=4.3 (2016-2019) to 7.7 mol/mol in 2020 and 2021 (Fig. 28). With the exception of the Odra Bight, nitrogen was a limiting factor in all investigated Baltic Sea areas, giving diazotrophic cyanobacteria an advantage compared to primary producer that depend on nitrate.
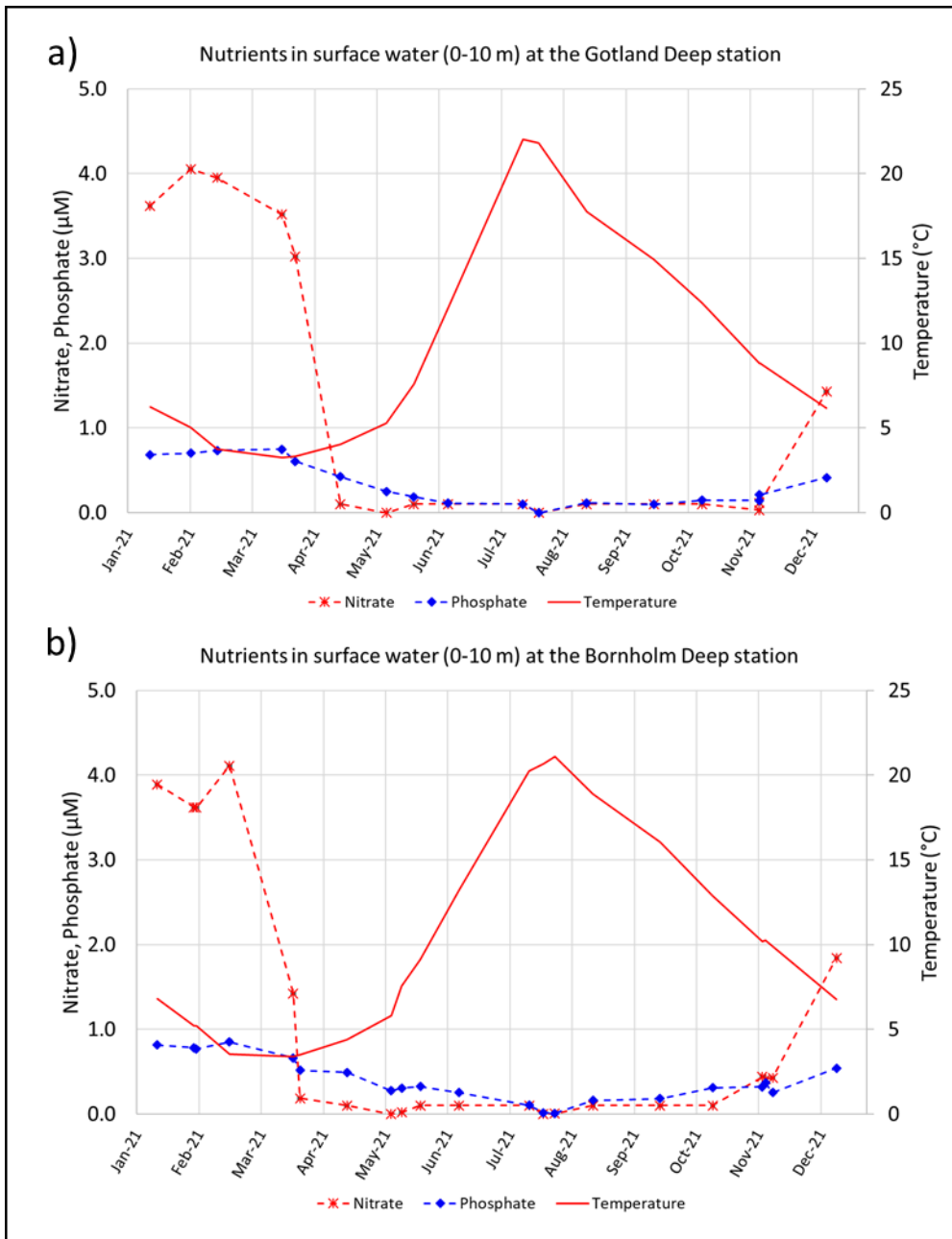
Fig. 27: *Seasonal Cycle of average phosphate and nitrate concentrations in 2021 compared to the temperature development in the surface layer (0-10 m) at the Gotland Deep station (a) and at the Bornholm Deep station (b), respectively, by depicting IOW and SMHI data.*
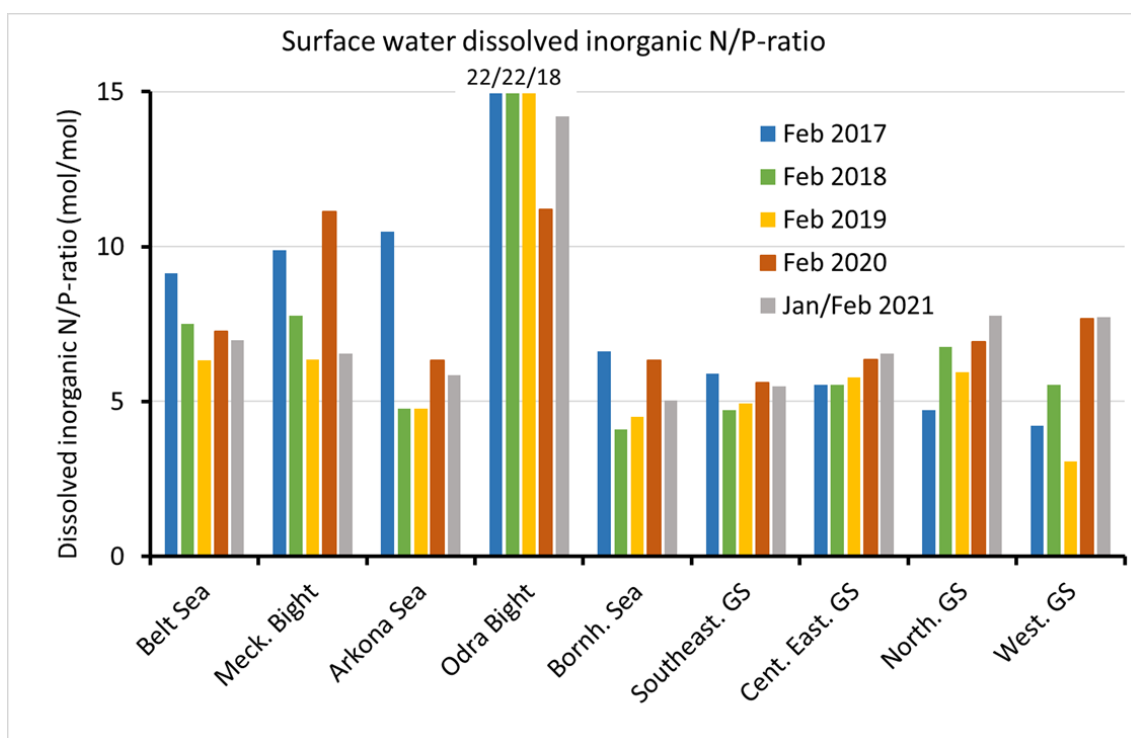
Fig. 28: Average winter dissolved inorganic nitrogen versus phosphate ratio in surface waters of selected Baltic Sea areas for 2017 to 2021.

Table 8 shows winter phosphate and nitrate concentrations in surface waters for the February months of recent years. For phosphate, clearly higher concentrations were determined for the western Baltic Sea and slightly higher concentrations for the Gotland Deep station were determined in January/February 2021 compared to previous years. For Fårö Deep, Landsort Deep, and Karlsö Deep stations 2021 reflects an average year. Thus phosphate in 2021 reflects the maximum concentrations in the western and southern part of the Baltic Sea. Most pronounced was the change again on the Fehmarn Belt station from 0.26 µmol/l in 2020 to 0.9 µmol/l in 2021, an increase by more than a factor of three. On the respective stations of the Gotland, Fårö and Karlsö Deeps the concentrations appear relatively stable during recent years with small increases compared to 2020 only.

The nitrate concentration of the selected stations determined for January/February 2021 were generally higher compared to previous years for the upper 10 m of the water column. For the Fehmarn Belt station, a strong increase was documented from 1.7 in 2019 and 1.1 µmol/L in 2020 to 5.0 µmol/l nitrate in 2021. On the Mecklenburg Bight station an ongoing rise was observed from 2.8 µmol/l (2019) to 3.8 µmol/l (2020) and further to 4.5 µmol/l nitrate in 2021. The Arkona Sea station reached with 3.7 µmol/l the highest surface water nitrate concentration since 2018. On the Gotland Deep station nitrate increased from 3.4 µmol/l in 2020 to 3.9 µmol/l in 2021, on Fårö Deep station from 3.6 µmol/l to 4.2 µmol/l, and on Landsort Deep station from 3.8 µmol/l to 4.8 µmol/l nitrate. The Bornholm Deep station showed after three years below 3 µmol/l again 3.8 µmol/l nitrate as in 2017. After the strong increase at the Karlsö Deep site from 2019 to 2020 by 2.4 µmol/l, the nitrate concentration increased again by 0.5 µmol/l reaching 4.1 µmol/l in 2021.

After a couple of winters with lower phosphate and nitrate concentrations in western Baltic Sea surface water, the concentration levels of phosphate and nitrate of the time before is reached. At the Gotland Deep and Fårö Deep sites the phosphate and nitrate concentrations remained relatively stable in the last 5 years with 0.69 ±0.02 µmol/L phosphate and 3.72 ±0.29 µmol/L nitrate and 0.65 ±0.05 µmol/L phosphate and 3.92 ±0.22 µmol/L nitrate, respectively. Statistically solid reductions of nutrient concentrations that have already been observed in coastal waters are up to now not reflected in the nutrients concentrations of the central Baltic Sea basins (NAUSCH et al. 2011, NAUSCH et al. 2014). However, by comparison with nutrient threshold values, a different development can be noticed for phosphate and dissolved inorganic nitrogen (DIN). The threshold values for DIN and DIP winter concentrations were elaborated for HOLAS II by the TARGEV project (HELCOM 2013) and were modified for HOLAS 3 in 2021: Kiel Bight 5.5/0.57 µmol/l (corresponding to Fehmarn Belt in Table 8), Mecklenburg Bight 4.3/0.49 µmol/l, the Arkona Sea 2.9/0.36 µmol/l, for the Bornholm Sea 1.8/0.28 µmol/l (now separated from Pomeranian Bay), and for the Eastern Gotland Basin 2.6/0.29 µmol/l, respectively. It appears that the nitrate winter concentration (ammonium and nitrite reflect minor contributions) may stabilzes at or below the respective target values in the western Baltic Sea within this decade, but for phosphate it may need some more decades to achieve the threshold values.

Table 8: Mean nutrient concentrations in the surface layer (0-10 m) in winter in the western and central Baltic Sea (IOW and SMHI data).
Table 8.1: Surface water phosphate concentrations (µmol/l) in February (Minima in bold).

Station	2017	2018	2019	2020	2021
360 (Fehmarn Belt)	0.54 ±0.01	0.66 ±0.02	0.42 ±0.00	**0.26 ±0.04**	0.90 ±0.03
022 (Lübeck Bight)	**0.53 ±0.09**	0.69 ±0.00	-	-	0.82 ±0.01
012 (Meckl. Bight)	**0.56 ±0.00**	0.70 ±0.00	0.58 ±0.00	0.58 ±0.00	0.83 ±0.01
113 (Arkona Sea)	0.53 ±0.00	0.67 ±0.01	0.59 ±0.00	**0.43 ±0.01**	0.72 ±0.03
213 (Bornholm Deep)	0.61 ±0.06	0.65 ±0.01	0.61 ±0.02	**0.51 ±0.03**	0.81 ±0.02
271 (Gotland Deep)	0.70 ±0.08	**0.67 ±0.01**	0.68 ±0.02	**0.67 ±0.00**	0.71 ±0.03
286 (Fårö Deep)	0.69 ±0.01	0.64 ±0.01	0.71 ±0.01	**0.57 ±0.01**	0.64 ±0.01
284 (Landsort Deep)	0.79 ±0.03	**0.59 ±0.01**	0.70 ±0.01	**0.59 ±0.00**	0.64 ±0.00
245 (Karlsö Deep)	0.91 ±0.07	0.70 ±0.01	0.65 ±0.01	**0.58 ±0.01**	0.74 ±0.04

Table 8.2: Surface water nitrate concentrations (μmol/l) in February (Minima in bold).

Station	2017	2018	2019	2020	2021
360 (Fehmarn Belt)	3.2 ± 0.1	3.7 ± 0.0	1.7 ± 0.1	**1.1 ± 0.8**	5.0 ±0.5
022 (Lübeck Bight)	4.5 ± 0.7	6.1 ± 0.0	-	-	4.3 ±0.2
012 (Meckl. Bight)	4.4 ± 0.0	4.7 ± 0.3	**2.8 ± 0.1**	3.8 ± 0.0	4.5 ±0.1
113 (Arkona Sea)	5.2 ± 0.0	2.8 ± 0.0	2.6 ± 0.0	**2.5 ± 0.0**	3.7 ±0.3
213 (Bornholm Deep)	3.8 ± 0.1	**2.5 ± 0.0**	2.6 ± 0.1	2.9 ± 0.0	3.8 ±0.1
271 (Gotland Deep)	3.9 ±0.3	**3.4 ±0.0**	4.0 ±0.0	**3.4 ±0.1**	3.9 ±0.2
286 (Fårö Deep)	3.9 ± 0.1	3.9 ± 0.0	4.0 ± 0.0	**3.6 ± 0.1**	4.2 ±0.1
284 (Landsort Deep)	**3.4 ± 0.2**	3.9 ± 0.0	4.0 ± 0.0	3.8 ± 0.0	4.8 ±0.0
245 (Karlsö Deep)	3.3 ±0.1	3.6 ±0.0	**1.2 ±0.1**	3.6 ±0.1	4.1 ±0.2

4.4.2 Deep water processes in 2021

In central Baltic Sea deep waters, the nutrient distribution is primarily influenced by the occurrence or absence of strong barotropic and/or baroclinic inflows and, thus, by its oxygen/hydrogen sulphide concentrations in deep waters. Since the MBI 2014/2015 the accumulation of phosphate in the deep water of the central basins has continued, however certain oxygen intrusions partly lead to lower values. During locally weak oxic water conditions phosphate could be bound to iron as well as to manganese and could be transported to the sediment by particles. The particles are dissolved during anoxia and then phosphate is released back to the water column. The annual mean phosphate concentration in the Bornholm Deep reflects a considerable variability each year that is visible in the large standard deviation. It showed some decline in the annual average phosphate concentration at 80 m depth since the high value in 2018 of 4.7 μmol/l to 2.9 μmol/l in 2020. This is in agreement with its slight oxygen excess on average during 2020. However, after the low value in 2020, the annual mean concentration increased in 2021 to 4.5 μmol/l, close to the former maximum in 2018 of 4.7 μmol/l phosphate. In the Gotland Deep at 200 m, phosphate reached 5.1 μmol/l in 2020 and increased to 5.4 μmol/l in 2021. The Fårö Deep showed a lower phosphate concentration of 3.4 μmol/l in 2020, but a 4.4 μmol/l in 2021. In contrast, the phosphate concentration in the Landsort Deep in

400 m depth was 4 µmol/l in 2020 and decreased to 3.7 µmol/l in 2021. The phosphate concentration in the Karlsö Deep at 100 m depth increased from 3.9 µmol/l in 2020 to almost 4.0 µmol/l in 2021 (Table 8).

The fading of the MBI impact (Naumann et al. 2018) is also reflected in the depletion of nitrate in deep waters. Only the Bornholm Deep showed intermittend a high nitrate concentration in deep waters of an annual average of 6.8 µmol/l in 2019, 7.7 µmol/l in 2020, and recently in 2021 only 2.9 µmol/l nitrate, because of its average weak oxic condition during these years. On Gotland Deep, Fårö Deep, Landsort Deep and Karlsö Deep stations no significant amounts of nitrate were detected since 2018, except the 0.3 µmol/l nitrate found at depth in the Fårö Deep in 2020 (Table 9). An explanation is that anoxic conditions prevent mineralization of organic matter to nitrate. Instead, ammonium is formed and represents the end product of the degradation of biogenic material. Therefore in general, ongoing accumulation of ammonium in deep waters was recorded in Baltic Sea deep waters, in the Gotland Deep from 12.2 µmol/l in 2019 to 20.1 µmol/l in 2020 and to 22.8 µmol/l ammonium in 2021. In the Fårö Deep also for ammonium the relatively low ammonium concentration of 7.3 µmol/l in 2020 changed to 12.2 µmol/l annual average ammonium in the 150 m reference depth. The Landsort Deep showed a moderate increase of ammonium since 2017 from 3.8 µmol/l to 10.3 µmol/l in 2021, and the Karlsö Deep was with 12.1 µmol/l annual average ammonium similar as in 2020 (12.8 µmol/l). In the Bornholm Deep annual average ammonium decreased from 1.9 µmol/l to 0.4 µmol/l between 2018 and 2020, but was 4 µmol/l in 2021 (Table 9).

Table 9: Annual means and standard deviations for phosphate (Tab. 9.1), nitrate (Tab. 9.2) and ammonium (Tab. 9.3) in the deep water of the central Baltic Sea (IOW and SMHI data).

Table 9.1: Annual mean deep water phosphate concentration (µmol/l; Maxima in bold).

Station	depth/m	2017	2018	2019	2020	2021
213 (Bornholm Deep)	80	2.51 ±1.15	**4.73 ±1.56**	3.78 ±1.40	2.88 ±1.03	4.49 ±2.65
271 (Gotland Deep)	200	2.91 ±0.92	4.08 ±0.13	4.38 ±0.25	5.14 ±0.34	**5.39 ±0.16**
286 (Fårö Deep)	150	2.49 ±0.12	3.55 ±0.68	4.02 ±0.45	3.36 ±0.42	**4.37 ±0.17**
284 (Landsort Deep)	400	3.08 ±0.22	3.12 ±0.22	3.64 ±0.57	**3.98 ±0.24**	3.69 ±0.14
245 (Karlsö Deep)	100	3.77 ±0.24	3.63 ±0.34	3.51 ±0.29	3.89 ±0.25	**3.98 ±0.32**

Table 9.2: Annual mean deep-water nitrate concentration (µmol/l; Minima in bold).

Station	depth/m	2017	2018	2019	2020	2021
213 (Bornholm Deep)	80	7.5 ±2.3	**1.6 ±1.5**	6.8 ±2.9	7.7 ±4.1	2.9 ±4.5
271 (Gotland Deep)	200	1.8 ±2.2	**0.0 ±0.0**	**0.0 ±0.0**	0.1 ±0.1	0.1 ±0.0
286 (Fårö Deep)	150	5.5 ±3.5	**0.0 ±0.0**	**0.0 ±0.0**	0.3 ±0.6	0.1 ±0.0
284 (Landsort Deep)	400	**0.0 ±0.1**	**0.0 ±0.0**	**0.0 ±0.0**	0.1 ±0.0	**0.0 ±0.1**
245 (Karlsö Deep)	100	0.1 ±0.0	**0.0 ±0.0**	**0.0 ±0.0**	0.1 ±0.0	0.1 ±0.1

Table 9.3: Annual mean deep water ammonium concentration (µmol/l; Maxima in bold).

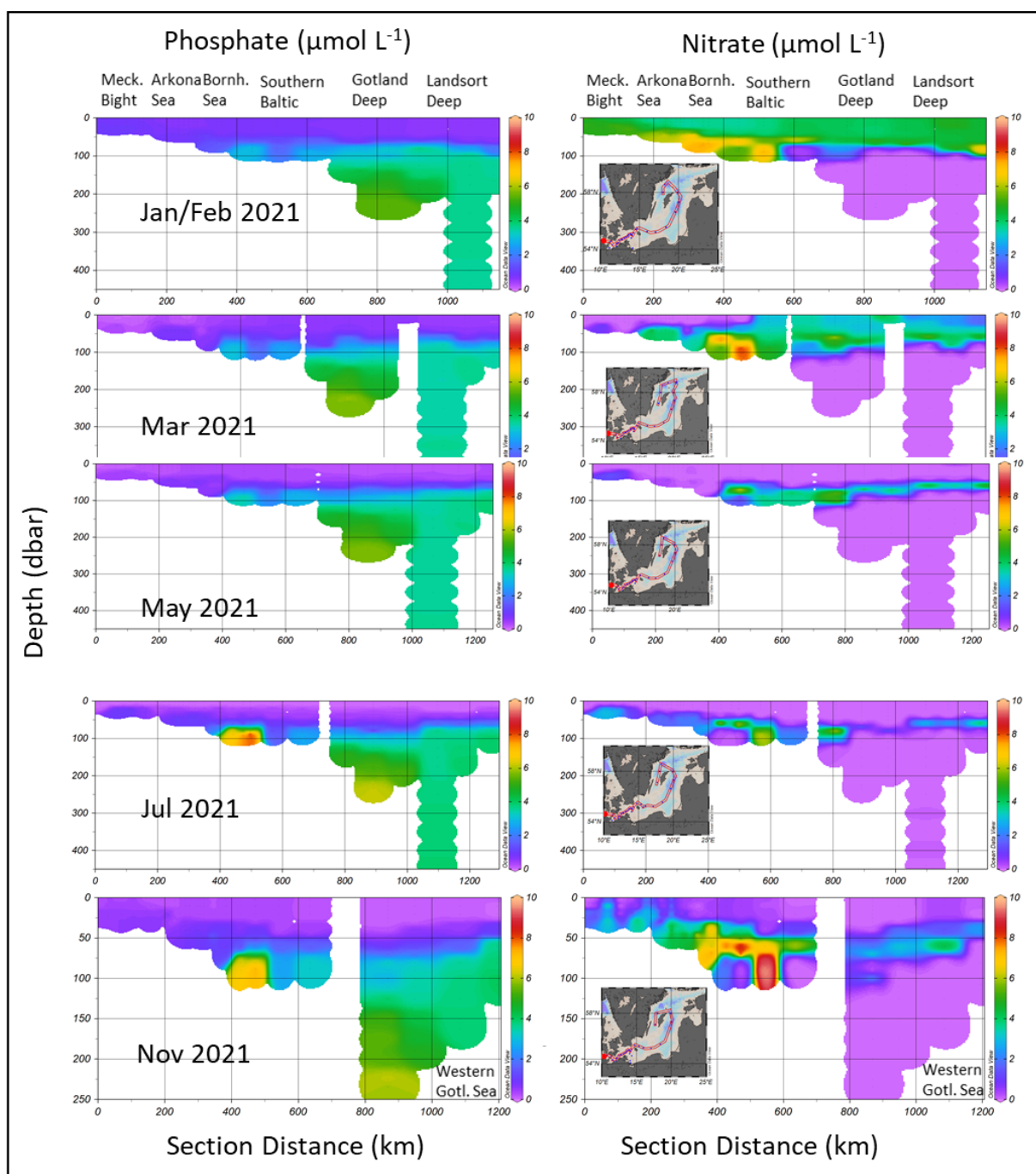| Station	depth/m	2017	2018	2019	2020	2021
213 (Bornholm Deep)	80	0.2 ±0.3	1.9 ±2.4	1.5 ±3.1	0.4 ±0.7	**4.0 ±4.9**
271 (Gotland Deep)	200	0.8 ±0.9	6.0 ±2.3	12.2 ±3.8	20.1 ±5.0	**22.8 ±0.9**
286 (Fårö Deep)	150	0.1 ±0.0	3.6 ±1.7	9.1 ±1.2	7.3 ±3.6	**12.2 ±1.6**
284 (Landsort Deep)	400	3.8 ±1.9	5.0 ±2.2	8.0 ±1.0	9.4 ±2.2	**10.3 ±0.3**
245 (Karlsö Deep)	100	8.4 ±1.5	10.4 ±2.9	9.4 ±5.1	**12.8 ±2.9**	12.1 ±3.8

Fig. 29: Vertical distribution of phosphate (left column) and nitrate (right column) in 2021 between the Mecklenburg Bight and the northern Gotland Basin measured on the monitoring cruises in January/February, March, May, July and November; Landsort Deep was not investigated in November. Figure panels were prepared by using ODV 5, (SCHLITZER 2018).

Fig. 29 illustrates the nutrient distributions in the water column on transects between the Mecklenburg Bight and the western Gotland Sea in January/February, March, May, July and November 2021 (small maps on the right side of Fig. 29 indicate the selected stations for each transect). Thereby, point measurements at their respective depth were enlarged to give an impression of spatial nutrient concentration distributions of phosphate and nitrate along transects. The purple shading corresponds to relatively low concentrations of 1 µmol/l. However,

this reflects for phosphate already the annual maximum in January/February value for surface water that constitutes the basis for primary production during spring and summer. Below the halocline, phosphate increased to a maximum of above 5 µmol/l in the Gotland Deep and below about 4 µmol/l in the Landsort Deep. Interestingly, intruded warm and haline water likely from autumn 2020 to the Bornholm Basin resided there for several month with oxygen depletion and mobilization of phosphate. This is especially visible in July when relatively high values of up to 9 µmol/l (yellow/red bubble) were reached. The affected volume enlarged until November decreasing the concentration to about 7 µmol/l phosphate (left side of Fig. 29). The nitrate concentration distribution along the transect from the western Baltic Sea to the western Gotland Sea is shown for the five monitoring campaigns. Clearly visible is the nitrate depletion in deep waters of the Central Gotland Sea, depicted in light purple being at the detection limit close to zero. In winter, the surface water concentration roughly ranges between 4 µmol/l and 6 µmol/l nitrate that is partly consumed end of March in the western Baltic Sea. In May 2021 only a relatively narrow ribbon of 20 m to 50 m thickness showed remaining nitrate in the halocline range. Above and below the layer, nitrate is depleted. The warm and haline Bornholm Sea bottom water was surpassed with colder less saline oxygenated water in winter that lead to a visible nitrate enrichment in the Bornholm Sea intermediate waters in March with concentrations of up to about 9 µmol/l. Afterwards, nitrate significantly declined during May and July. In November, oxygenated water caused again elevated nitrate concentration in the Bornholm Sea at 50 m to 70 m depth that subsequently even reached the bottom of the southern Gotland Sea increasing the nitrate concentration to about 9 µmol/l there (Fig. 29).

4.5   Nutrients: Particulate organic carbon and nitrogen (POC, PON)

POM includes biomass from living microbial cells, detrital material including dead cells, fecal pellets, other aggregated material, and terrestrially-derived organic matter (KHARBUSH et al. 2020). It constitutes the main pathway by which organic matter is channeled through the biological pump to depths (LE MOIGNE 2019). In the photic surface waters of the Baltic Sea, particulate organic carbon (POC) and nitrogen (PON) concentrations are mainly controlled by the presence, growth, and degradation of biologically produced material (SZYMCZYCHA et al. 2017, WINOGRADOW et al. 2019). Although terrestrial inputs are a significant source of organic matter to the Baltic Sea regarding the dissolved fraction (NAUSCH et al. 2008, SEIDEL et al. 2017), the weak correlation of salinity and POC (Pearson's r=0.07, p<0.001, n=2598) indicated that terrestrial particulate organic matter (POM) played a negligible role at the sampled stations.

POC and PON concentrations were elevated in the surface waters of all stations to varying degrees from March to July (Fig. 30). The seasonal POC and PON signal induced by primary production decreased with water depths, but was often visible down to the bottom water layers especially at the shallow stations TF5 near Warnemünde and TF0360 at Kiel Bight. At the shallow stations, sediment resuspension likely contributes to PON and POC at depth. In the bottom waters of the Bornholm Basin (TF0213), slightly elevated PON concentrations throughout the year potentially resulted from the hypoxic conditions prevailing in 2021 (see Chapter 4.3), supporting organic matter preservation (JESSEN et al. 2017).

Generally, POC and PON concentrations were highly correlated (1995 to 2021, Pearson's r=0.94, p<0.001, n=2764). The particulate C/N ratios were for 2021 on average 6.5±0.7 for the bottom waters and 6.2±0.5 for the surface waters and thus significantly below the long-term means of 7.9±0.9 and 7.6±0.8, respectively (Table 10). The deviation towards lower values in surface and deep waters were visible during all months, except for the surface water C/N ratio in March (Fig. 31). The overall 2021 C/N ratio of 6.0±1.4 was lower than the ratio for living plankton of 6.6 (REDFIELD 1934) and may indicate a combined effect of low terrigenous input of usually higher C/N ratio, primary production, and enhanced heterotrophic biomass contribution during the extremely warm summer (see Chapter 2, (ZIMMERMAN et al. 2014)).
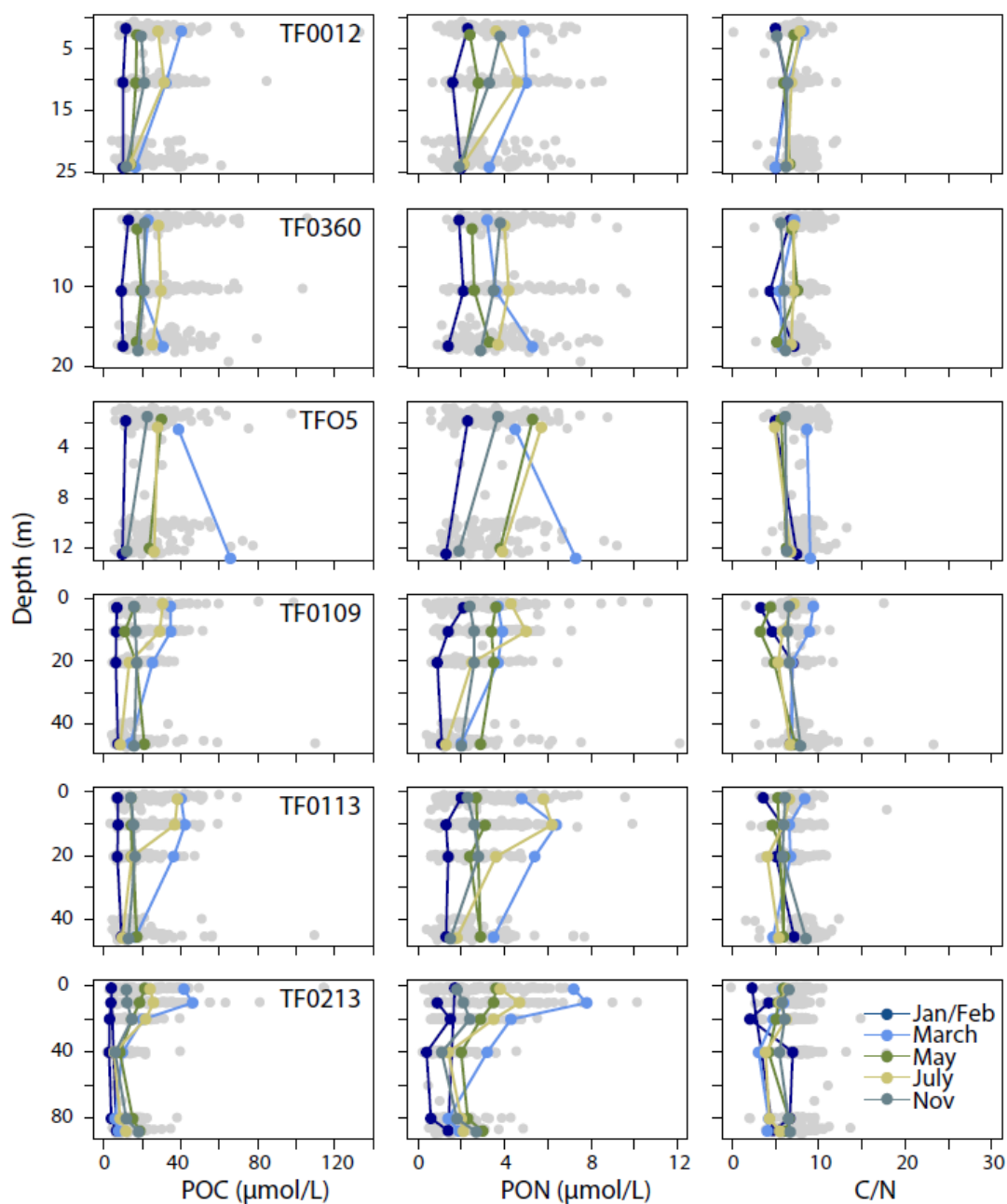

Fig. 30: POC, PON concentrations as well as the particulate C/N ratio over water depth in 2021 by month and station (stations: TF0012 – Mecklenburg Bight, TF0360 – Kiel Bight, TFO5 – Warnemünde, TF0109 – southeastern Arkona Basin, TF0113 – central Arkona Basin, TF0213 – Bornholm Basin/Bornholm Deep). Gray symbols show historic values (1995-2020).
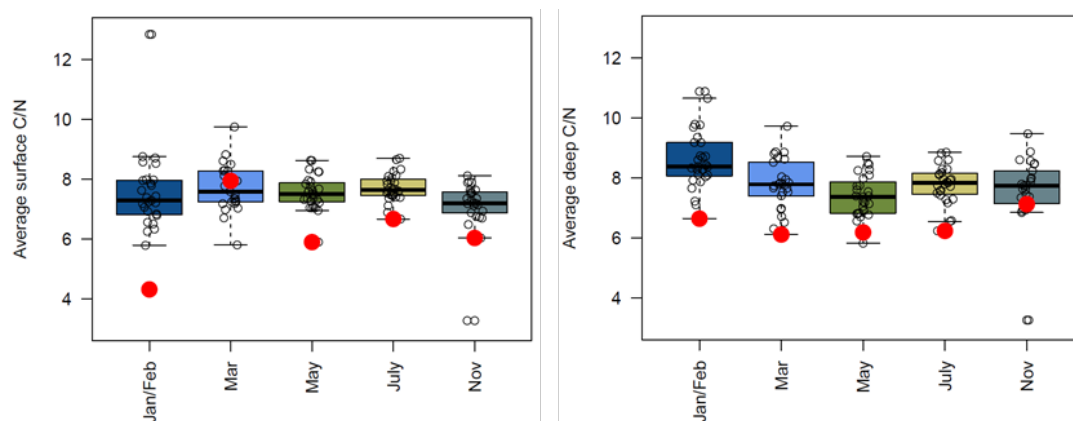
Fig. 31: Yearly averages of surface and deepwater particulate C/N ratios by month with 2021 values shown in red.

Table 10: Average concentrations and C/N ratio of POC and PON in the surface and deep waters in 2021 in comparison to historic data. Differences in means were analyzed via Welch test, significance and degrees of freedom (df) are provided.

	Surface POM			Deep POM		
	2021	1995-2020	Welch-Test	2021	1995-2020	Welch-Test
POC (µmol/L)	**22.4±2.2**	**25.3±7.9**	$p<0.05$, df=11.0	17.4±6.5	19.9±9.0	p=043, df=4.6
PON (µmol/L)	3.5±0.4	3.3±0.9	p=0.30, df=6.7	2.6±0.8	2.5±1.1	p=0.80, df=4.6
C/N	**6.2±0.5**	**7.6±0.8**	$p<0.001$, df=6.0	**6.5±0.7**	**7.9±0.9**	$p<0.01$, df=4.6

4.6 Organic hazardous substances in surface water of the Baltic Sea in January/February 2021

The Baltic Sea is largely affected through contamination since the onset of the industrialization in the late 19th century. Riverine transport and atmospheric deposition are the main transport pathways of organic hazardous substances from land based sources in the catchment area into the Baltic Sea (HELCOM 2018c).

During the monitoring cruise in January/February 2021, Baltic Sea surface water was sampled and analyzed for polycyclic aromatic (PAH) and chlorinated (CHC) hydrocarbons (Table 11). In this report the obtained data are summarized (for an overview see Fig. 32) and time series data for the Mecklenburg Bight, Arkona Sea and the Pomeranian Bight are continued. The results are assessed based on criteria of HELCOM as well as the Marine Strategy Framework Directive (MSFD) and the Water Framework Directive (WF).
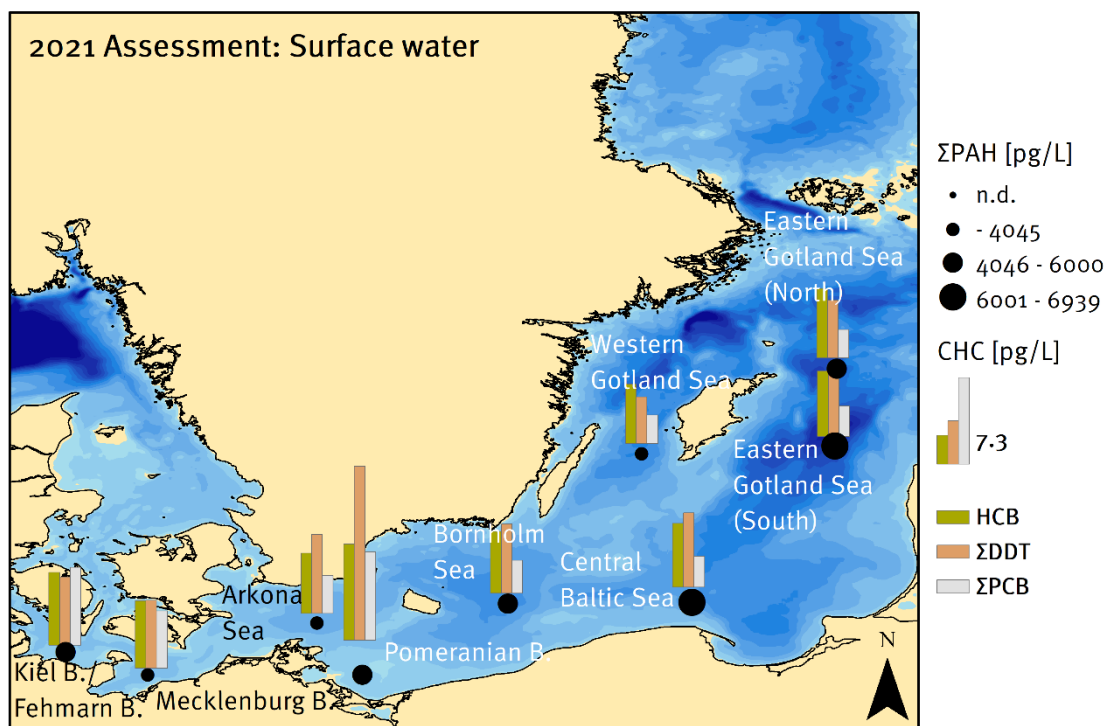
Fig. 32: Summary of obtained data for polycyclic aromatic hydrocarbons (PAH) and chlorinated hydrocarbons (CHC) for the study areas in Baltic Sea surface water in Jan/Feb 2021. ΣPAH_{sum}: summarized concentrations for U.S. EPA PAH indicator compounds (exc. Naph) in dissolved and particulate water fraction, HCB_{sum}: summarized HCB concentration for dissolved and particulate water fraction, ΣDDT_{sum}: summarized concentrations of DDT and metabolites in dissolved and particulate water fraction, ΣPCB_{sum}: summarized concentrations of PCB_{ICES} congeners of dissolved and particulate water fraction.

Table 11: Analyzed compounds in Baltic Sea surface water samples obtained during the January/February 2021 observation.

Compound group	Subgroup	Determined substances
Chlorinated hydrocarbons	ICES-polychlorinated biphenyls (PCB$_{ICES}$)	PCB28/31, PCB52, PCB101, PCB118, PCB153, PCB138, PCB180
	dichlorodiphenyl-trichloroethane (DDT) and metabolites	p,p'-DDT, o,p'-DDT dichlorodiphenyldichloroethylene (DDE): p,p'-DDE dichlorodiphenyldichloroethane (DDD): p,p'-DDD
		hexachlorobenzene (HCB)

	U.S. EPA PAH indicator compounds except naphthalene	acenaphthylene (ACNLE), acenaphthene (ACNE), fluorine (FlE), pheanthrene (PA), anthracene (ANT), fluoranthene (FLU), pyrene (PYR), benzo(*a*)anthracene (BAA), chrysene (CHR), benzo(*b*)fluoranthene (BBF), benzo(*k*)fluoranthene (BKF), benzo(*a*)pyrene (BAP), indeno(1,2,3-*cd*)pyrene (ICDP), dibenzo(*a,h*)anthracene (DBAH), benzo(*g,h,i*)perylene (BGHIP)
Polycyclic aromatic hydrocarbons (PAH)		

Samples were taken in winter season during the expedition EMB256 with RV "Elisabeth Mann Borgese" in January/February 2021, at which the Baltic Sea water is most unaffected by biological conditions such as through algal blooms. Surface water transect samples were obtained in different Baltic Sea study areas (Fig. 33).
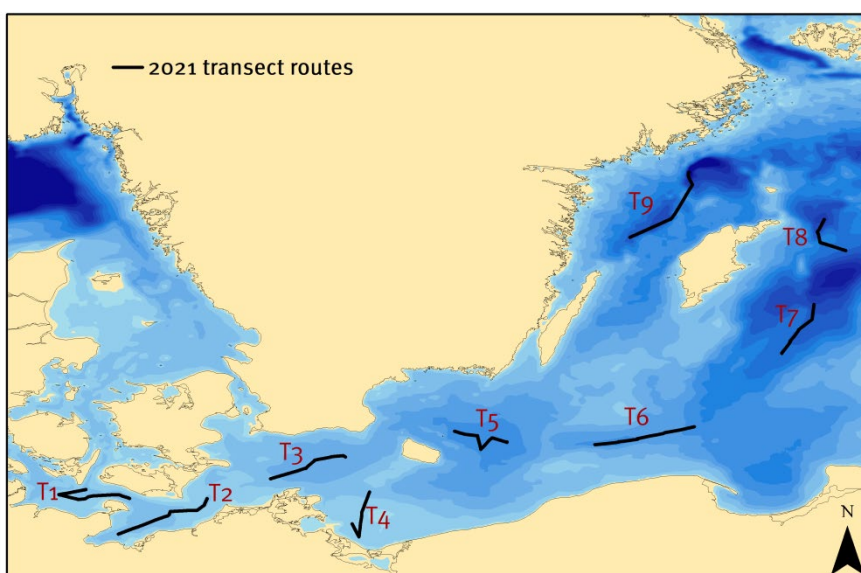
Fig. 33: Surface water sampling transect routes of the research vessel during the January/February 2021 monitoring. T1: Kiel Bight/Fehmarn Belt,T2: Mecklenburg Bight, T3: Arkona Sea, T4: Pomeranian Bight, T5: Bornholm Sea, T6: Central Baltic Sea, T7: Eastern Gotland Sea (South), T8: Eastern Gotland Sea (North), T9: Western Gotland Sea.

During the transect route a pump/filtration system was used to continuously pump surface water from 5 m below the surface through a GF/F filter and subsequently through an XAD-2 resin packed column with a flow rate of about 1.1 l/min for 4 to 6 hours.

Chemical analysis of the CHC and PAH in the dissolved and particulate water fractions was conducted as described before (SCHULZ-BULL et al. 2011; KANWISCHER et al. 2020). All analysis followed accredited procedures.

4.6.1 Chlorinated Hydrocarbons: DDT and metabolites, hexachlorobenzene (HCB) and polychlorinated biphenyls (PCB)

The insecticide <u>DDT</u> has been used as a contact and feeding poison in agriculture and forestry since the 1940s. DDT technical formulations were mixtures of *o,p'* and *p,p'* congeners with *p,p'*-DDT as the predominant one. In the environment DDT degrades to the stable metabolites DDE and DDD. Due to their chemical stability and lipophilic properties, these contaminants accumulate in the tissues of animals and humans *via* the food chain.

<u>HCB</u> is a fungicide which was mainly used for seed treatment and as wood preservative. It is persistent and toxic to aquatic organisms.

Since the 1930s <u>PCBs</u> had been used as fluids in hydraulic systems, as lubricants and insulating and cooling fluids in transformers and electrical capacitors. Commercial PCB formulations usually consisted of a wide range of PCB congeners which differ in the number and position of substituted chlorine on the biphenyl rings. Seven PCB congeners were suggested as indicators for environmental monitoring by the International Council of the Exploration of the Sea (ICES, PCB_{ICES}).

Production and use of DDT, HCB and PCBs is internally restricted or banned by the Stockholm Convention of 2004.

<u>Results for DDT and metabolites in Baltic Sea surface water</u>

In Baltic Sea surface water, concentrations for DDT and its metabolites (ΣDDT_{sum}[1]) ranged from 4.0 pg/L in the Western Gotland Sea (T9) to 14.7 pg/L at the Pomeranian Bight (T4) (median: 5.8 pg/L, Fig. 34, Table Appendix 1). For the western part of the Baltic Sea (T1 – T4) basically higher ΣDDT_{sum} concentrations were determined than for the areas T5 – T9.

The observed high suspended matter (SPM) load at the Pomeranian Bight (about 1.5 mg/L) is accompanied with the highest particulate ΣDDT_{part}[2] concentration of 7.2 pg/L at this site (Fig. 34).

As observed in previous years, too, basically higher concentrations of the long-lived degradation products *p,p'*-DDE and *p,p'*-DDD as compared to *p,p'*-DDT were determined (Fig. 34). This implies no recent inputs of DDT which is also reflected by *p,p'*-DDT/*p,p'*-DDE ratios mostly below 0.5 (STRANDBERG et al. 1998) (Table 12).

Table 12: Ratios of p,p'-DDT/p,p'-DDE for the determined concentrations of DDT and metabolites in Baltic Sea surface water. [a] ratios were determined from summarized particulate and dissolved concentrations

	T1	T2	T3	T4	T5	T6	T7	T8	T9
p,p'-DDT/*p,p'*-DDE [a]	0.24	0.28	0.36	0.26	0.49	0.47	0.46	0.43	0.61

---

[1] ΣDDT_{sum}: summarized concentration of DDT congeners and metabolites in particulate and dissolved water fraction

[2] ΣDDT_{part}: summarized concentration of DDT congeners and metabolites in particulate water fraction
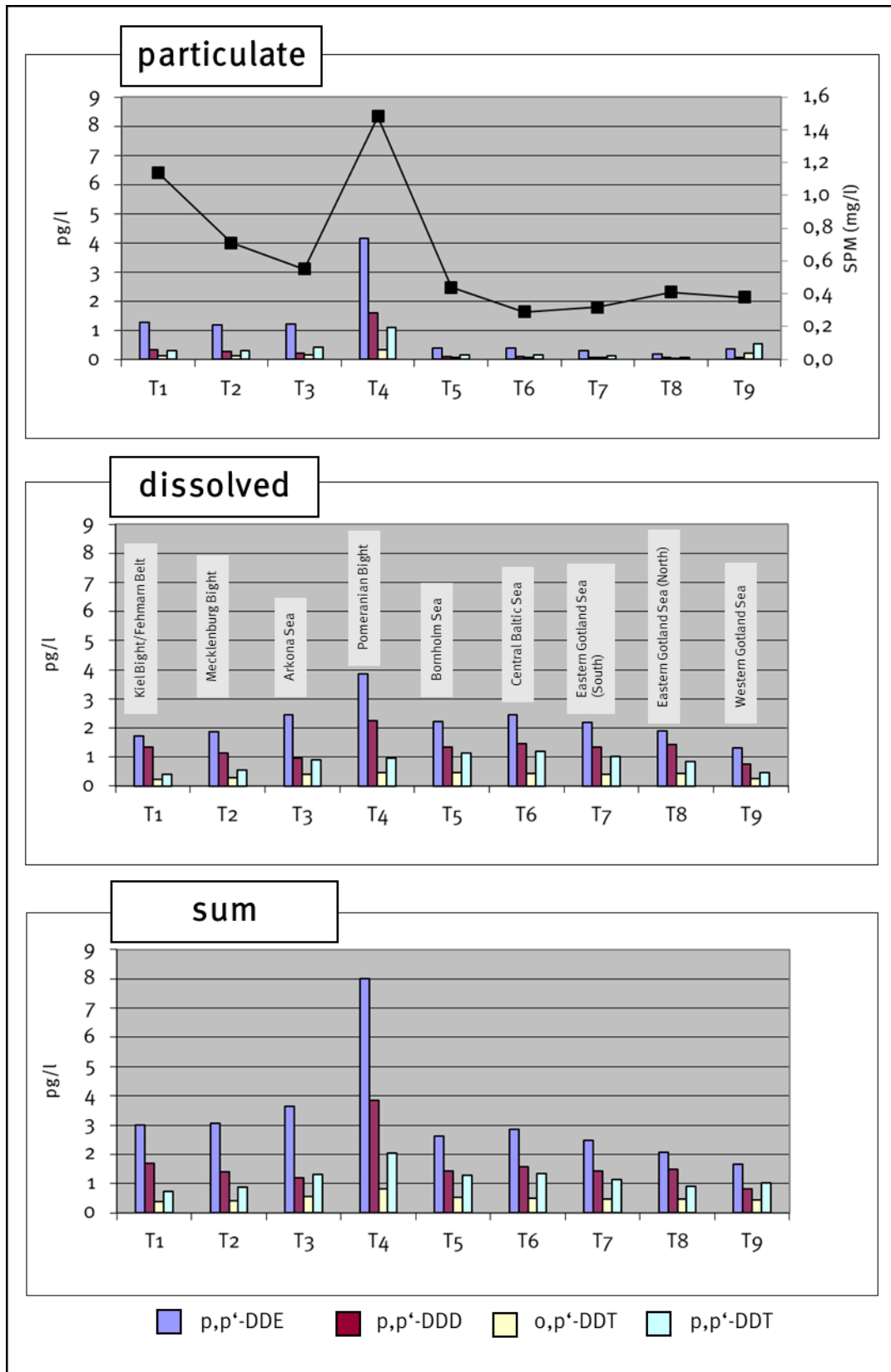
Fig. 34: Concentrations of DDT and metabolites in the dissolved and particulate fractions of Baltic Sea surface water samples of the January/February 2021 surveillance.

Fig. 35 depicts concentrations of *p,p'*-DDE and *p,p'*-DDT of past winter observations for the study areas Mecklenburg Bight, Arkona Sea and Pomeranian Bight. Trends of decreasing concentration for both compounds continue at these sites.
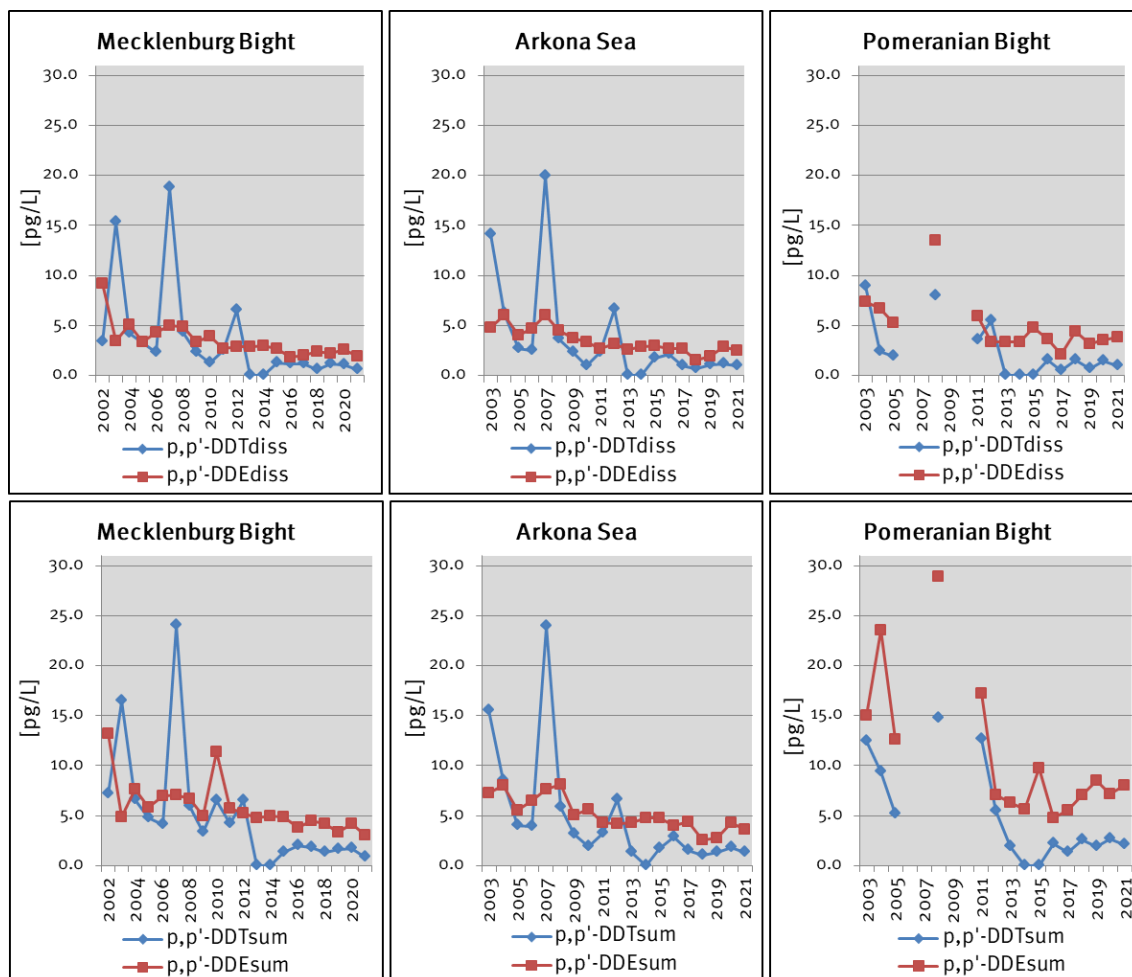
Fig. 35: Time series of p,p'-DDT and p,p'-DDE concentrations in surface water of the Mecklenburg Bight, Arkona Sea and Pomeranian Bight. Upper panel: dissolved water fraction, lower panel: summarized dissolved and suspended water fraction. Gaps in the time line indicate no sampling at the respective year; concentrations at "0 ng/L" mean that the compound was not detected in the sample.

Results for HCB in Baltic Sea surface water

HCB was mainly found in the dissolved water fractions (Table Appendix 2) and determined concentrations for HCB_{sum}[3] ranged from 5.1 to 8.1 pg/L (median: 5.6 pg/L). As for DDT/metabolites and the PCB_{ICES}, too, the highest HCB_{part}[4] concentration of 1.3 pg/L found for the site Pomeranian Bight is accompanied by a high SPM load.

Long-term developments of HCB concentrations for the areas Mecklenburg Bight, Arkona Sea and Pomeranian Bight are shown in Fig. 36. Overall, since 2001 HCB concentrations have

[3] HCB_{sum}: summarized HCB concentrations of particulate and dissolved water fraction
[4] HCB_{part}: HCB concentrations in the particulate water fractions

decreased only slightly which reflects the persistence of this contaminant in the marine environment.

Fig. 36: Concentrations of HCB in Baltic Sea surface water of the Mecklenburg Bight, Arkona Sea and the Pomeranian Bight. Upper panel: dissolved water fraction, lower panel: summarized dissolved and suspended water fraction. Gaps in the time line indicate no sampling at the respective year.

Results for PCBICES in Baltic Sea surface water

Determined concentrations for PCBICES ranged from 2.4 in the Western GotlandSea (T9) to 7.5 pg/L ΣPCBsum[5] in the Pomeranian Bight (T4) (Fig. 37, Table Appendix 2). In the study areas T1 to T4, PCB concentrations were basically higher than for T5 to T9.

High SPM loads accompany with high ΣPCBpart[6] concentrations in the areas Fehmarn Belt/Kiel Bight with 3.0 pg/L ΣPCBpart (SPM 1.1 mg/L) and the Pomeranian Bight with 4.4 pg/L ΣPCBpart (SPM 1.5 mg/L). The high particulate PCB concentrations at the site Fehmarn Belt/Kiel Bight might have derived from bad weather conditions with strong winds at this shallow site and resuspension of

---

[5] ΣPCBSUM: summarized concentrations of PCBICES congeners of the dissolved and particulate water fraction

[6] ΣPCBpart: summarized concentrations of PCBICES congeners in the particulate water fraction

[7] ΣPCBdiss: summarized concentrations of PCBICES congeners in the dissolved water fraction

the contaminants from the surface sediments. At the Pomeranian Bight the high load of SPM presumably derives from the riverine inflow of the river Odra.

Fig. 38 shows PCB concentrations in surface water for the areas Mecklenburg Bight, Arkona Sea and Pomeranian Bight of past winter observations. At these sites concentrations for ΣPCB_{diss}[7] decreased continuously from about 20 pg/L to currently about 3 pg/L.

Fig. 37: Concentrations of PCB*ICES* in the particulate and dissolved water fractions of Baltic Sea surface water in January/February 2021.
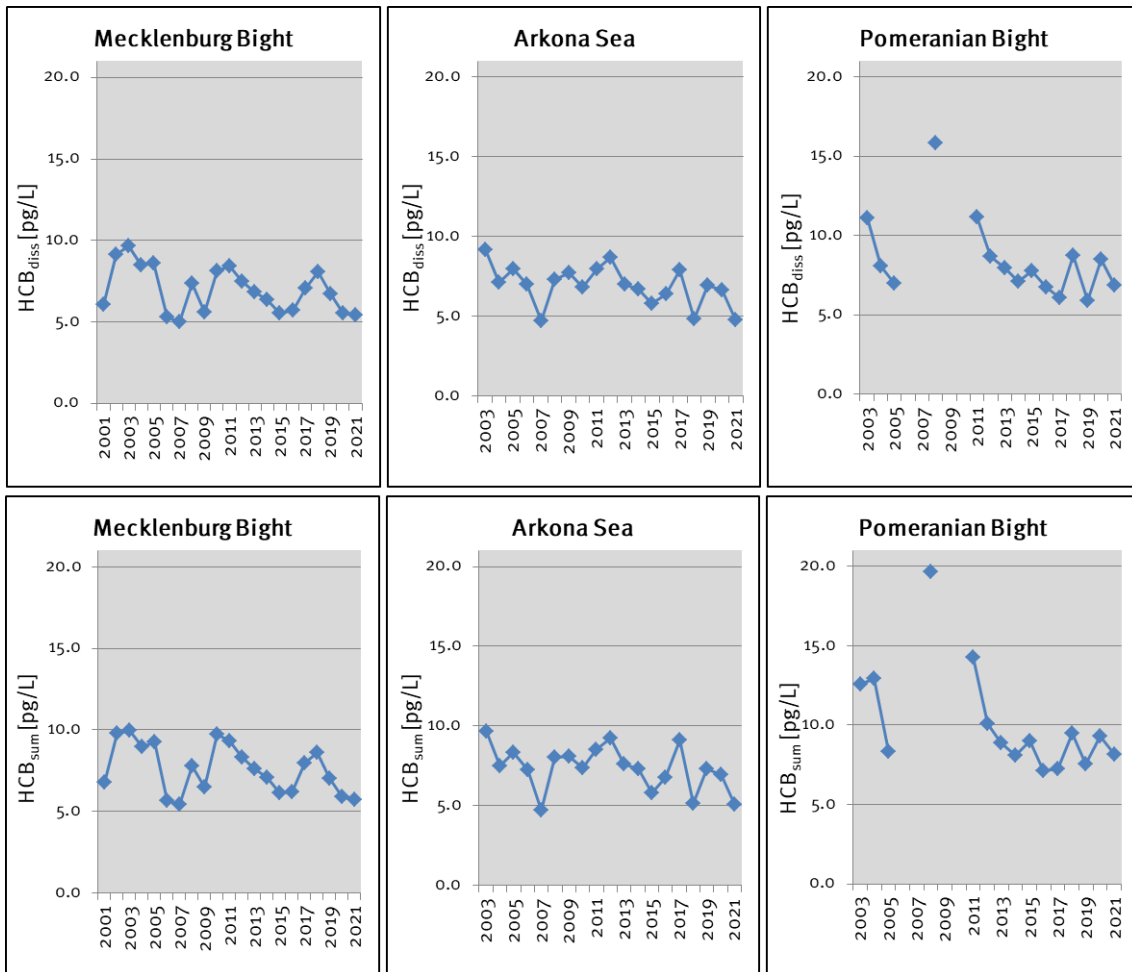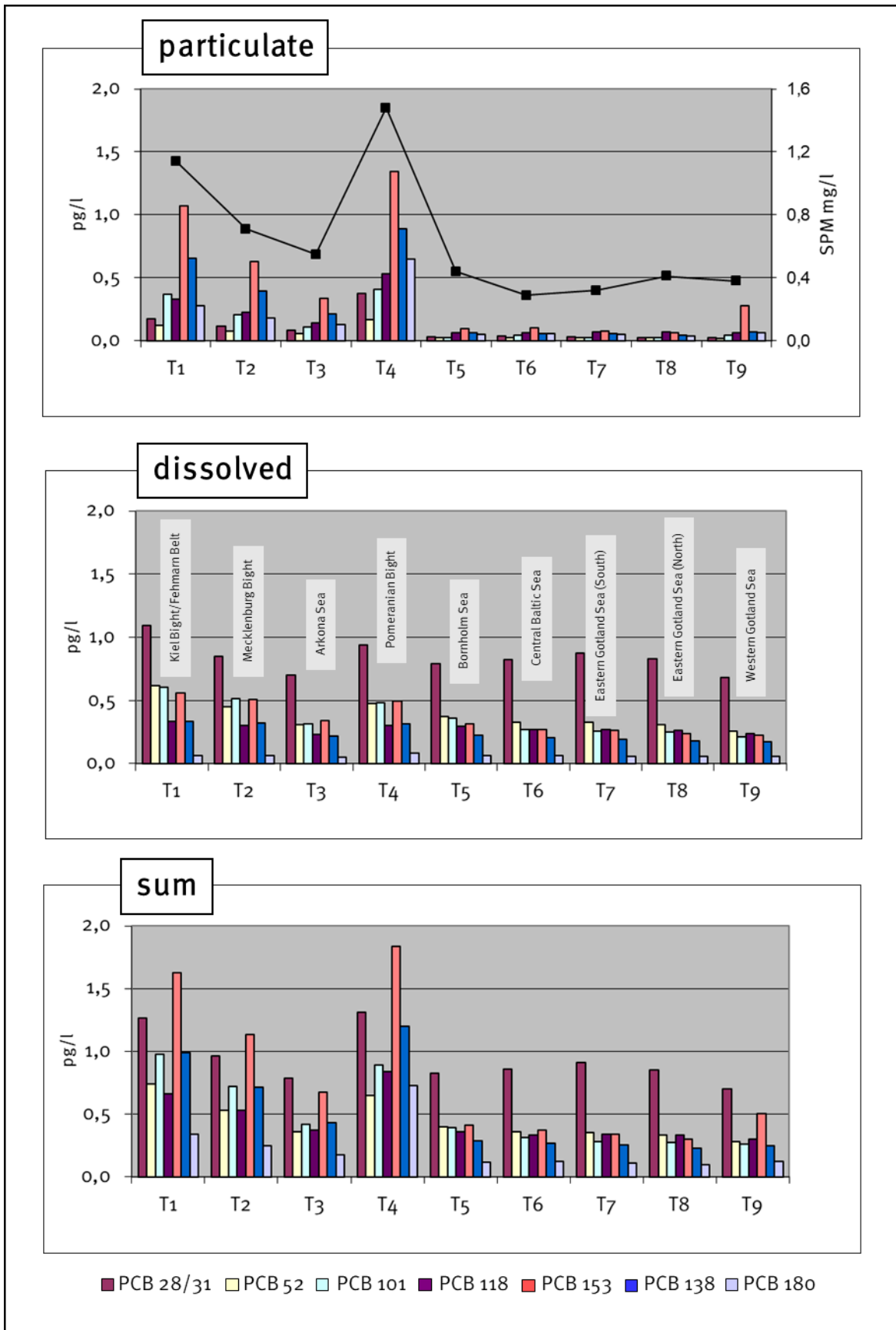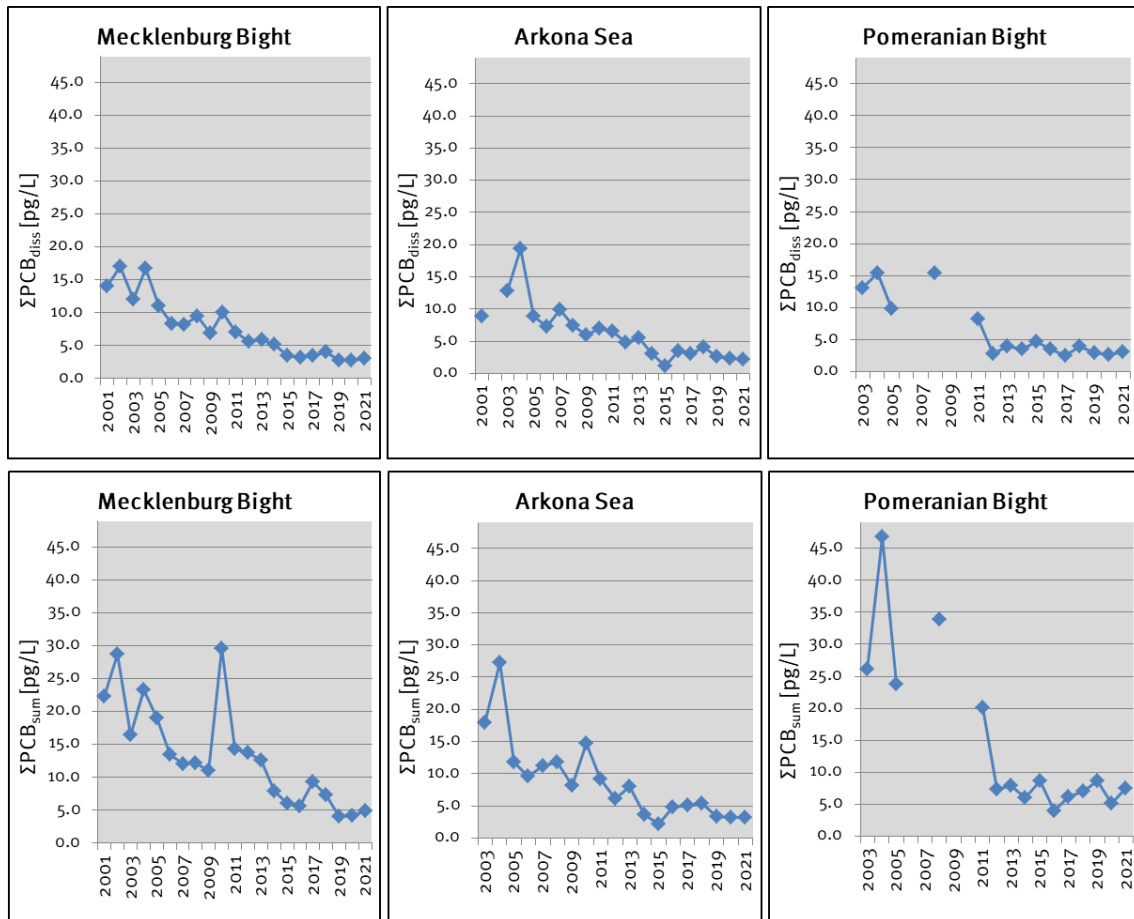
Fig. 38: Time series of ΣPCB$_{ICES}$ concentrations in Baltic Sea surface water at the Mecklenburg Bight, the Arkona Sea and the Pomeranian Bight. Upper panel: dissolved water fraction, lower panel: summarized dissolved and suspended water fraction. Gaps in the time line indicate no sampling at the resp. year.

4.6.2 Results for polycyclic aromatic hydrocarbons (PAHs) in Baltic Sea surface water

PAHs result from incomplete combustion of organic material. They largely derive from industrial combustion processes such as from fossil fuel or wood combustion. Thus, the presence of these pollutants in the environment is strongly associated to anthropogenic activities. PAHs enter the marine environment particularly through oil spills from shipping, river discharges and the atmosphere. PAHs are persistent in the environment and have toxic, carcinogenic as well as reprotoxic properties. PAHs belong to the main environmental pollutants. The 16 U.S. EPA PAH indicator compounds serve as representatives for PAH contamination in the environment (KEITH 2015).

Obtained concentrations for ΣPAH$_{sum}$[8] in Baltic Sea surface water ranged from 3665 pg/L in the Arkona Sea (T3) to 6939 pg/L in the Eastern Gotland Sea (South, T7). In contrast to observed PAH data for the year 2020 (NAUMANN et al. 2021) highest PAH concentrations were found in the areas from the Central Baltic Sea to the Eastern Gotland Sea (T6–T8, Fig. 39, Table Appendix 3). Highest

---

[8] ΣPAH$_{SUM}$: summarized U.S. EPA PAH indicator compounds (exc. Naph) in particulate and dissolved water fraction
[9] ΣPAH$_{part}$: summarized U.S. EPA PAH indicator compounds (exc. Naph) in particulate water fraction

ΣPAH_{part9} concentrations of 1872 pg/L at the Pomeranian Bight accompany with the high SPM load there.
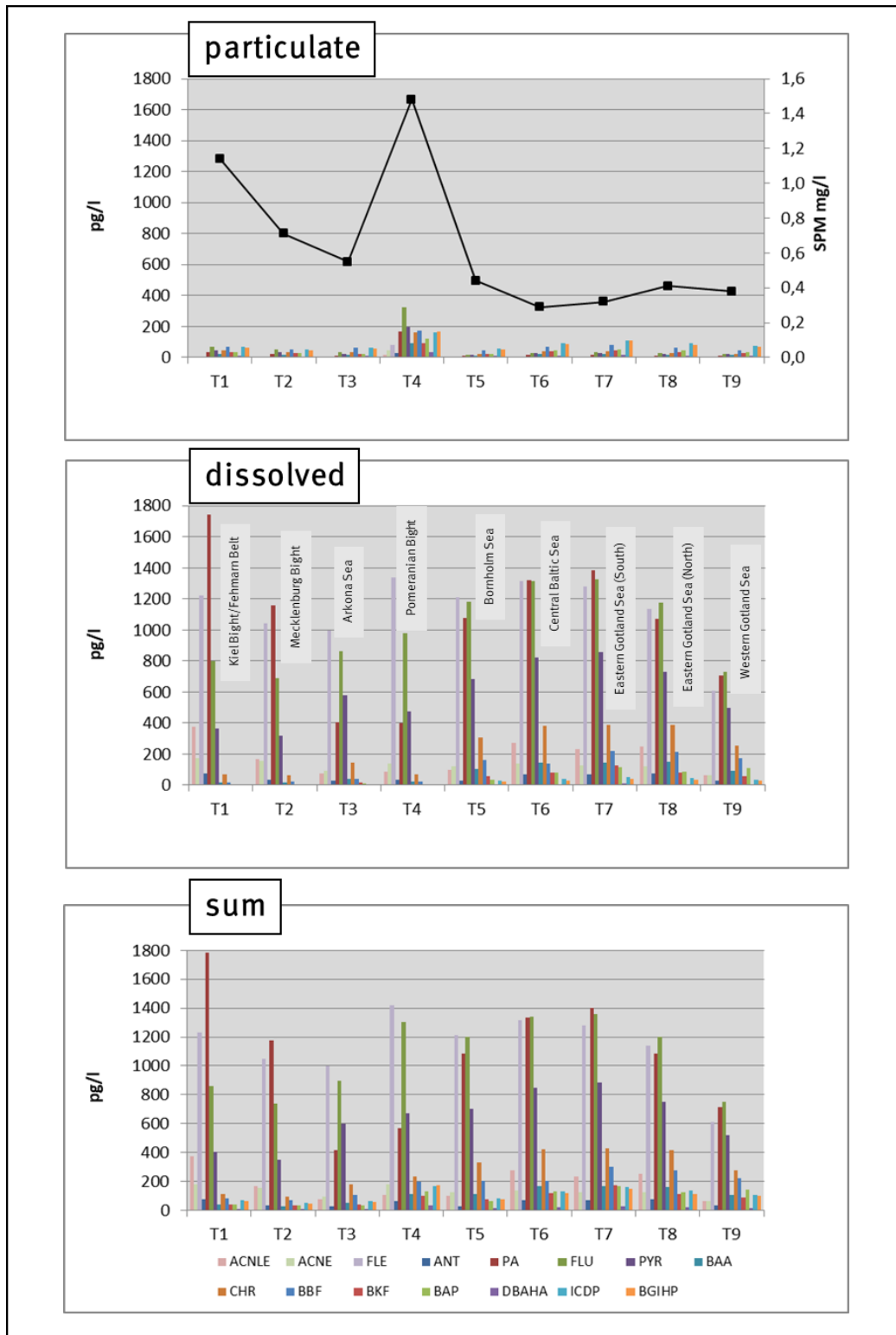

Fig. 39: Concentrations of PAHs in the dissolved and particulate fraction of Baltic Sea surface waters in January/February 2021.

Diagnostic ratios as described by e.g., Yunker et al. 2002; Katsoyiannis & Breivik 2014 can be utilized to identify sources of PAH contamination. Application of the diagnostic ratio BAA/(BAA+CHR) to the observed data reveals petrogenic and combustion processes as PAH sources (Table 13). The BAP/BGHIP ratio of the determined PAH was above 0.6 in all studied areas which identifies marine traffic as a source of PAH contamination, too.

Table 13: Diagnostic ratios BAP/BGHIP and BAA/(BAA+CHR) for the identification of putative PAH sources in Baltic Sea surface water in January/February 2021. Boundaries: BAA/(BAA+CHR) ‹ 0.2: petrogenic PAH source, BAA/(BAA+CHR) › 0.35: combustion derived PAH, 0.2 ‹ BAA/(BAA+CHR) ‹ 0.35: mixed sources, BAP/BGHIP › 0.6: traffic derived PAH; data for dissolved and particulate water fraction are summarized

	T1	T2	T3	T4	T5	T6	T7	T8	T9
BAP/BGHIP	0.61	0.66	0.58	0.75	0.83	1.10	1.12	1.11	1.46
BAA/(BAA+CHR)	0.26	0.24	0.23	0.33	0.26	0.28	0.28	0.28	0.28

The BAP/BGHIP ratio was predominantly high for the areas Central Baltic Sea, Eastern Gotland Sea and Western Gotland Sea (T6 to T9), i.e., ratios were above 1.0 and for T6, T8 and T9 the ratio was highest since 2004 (Fig. 40).
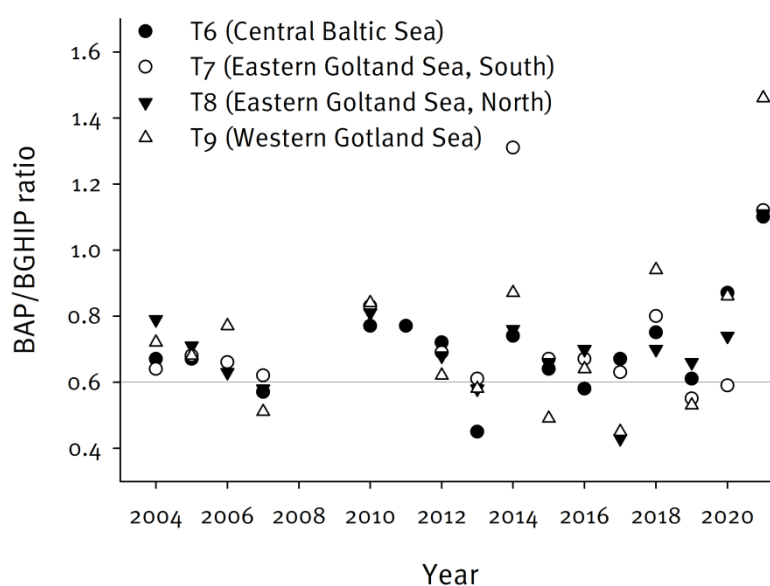
Fig. 40: Results for the diagnostic ratio BAP/BGHIP of the determined PAH for the areas T6-T9 since 2004. The reference line at 0.6 indicates the boundary value for this ratio; data for dissolved and particulate water fraction are summarized.

Analysis of the distribution of the data for the PAH compound BAP, which derives from traffic sources (e.g., Lee et al. 1995; Nielsen 1996), and total PAH for the time period from 2004 to 2021

for the study areas shows that for the year 2021 the obtained BAP concentrations were particularly high in the areas T6 to T9 (Fig. 41) whereas total PAH concentrations where within the 75th and 25th percentile. Thus, for the sites T6 to T9 the proportion of the traffic derived PAH compound BAP on total PAH was exceptionally high.
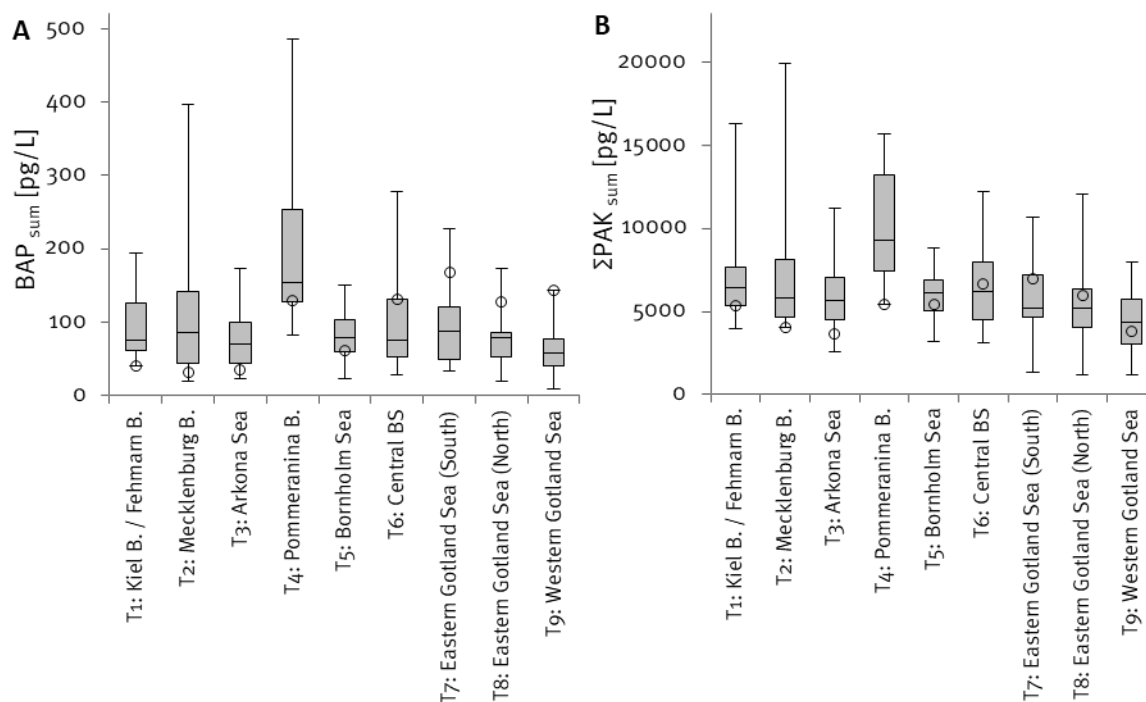
*Fig. 41: Distribution of data for **A** BAP and **B** total PAH in Baltic Sea surface water in the time period from 2004 to 2021. Shown are the values for minimum, maximum, 25th, 50th (median) and 75th percentile. Open circles represent the data obtained during the 2021 monitoring. Data for dissolved and particulate water fraction are summarized.*

Time series PAH data for Baltic Sea surface water since 2003 for the areas Mecklenburg Bight, Arkona Sea and Pomeranian Bight are shown in Fig. 42. The pattern depicts high variation of the PAH concentrations indicating temporally intense PAH sources.

4.6.3   Assessment of the results

Quantitative limits for contaminants in the Baltic Sea have been defined within the framework of European water policy and the HELCOM commitment within the scope of the Baltic Sea Action Plan. Under European legislation monitoring of hazardous substances in the Baltic Sea is directed through the MSFD[10] and the WFD[11]. The Environmental Quality Standards (EQS) for

---

[10] Directive 2008/56/EC of the European Parliament and of the Council of 17 June 2008 establishing a framework for community action in the field of marine environmental policy

[11] Directive 2000/60/EC of the European Parliament and of the Council of 23 October 2000 establishing a framework for Community action in the field of water policy

surface waters of the EQS-Directive[12] serve as the basis to evaluate obtained results for Baltic Sea surface water in January/February 2021 (Table 14).
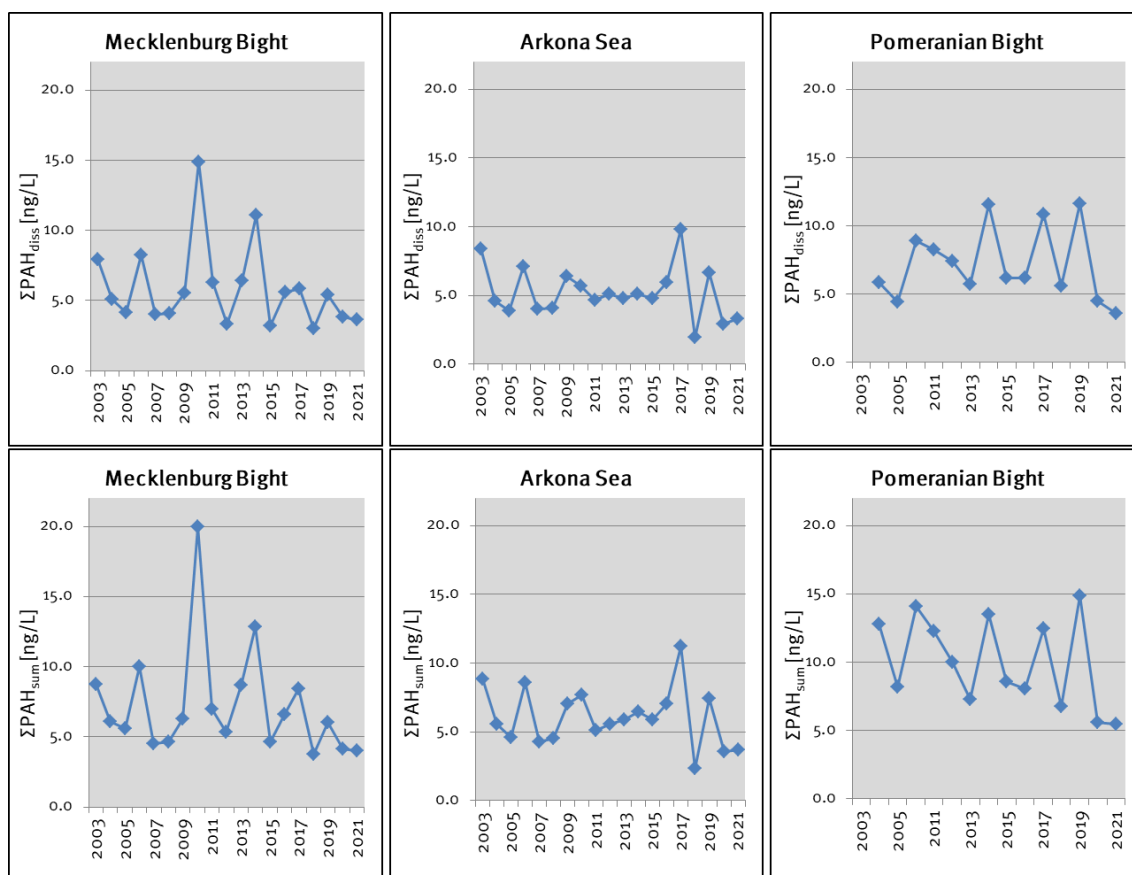
Fig. 42: Concentrations of ΣPAH in surface water of the Mecklenburg Bight, the Arkona Sea and the Pomeranian Bight. Upper panel: dissolved water fraction, lower panel: summarized dissolved and suspended water fraction.

None of the obtained contaminant data in the Baltic Sea surface water exceeded defined maximum allowable concentrations (MAC-EQS, Table 14). In addition, determined concentrations for DDT and metabolites as well as HCB do not exceed annual average EQS (AA-EQS) values.

However, concentrations for the high molecular weight PAH compound BBF exceeding the AA-EQS values were found in the areas Pomeranian Bight, Bornholm Sea, Central Baltic Sea, Eastern Gotland Sea and the Western Gotland Sea. Concentrations of BGHIP and ICDP (Pomeranian Bight) as well as BKF and BAP (Eastern Gotland Sea, South) are at the AA-EQS concentration of 0.00017 µg/L. Although the EQS values are not exceeded there, the concentrations of these PAH compounds might be considered as of concern for marine organisms, too.

---

[11]Directive 2008/105/EC of the European Parliament and of the Council of 16 December 2008 on environmental quality standards in the field of water policy; amended by directive 2013/39/EU

Table 14: Assessment of obtained Baltic Sea surface water contaminant concentrations in Jan/Feb 2021 on the basis of Environmental Quality Standards (EQS) of the EQS-Directive. red values: exceeded EQS, AA-EQS: annual average EQS, MAC-EQS: maximum allowable concentration, data for dissolved and particulate water fraction are summarized.

Substance	Other Surface waters AA-EQS	Other Surface waters MAC-EQS	Kiel Bight/ Fehmarn-belt (T1)	Mecklenburg Bight (T2)	Arkona Sea (T3)	Pomeranian Bight (T4)	Bornholm Sea (T5)	Central Baltic Sea (T6)	Eastern Gotland Sea (South) (T7)	Eastern Gotland Sea (North) (T8)	Western Gotland Sea (T9)
						[µg/L]					
ΣDDTsum	0.025	-	0.000001	0.000001	0.000001	0.000002	0.000001	0.000001	0.000001	0.000001	0.000001
p.p'-DDTsum	0.01	-	0.000006	0.000006	0.000007	0.000015	0.000006	0.000006	0.000005	0.000005	0.000004
HCBsum	-	0.05	0.000006	0.000006	0.000005	0.000008	0.000005	0.000005	0.000006	0.000006	0.000005
ANTsum	0.1	0.1	0.00008	0.00003	0.00003	0.00006	0.00003	0.00007	0.00007	0.00008	0.00003
FLUsum	0.0063	0.12	0.0009	0.0007	0.0009	0.0013	0.0012	0.0013	0.0014	0.0012	0.0008
BBFsum	0.00017	0.017	0.00008	0.00007	0.00010	0.00020	0.00021	0.00021	0.00030	0.00028	0.00022
BKFsum	0.00017	0.017	0.00004	0.00003	0.00004	0.00010	0.00008	0.00012	0.00017	0.00011	0.00009
BAPsum	0.00017	0.027	0.00004	0.00003	0.00003	0.00013	0.00006	0.00013	0.00017	0.00013	0.00014
BGHIPsum	0.00017	0.0082	0.00007	0.00005	0.00006	0.00017	0.00007	0.00012	0.00015	0.00011	0.00010
ICDPsum	0.00017	-	0.00007	0.00005	0.00007	0.00017	0.00008	0.00013	0.00016	0.00014	0.00011

Acknowledgements

References

BSH, 2009: Flächenbezogene Eisvolumensumme.
http://www.bsh.de/de/Meeresdaten/Beobachtungen/Eis/Kuesten.jsp

v.BODUNGEN, B., GRAEVE, M., KUBE, J., LASS, H.U., MEYER-HARMS, B., MUMM, N., NAGEL, K., POLLEHNE, F., POWILLEIT, M., RECKERMANN, M., SATTLER, C., SIEGEL, H., WODARG, D., 1995: Stoff-Flüsse am Grenzfluss – Transport- und Umsatzprozesse im Übergangsgebiet zwischen Oderästuar und Pommerscher Bucht (TRUMP). Geowiss. 13, 479-485.

DIAZ, R.J., ROSENBERG, R., 2008: Spreading dead zones and consequences for marine ecosystems. Science 321 (5891), 926-929.

DUARTE, C.M., CONLEY, D.J., CARSTENSEN, J., SÁNCHEZ-CAMACHO, M., 2009: Return to Neverland: Shifting baselines affect eutrophication restoration targets. Estuaries and Coasts 32 (1), 29-36.

DWD, 2022: Monatlicher Klimastatus, Nr. 1 – 12. Deutscher Wetterdienst.

https://www.dwd.de/DE/leistungen/pbfb_verlag_monat_klimastatus/monat_klimastatus.html

DWD, 2022a: Windmessungen der Station Arkona in Stundenmittelwerten des Jahres 2021. ftp://ftp-cdc.dwd.de/pub/CDC/observations_germany/climate/

DWD, 2022b: Langzeitdaten von Windmessungen der Station Arkona in Tagesmittelwerten. ftp://ftp-cdc.dwd.de/pub/CDC/observations_germany/climate/daily/kl/historical/

FEISTEL, R., NAUSCH, G., HAGEN, E., 2006: Unusual Baltic inflow activity in 2002–2003 and varying deep-water properties. Oceanologia 48, pp. 21–35.

FEISTEL, R. SEIFERT, T., FEISTEL, S., NAUSCH, G., BOGDANSKA, B., BROMAN, B., HANSEN, L., HOLFORT, J., MOHRHOLZ, V., SCHMAGER, G., HAGEN, E., PERLET, I., WASMUND, N., 2008: Digital supplement. In: FEISTEL, R., NAUSCH, G. WASMUND, N. (eds.): State and evolution of the Baltic Sea 1952-2005. John Wiley & Sons, Inc., Hoboken, New Jersey, pp. 625-667.

GRASSHOFF, K., ERHARDT, M., KREMLING, K., 1983: Methods of seawater analysis. 2nd ed., Verlag Chemie, Weinheim.

GRÄWE, U., NAUMANN, M., MOHRHOLZ, V., BURCHARD, H., 2015: Anatomizing one of the largest saltwater inflows in the Baltic Sea in December 2014. J. Geophys. Res. 120, 7676-7697.

HAGEN, E., FEISTEL, R., 2008: Baltic climate change. In: FEISTEL, R., NAUSCH, G., WASMUND, N. (eds.), State and evolution of the Baltic Sea 1952 – 2005. John Wiley & Sons, Inc., Hoboken, New Jersey, pp. 93-120.

HELCOM, 2000: Manual of marine monitoring in the COMBINE programme of HELCOM. Baltic Marine Environment Protection Commission, Helsinki, Updated 2002: www.helcom.fi/Monas/CombineManual2/CombineHome.htm

HELCOM, 2013: Approaches and methods for eutrophication target setting in the Baltic Sea region. Helsinki Commission, Helsinki, Finland.

HELCOM, 2018a: State of the Baltic Sea - Second HELCOM holistic assessment 2011-2016. Balt. Sea Environ. Proc. 155. Helsinki, Finland. http://stateofthebalticsea.helcom.fi

HELCOM, 2018b: Sources and pathways of nutrients to the Baltic Sea - HELCOM PLC-6. Helsinki, Finland. www.helcom.fi/Lists/Publications/BSEP143.pdf

HELCOM, 2018c: Inputs of hazardous substances to the Baltic Sea. Baltic Sea Environment Proceedings 162.

HOLFORT, J., 2021: Der Eiswinter 2020/21 an den deutschen Küsten und an der gesamten Ostsee. Eisdienst, Bundesamt für Seeschifffahrt und Hydrographie Rostock,

https://www.bsis-ice.de/Beschreibung_Eiswinter2021/Eiswinter2021.html#:~:text=Der%20Eiswinter%20 2020%2F21%20an,Eisbildung%20im%20gesamten%20deutschen%20Küstengebiet.

IMGW, 2022: Solar radiation in J/m² at the station Gdynia 2021 – unpublished data

JACOBSEN, T.S., 1980: Sea water exchange of the Baltic. Measurements and methods. The Belt Project. The National Agency for Environmental Protection, Denmark: p107

JESSEN, G.L., LICHTSCHLAG, A., RAMETTE, A., PANTOJA, S., ROSSEL, P.E., SCHUBERT, C.J., STRUCK, U., BOETIUS, A., 2017: Hypoxia causes preservation of labile organic matter and changes seafloor microbial community composition (Black Sea). Science Advances 3: e1601897.

KANWISCHER, M., BUNKE, D., LEIPE, T., MOROS, M., SCHULZ-BULL, D. E., 2020: Polycyclic aromatic hydrocarbons in the Baltic Sea — Pre-industrial and industrial developments as well as current status. Marine Pollution Bulletin 160. Elsevier: 111526. doi:10.1016/j.marpolbul.2020.111526.

KATSOYIANNIS, A., BREIVIK, K., 2014: Model-based evaluation of the use of polycyclic aromatic hydrocarbons molecular diagnostic ratios as a source identification tool. Environmental Pollution, 184, pp. 488-494. doi: 10.1016/j.envpol.2013.09.028.

KEITH, L.H., 2015: The source of U.S. EPA's sixteen PAH priority pollutants, polycyclic aromatic compounds. Taylor & Francis, 35 (2–4), pp. 147–160. doi: 10.1080/10406638.2014.892886.

KHARBUSH, J. J., CLOSE, H. G., VAN MOOY, B. A. S., ARNOSTI, C., RSMITTENBERG, . H., LE MOIGNE, F. A. C., MOLLENHAUER, G., SCHOLZ-BÖTTCHER, B., OBREHT, I., KOCH, B. P., BECKER, K. W., IVERSEN, M. H. MOHR, W., 2020: Particulate Organic Carbon Deconstructed: Molecular and Chemical Composition of Particulate Organic Carbon in the Ocean. Frontiers in Marine Science 7(518).

KOSLOWSKI, G., 1989: Die flächenbezogene Eisvolumensumme, eine neue Maßzahl für die Bewertung des Eiswinters an der Ostseeküste Schleswig-Holsteins und ihr Zusammenhang mit dem Charakter des meteorologischen Winters. Dt. Hydrogr. Z. 42, 61-80.

KRÜGER, S., 2000: Basic shipboard instrumentation and fixed autonomic stations for monitoring in the Baltic Sea. In: EL-HAWARY, F. (ed.): The ocean engineering handbook. CRC Press, Boca Raton, USA, pp. 52-61.

Krüger, S., Roeder, W., Wlost, K.-P., Koch, M., Kämmerer, H., Knutz, T., 1998: Autonomous instrumentation carrier (APIC) with acoustic transmission for shallow water profiling. Oceanology International 98: The Global Ocean Conf. Proc. 2, 149-158.

Lass, H.U., Mohrholz, V., Seifert, T., 2001: On the dynamics of the Pomeranian Bight. Cont. Shelf. Res. 21, 1237-1261.

Le Moigne, F. A. C., 2019: Pathways of Organic Carbon Downward Transport by the Oceanic Biological Carbon Pump. Frontiers in Marine Science 6(634).

Lee, W.-J., Y.-F. Wang, T.-C. Lin, Y.-Y. Chen, W.-C. Lin, C.-C. Ku, and J.-T. Cheng., 1995. PAH characteristics in the ambient air of traffic-source. Science of The Total Environment 159: 185–200. doi:10.1016/0048-9697(95)04323-S.

Lisitzin, E., 1974: Sea-level changes. Elsevier Oceanography Series, Vol. 8, Amsterdam: p286

Matthäus W., Franck, H., 1992: Characteristics of major Baltic inflows - a statistical analysis. Cont. Shelf Res., 12, 1375-1400.

Mohrholz, V., 1998: Transport- und Vermischungsprozesse in der Pommerschen Bucht. Meereswiss. Ber. Warnemünde 33, 1-106.

Mohrholz, V., Naumann, M., Nausch, G., Krüger, S. and Gräwe, U. (2015): Fresh oxygen for the Baltic Sea – an exceptional saline inflow after a decade of stagnation. – Journal Mar. Syst. 148, 152-166.

Mohrholz, V., 2018: Major Baltic inflow statistics – reviewed. Front. Mar. Sci. 5, 384. doi: 10.3389/fmars.2018.00384

Naumann, M., Mohrholz, V., Waniek, J.J., 2017: Water exchange between the Baltic Sea and the North Sea, and conditions in the deep basins. – HELCOM Baltic Sea Environmental Fact Sheet Online, https://helcom.fi/wp-content/uploads/2020/07/BSEFS-Water-exchange-between-the-Baltic-Sea-and-the-North-Sea-and-conditions-in-the-deep-basins-2017.pdf

Naumann, M., Umlauf, L., Mohrholz, V., Kuss, J., Siegel, H., Waniek, J.J., Schulz-Bull, D.E., 2018: Hydrographic-hydrochemical assessment of the Baltic Sea 2017, Meereswiss. Ber. Warnemünde 107, 97 pp. doi:10.12754/msr-2018-0107

Naumann, M., Gräwe, U., Mohrholz, V., Kuss, J., Kanwischer, M., Osterholz, H., Feistel, S., Hand, I., Waniek, J.J., Schulz-Bull, D.E., 2021: Hydrographic-hydrochemical assessment of the Baltic Sea 2020. Meereswiss. Ber. Warnemünde 119, 100 pp. doi:10.12754/msr-2021-0119.

Nausch, G. and Nehring, D. (1996): Baltic Proper, Hydrochemistry. In: Third Periodic Assessment of the State of the Marine Environment of the Baltic Sea. – Balt. Sea Environ. Proc. 64B, 80-85.

Nausch, G., Bachor, A., Petenati, T., Voss, J., V. Weber, M., 2011: Nährstoffe in den deutschen Küstengewässern der Ostsee und angrenzenden Seegebieten. Meeresumwelt Aktuell Nord- und Ostsee 2011/1.

NAUSCH, G., FEISTEL, R., LASS, H.-U., NAGEL, K., SIEGEL, H., 2002: Hydrographisch-chemische Zustandseinschätzung der Ostsee 2001. Meereswiss. Ber. Warnemünde 49, 3-77.

NAUSCH, G., NAUMANN, M., UMLAUF, L., MOHRHOLZ, V., SIEGEL,H., 2014: Hydrographisch-hydrochemische Zustandseinschätzung der Ostsee 2013. Meereswiss. Ber. Warnemünde 93, 1-104.

NAUSCH, G., NEHRING, D., NAGEL, K., 2008: Nutrient concentrations, trends and their relation to eutrophication. In: FEISTEL, R., NAUSCH, G., WASMUND, N. (eds.): State and evolution of the Baltic Sea, 1952-2005. John Wiley & Sons, Inc. Hoboken, New Jersey, 337-366.

NEHRING, D., MATTHÄUS, W., 1991: Current trends in hydrographic and chemical parameters and eutrophication in the Baltic Sea. Int. Revue ges. Hydrobiol. 76, 297-316.

NEHRING, D., MATTHÄUS, W., LASS, H.U., 1993: Die hydrographisch-chemischen Bedingungen in der westlichen und zentralen Ostsee im Jahre 1992. Dt. Hydrogr. Z. 45, 281-331.

NEHRING, D., MATTHÄUS, W., LASS, H.U., NAUSCH, G., NAGEL, K., 1995: Hydrographisch-chemische Zustandseinschätzung der Ostsee 1994. Meereswiss. Ber. Warnemünde 9, 1-71.

NIELSEN, T., 1996. Traffic contribution of polycyclic aromatic hydrocarbons in the center of a large city. Atmospheric Environment 30: 3481–3490. doi:10.1016/1352-2310(96)00096-9.

REDFIELD, A. C., 1934: On the proportions of organic derivations in sea water and their relation to the composition of plankton. James Johnstone Memorial Volume. R. J. Daniel. Liverpool, University Press: 177-192.

REDFIELD, A.C., KETCHUM, B.H., RICHARDS, F.A., 1963: The influence of organisms on the composition of sea water. In: HILL, M.N. (ed.): The sea. J. Wiley & Sons, pp. 26-77.

REYNOLDS, R. W., SMITH, T.M., LIU, C., CHELTON, D.B., CASEY, K.S., SCHLAX, M.G., 2007: Daily high-resolution-blended analyses for sea surface temperature. J. Clim. 20, 5473–5496.

SCHLITZER, R., 2018: Ocean Data View 5, ODV5 Release 5.1.7 (Windows 64bit) Oct. 2018. AWI-Bremerhaven, 2018.

SCHMELZER, N., SEINÄ, A., LUNDQUIST, J.-E. and SZTOBRYN, M. (2008): Ice, in: Feistel, R., Nausch, G., and Wasmund, N. (Eds.), State and Evolution of the Baltic Sea 1952 – 2005. – John Wiley & Sons, Inc., Hoboken, New Jersey, p. 199-240.

SCHULZ-BULL, D., HAND, I., LERZ, A., SCHNEIDER, R., TROST, E., WODARG, D., 2011: Regionale Verteilung chlorierter Kohlenwasserstoffe (CKW) und polycyclischer aromatischer Kohlenwasserstoffe (PAK) im Pelagial und Oberflächensediment in der deutschen ausschließlichen Wirtschaftszone (AWZ) im Jahr 2010. Leibniz-Institut für Ostseeforschung an der Universität Rostock im Auftrag des Bundesamtes für Seeschifffahrt und Hydrographie Hamburg, Rostock Warnemünde.

SEIDEL, M., MANECKI, M., HERLEMANN, D. P. R., DEUTSCH, B., SCHULZ-BULL, D., JÜRGENS K., DITTMAR, T., 2017: Composition and Transformation of Dissolved Organic Matter in the Baltic Sea. Frontiers in Earth Science 5: 31.

SIEGEL, H., GERTH, M., SCHMIDT, T., 1996: Water exchange in the Pomeranian Bight – investigated by satellite data and shipborne measurements. Cont. Shelf Res 16, 1793-1817.

SMHI, 2022a: Tide gauge data at station Landort Norra in hourly means of the year 2021; geodesic reference level RH2000. http://opendata-download-ocobs.smhi.se/explore/

SMHI, 2022b: Accumulated inflow through the Öresund 2014-2021. http://www.smhi.se/hfa_coord/BOOS/Oresund.html

STRANDBERG, B., VAN BAVEL, B., BERGQVIST, P.-A., BROMAN, D., ISHAQ, R., NÄF, C., PETTERSEN, H., RAPPE, C., 1998: Occurrence, sedimentation, and spatial variations of organochlorine contaminants in settling particulate matter and sediments in the northern part of the Baltic Sea. Environmental Science & Technology. American Chemical Society 32 (12), pp. 1754–1759. doi: 10.1021/es970789m.

SZYMCZYCHA, B., WINOGRADOW, A., KULIŃSKI, K., KOZIOROWSKA, K. PEMPKOWIAK, J. 2017: Diurnal and seasonal DOC and POC variability in the land-locked sea. Oceanologia 59(3): 379-388.

TRUMP, 1998: Transport- und Umsatzprozesse in der Pommerschen Bucht (TRUMP) 1994-1996. Abschlussbericht, Warnemünde, 1-32 (unveröffentlicht).

WEIDIG, B. (2021): Sturmflut vom 08.02.2021. https://www.bsh.de/DE/THEMEN/Wasserstand_und_Gezeiten/Sturmfluten/_Anlagen/Downloads/Ostsee_Sturmflut_20210208.pdf;jsessionid=D44C33805E1EC2FE9626A0FF4C39A5D1.live11312?__blob=publicationFile&v=2

WINOGRADOW, A., MACKIEWICZ, A., PEMPKOWIAK, J., 2019: Seasonal changes in particulate organic matter (POM) concentrations and properties measured from deep areas of the Baltic Sea. Oceanologia 61(4): 505-521.

YUNKER, M. B., MACDONALD, R.W., VINGARZAN, R., MITCHELL, R., GOYETTE, D., SYLVESTRE, S., 2002: PAHs in the Fraser River basin: A critical appraisal of PAH ratios as indicators of PAH source and composition. Organic Geochemistry 33 (4), 489–515. doi: 10.1016/S0146-6380(02)00002-5.

ZIMMERMAN, A.E., ALLISON, S.D., MARTINY, A.C., 2014: Phylogenetic constraints on elemental stoichiometry and resource allocation in heterotrophic marine bacteria. Environmental Microbiology 16: 1398-1410.

Appendix: Organic hazardous substances

Table Appendix 1: Concentrations of DDT and metabolites in Baltic surface water in winter 2021.

Dissolved	Transect	*p,p*'DDE	*p,p*'DDD	*o,p*'DDT	*p,p*'DDT	ΣDDT_{diss}
				pg/L		
Kiel Bight/ Fehmarn Belt	T1	1.7	1.4	0.24	0.41	3.7
Mecklenburg Bight	T2	1.9	1.1	0.28	0.56	3.9
Arkona Sea	T3	2.4	0.97	0.40	0.90	4.7
Pomeranian Bight	T4	3.9	2.3	0.47	0.95	7.5
Bornholm Sea	T5	2.2	1.4	0.46	1.1	5.2
Central Baltic Sea	T6	2.5	1.5	0.45	1.2	5.6
Eastern Gotland Sea (South)	T7	2.2	1.3	0.41	1.0	5.0
Eastern Gotland Sea (North)	T8	1.9	1.4	0.42	0.8	4.6
Western Gotland Sea	T9	1.3	0.76	0.25	0.5	2.8

Particulate	Transect	*p,p*'DDE	*p,p*'DDD	*o,p*'DDT	*p,p*'DDT	ΣDDT_{part}
				pg/L		
Kiel Bight/ Fehmarn Belt	T1	1.3	0.34	0.13	0.31	2.1
Mecklenburg Bight	T2	1.2	0.28	0.13	0.30	1.9
Arkona Sea	T3	1.2	0.21	0.17	0.41	2.0
Pomeranian Bight	T4	4.1	1.6	0.34	1.1	7.2
Bornholm Sea	T5	0.38	0.08	0.06	0.15	0.68
Central Baltic Sea	T6	0.40	0.11	0.06	0.15	0.71
Eastern Gotland Sea (South)	T7	0.29	0.08	0.05	0.11	0.53
Eastern Gotland Sea (North)	T8	0.17	0.06	0.04	0.07	0.35
Western Gotland Sea	T9	0.37	0.06	0.20	0.55	1.2

Sum (dissolved + particulate)	Transect	*p,p*'DDE	*p,p*'DDD	*o,p*'DDT	*p,p*'DDT	ΣDDT_{sum}
				pg/L		
Kiel Bight/ Fehmarn Belt	T1	3.1	1.7	0.37	0.72	5.8
Mecklenburg Bight	T2	3.1	1.4	0.41	0.87	5.7
Arkona Sea	T3	3.6	1.2	0.57	1.3	6.7
Pomeranian Bight	T4	8.0	3.8	0.81	2.1	14.7
Bornholm Sea	T5	2.7	1.4	0.52	1.3	5.9
Central Baltic Sea	T6	2.9	1.6	0.51	1.3	6.3
Eastern Gotland Sea (South)	T7	2.5	1.4	0.46	1.1	5.5
Eastern Gotland Sea (North)	T8	2.1	1.5	0.46	0.90	4.9
Western Gotland Sea	T9	1.7	0.82	0.45	1.0	4.0

Table Appendix 2: Concentrations of HCB and PCB$_{ICES}$ in Baltic surface water in Jan/Feb 2021.

Dissolved	Transect	HCB	PCB 28/31	PCB 52	PCB 101	PCB 118	PCB 153	PCB 138	PCB 180	ΣPC$_{diss}$
						pg/L				
Kiel Bight/ Fehmarn Belt	T1	5.8	1.1	0.62	0.61	0.33	0.56	0.33	0.06	3.6
Mecklenburg Bight	T2	5.4	0.85	0.45	0.52	0.30	0.51	0.32	0.07	3.1
Arkona Sea	T3	4.8	0.70	0.31	0.31	0.23	0.34	0.22	0.05	2.2
Pomeranian Bight	T4	6.9	0.94	0.48	0.48	0.30	0.49	0.32	0.08	3.1
Bornholm Sea	T5	5.1	0.79	0.37	0.36	0.30	0.31	0.22	0.06	2.4
Central Baltic Sea	T6	5.3	0.82	0.33	0.27	0.27	0.27	0.21	0.06	2.2
Eastern Gotland Sea (South)	T7	5.4	0.88	0.33	0.26	0.27	0.26	0.19	0.06	2.3
Eastern Gotland Sea (North)	T8	5.8	0.83	0.31	0.25	0.26	0.23	0.18	0.06	2.1
Western Gotland Sea	T9	4.9	0.68	0.26	0.21	0.23	0.22	0.18	0.06	1.8

Particulate	Transect	HCB	PCB 28/31	PCB 52	PCB 101	PCB 118	PCB 153	PCB 138	PCB 180	ΣPCB$_{part}$
						pg/L				
Kiel Bight/ Fehmarn Belt	T1	0.40	0.17	0.12	0.37	0.33	1.1	0.65	0.28	3.0
Mecklenburg Bight	T2	0.31	0.12	0.08	0.20	0.23	0.63	0.39	0.18	1.8
Arkona Sea	T3	0.31	0.08	0.06	0.11	0.14	0.34	0.22	0.13	1.1
Pomeranian Bight	T4	1.3	0.37	0.17	0.41	0.53	1.3	0.89	0.65	4.4
Bornholm Sea	T5	0.14	0.03	0.02	0.03	0.06	0.10	0.07	0.05	0.37
Central Baltic Sea	T6	0.15	0.04	0.03	0.04	0.06	0.10	0.06	0.06	0.39
Eastern Gotland Sea (South)	T7	0.18	0.03	0.02	0.02	0.07	0.08	0.06	0.05	0.33
Eastern Gotland Sea (North)	T8	0.10	0.03	0.02	0.03	0.07	0.06	0.05	0.04	0.29
Western Gotland Sea	T9	0.12	0.02	0.02	0.05	0.07	0.28	0.07	0.06	0.57

Sum (dissolved+ particulate)	Transect	HCB	PCB 28/31	PCB 52	PCB 101	PCB 118	PCB 153	PCB 138	PCB 180	ΣPCB$_{sum}$
						pg/L				
Kiel Bight/ Fehmarn Belt	T1	6.2	1.3	0.74	0.98	0.66	1.6	0.99	0.34	6.6
Mecklenburg Bight	T2	5.7	0.96	0.53	0.72	0.53	1.1	0.71	0.25	4.8
Arkona Sea	T3	5.1	0.79	0.36	0.42	0.37	0.67	0.43	0.18	3.2
Pomeranian Bight	T4	8.1	1.3	0.65	0.89	0.84	1.8	1.2	0.73	7.5
Bornholm Sea	T5	5.2	0.82	0.40	0.39	0.36	0.41	0.29	0.12	2.8
Central Baltic Sea	T6	5.4	0.86	0.36	0.31	0.33	0.37	0.27	0.12	2.6
Eastern Gotland Sea (South)	T7	5.6	0.91	0.35	0.28	0.34	0.34	0.25	0.11	2.6
Eastern Gotland Sea (North)	T8	5.9	0.85	0.33	0.28	0.33	0.30	0.23	0.10	2.4
Western Gotland Sea	T9	5.1	0.70	0.28	0.26	0.30	0.50	0.25	0.12	2.4

Table Appendix 3: Concentrations of of PAHs in Baltic surface water in Jan/Feb 2021

Dissolved	Transect	ACNLE	ACNE	FLE	ANT	PA	FLU	PYR	BAA	CHR	BBF	BKF	BAP	DBAHA	ICDP	BGHIP	ΣPAH$_{diss}$
										pg/L							
Kiel Bight/ Fehmarn Belt	T1	375	176	1221	72	1744	796	362	17	68	15	7.3	5.0	0.6	2.2	2.3	4865
Mecklenburg Bight	T2	168	155	1040	32	1155	686	318	15	61	20	6.5	4.9	0.7	2.6	2.5	3667
Arkona Sea	T3	77	92	995	28	404	860	576	38	145	39	17	10	1.4	5.9	5.4	3294
Pomeranian Bight	T4	89	136	1336	32	399	979	472	22	69	26	8	5.0	0.9	3.8	3.5	3581
Bornholm Sea	T5	101	122	1209	30	1075	1181	684	104	305	162	56	37	5.0	26	22	5117
Central Baltic Sea	T6	271	139	1312	68	1320	1312	822	147	382	138	79	83	6.9	37	30	6146
Eastern Gotland Sea (South)	T7	231	126	1277	69	1383	1325	855	147	390	219	126	114	8.9	52	41	6363
Eastern Gotland Sea (North)	T8	248	124	1136	75	1073	1174	727	147	389	213	78	85	7.9	45	35	5555
Western Gotland Sea	T9	62	63	608	31	704	729	498	95	254	175	59	108	5.4	32	28	3450

Particulate	Transect	ACNLE	ACNE	FLE	ANT	PA	FLU	PYR	BAA	CHR	BBF	BKF	BAP	DBAHA	ICDP	BGHIP	ΣPAH$_{part}$
										pg/L							
Kiel Bight/ Fehmarn Belt	T1	2.5	2.3	6.9	3.0	37	67	44	22	44	67	32	35	11	67	63	504
Mecklenburg Bight	T2	2.0	1.2	5.3	2.0	22	50	35	15	35	51	26	27	8.0	51	47	378
Arkona Sea	T3	1.8	1.5	4.6	1.5	12	36	25	14	34	65	25	25	8.0	61	55	371
Pomeranian Bight	T4	19	44	80	30	166	322	198	91	164	174	94	124	32	164	169	1872
Bornholm Sea	T5	1.9	0.5	2.0	1.1	9	19	16	11	25	45	24	25	8.0	58	52	297
Central Baltic Sea	T6	4.3	0.4	2.8	2.0	15	30	27	20	39	67	39	48	14	95	89	493
Eastern Gotland Sea (South)	T7	5.0	0.5	3.0	2.5	16	33	31	24	41	81	46	54	17	112	109	575
Eastern Gotland Sea (North)	T8	3.8	0.4	1.9	1.9	12	27	24	16	30	63	34	43	13	93	80	444
Western Gotland Sea	T9	3.6	0.4	1.7	1.5	11	23	20	15	25	45	31	36	11	77	71	371

App. Table 3 continued

Sum (particulate + dissolved)	Transect	ACNLE	ACNE	FLE	ANT	PA	FLU	PYR	BAA	CHR	BBF	BKF	BAP	DBAHA	ICDP	BGHIP	ΣPAH_{sum}
								pg/L									
Kiel Bight/ Fehmarn Belt	T1	377	178	1228	75	1781	863	407	39	112	82	39	40	11	69	65	5368
Mecklenburg Bight	T2	170	156	1046	34	1177	737	353	30	96	71	33	32	8,7	53	49	4045
Arkona Sea	T3	78	94	999	30	416	896	601	53	179	104	42	35	10	67	61	3665
Pomeranian Bight	T4	108	180	1416	62	566	1301	670	113	232	200	102	129	33	167	173	5453
Bornholm Sea	T5	103	122	1211	31	1084	1201	700	115	329	207	79	62	13	84	74	5414
Central Baltic Sea	T6	275	139	1314	70	1335	1343	848	167	421	205	119	130	21	132	119	6639
Eastern Gotland Sea (South)	T7	236	127	1280	72	1399	1357	886	171	431	300	172	168	26	164	150	6939
Eastern Gotland Sea (North)	T8	251	124	1138	77	1085	1201	751	164	419	276	113	128	21	137	115	6000
Western Gotland Sea	T9	65	64	610	32	715	752	518	109	279	220	90	144	16	108	99	3821

Naumann, M., Gräwe, U., Mohrholz, V., Kuss, J., Kanwischer, M., Osterholz, H., Feistel, S., Hand, I., Waniek, J.J., Schulz-Bull, D.E.: Hydrographic-hydrochemical assessment of the Baltic Sea 2021

CONTENT

LEIBNIZ-INSTITUT FÜR
OSTSEEFORSCHUNG
WARNEMÜNDE